Universidade de Aveiro
2019

Departamento de Biologia

Sara Maria de Cabral Martins Pêgo

DEVELOPING REAL-TIME PCR GENETIC TESTS FOR FAST DIAGNOSIS OF LHON AND HEARING LOSS

DESENVOLVIMENTO DE TESTES GENÉTICOS POR PCR EM TEMPO-REAL PARA DIAGNÓSTICO RÁPIDO DE LHON E SURDEZ

DECLARAÇÃO

Declaro que este relatório é integralmente da minha autoria, estando devidamente referenciadas as fontes e obras consultadas, bem como identificadas de modo claro as citações dessas obras. Não contém, por isso, qualquer tipo de plágio quer de textos publicados, qualquer que seja o meio dessa publicação, incluindo meios eletrónicos, quer de trabalhos académicos.

Universidade de Aveiro
2019

Departamento de Biologia

SARA MARIA DE CABRAL MARTINS PÊGO

DEVELOPING REAL-TIME PCR GENETIC TESTS FOR FAST DIAGNOSIS OF LHON AND HEARING LOSS

DESENVOLVIMENTO DE TESTES GENÉTICOS POR PCR EM TEMPO-REAL PARA DIAGNÓSTICO RÁPIDO DE LHON E SURDEZ

Dissertação apresentada à Universidade de Aveiro para cumprimento dos requisitos necessários à obtenção do grau de Mestre em Biologia Aplicada, realizada sob a orientação científica da Doutora Maria Manuela Monteiro Grazina, Professora da Faculdade de Medicina da Universidade de Coimbra, e da Doutora Rita Maria Pinho Ferreira, Professora Auxiliar do Departamento de Química da Universidade de Aveiro

O Laboratório de Biomedicina Mitocondrial e Teranóstica recebeu apoio financeiro da Santhera Pharmaceuticals que permitiu implementação do projeto nacional "Investigação Translacional Epidemiológica, Bigenómica e Funcional nas Atrofias Ópticas" (IP Professora Doutora Manuela Grazina).

Apoio financeiro do CNC.IBILI no âmbito do Plano Estratégico UID/NEU/04539/2019.

o júri

presidente	Doutora Isabel Maria Cunha Antunes Lopes Equiparada a investigadora auxiliar da Universidade de Aveiro
vogal (arguente principal)	Prof. Doutora Ana Teresa Moreira de Almeida Santos professor auxiliar com agregação da Universidade de Coimbra
vogal (co-orientadora)	Prof. Doutora Maria Manuela Monteiro Grazina professor auxiliar do Instituto de Bioquímica da Faculdade de Medicina da Universidade de Coimbra

agradecimentos

Este trabalho está de pé sobre ombros de gigantes e, por isso, quero dirigir os meus agradecimentos a quem, de uma forma ou outra, o impactou.

Em primeiro lugar, agradeço à professora Manuela Grazina, por me ter aceitado como orientanda e me ter recebido no seu laboratório, com todo o apoio possível, e permitindo toda a realização deste trabalho. À professora Rita Ferreira, por também me ter aceitado como orientanda, e pela sua ajuda nesta dissertação.

Agradeço à Universidades de Aveiro, à Universidade de Coimbra e ao Centro de Neurociências e Biologia Celular por terem apoiado o desenvolvimento deste trabalho. Em particular, agradeço ao Laboratório de Biomedicina Mitocondrial e Teranóstica por me ter acolhido durante este último ano, tanto na pessoa da Professora Manuela Grazina, como nos restantes membros da equipa – Maria João Santos, Marta Simões, Márcia Teixeira e Vanessa Costa. Um especial obrigado à Maria João, essencial no decorrer deste projeto.

Quero ainda agradecer a todos os que, de uma maneira ou de outra, traçaram o meu caminho até aqui:

Um agradecimento especial a todos os professores que me traçaram o caminho até aqui, da Universidade de Aveiro e de Coimbra, do Colégio São Teotónio e São José. Em particular, à minha avó Emília e ao meu avô Raúl, que foram os meus primeiros professores.

Ao resto da minha família, por terem criado e moldado a pessoa que escreveu este trabalho; a culpa é vossa, não assumo responsabilidades.

Aos meus amigos de longa data: Bea, Carolina, Diogo, Inês, Joana, Margarida, Nuno, Pedro e Rita; e Maria João, Inês, Bia e Ana Luísa. Aos meus colegas e amigos que andaram por biologias: Ana Lousã, Ana Fonseca, Constança e Ricardo, Elsa, Inês Cardoso, Inês Carvalho e Romão. Um pequeno agradecimento a todas as outras pessoas e comunidades que fui encontrando, cara-a-cara ou não. *“My friends have always been the best of me.”*

À minha mãe. Não tenho palavras que te façam justiça (tu é que andaste em Direito). Obrigada pelas mitocôndrias!

E, finalmente, como não poderia deixar de ser, ao Simão, que tem sempre uma pata amiga disponível!

palavras-chave

Doença mitocondrial, *screening* de mutações, *High-Resolution Melting*, *ARMS*, DNA mitocondrial, variação de sequência.

resumo

As citopatias mitocondriais são um conjunto de doenças causadas por um distúrbio na produção de energia celular. A disfunção mitocondrial prejudica a eficiência da cadeia respiratória mitocondrial (CRM) e a produção de ATP, afetando o equilíbrio energético do organismo. As variações de sequência patogénicas no DNA mitocondrial (mtDNA) que levam a estas patologias são mais frequentes em tecidos que necessitam de maiores níveis de energia para funcionar.

O presente trabalho explora duas dessas doenças: Neuropatia ótica hereditária de Leber (LHON) e Surdez mitocondrial induzida por aminoglicosídeos.

A LHON é caracterizada pela presença de alterações genéticas do mtDNA, existindo três variações de sequência patogénicas primárias principais, que representam 90-95% de casos de LHON com identificação da causa genética: m.3460G>A, no gene que codifica a subunidade ND1; m.11778G>A, no gene que codifica a subunidade ND4; e m.14484T>C, no gene que codifica a subunidade ND6. Todas estas subunidades pertencem ao complexo I da CRM. Estas alterações no mtDNA levam a disfunção mitocondrial no complexo I, criando depleção de ATP, aumento de espécies reativas de oxigénio (ROS) e stresse oxidativo.

A LHON é comummente caracterizada pela perda sequencial de visão e, 1 ano após o início dos sintomas, 97% dos casos com perda de visão num olho desenvolvem perda de visão no segundo. A administração de terapia produz bons resultados, quando realizada num curto período de tempo após a primeira perda de visão. Assim, é essencial pesquisar variações de sequência patogénicas genéticas de forma rápida e fiável, para atuar rapidamente e recuperar a função visual.

A Surdez mitocondrial não-sindrómica (MNSHL), em particular a induzida por aminoglicosídeos, tem também três mutações principais associadas à perda de audição: m.1494C>T e m.1555A>G, ambas no gene *MTRNR1*, e m.7445A>G, nos genes *MTCO1* e *MTTS1*. Estas são responsáveis pela depleção de ATP, aumento de ROS e stresse oxidativo, devido a alterações no ribossoma ou no tRNA mitocondrial.

Aqui, o tecido afetado é a cóclea. Nesta doença, o fator modificador em destaque é a administração de antibióticos de tipo aminoglicosídeos, que despoletam uma cascata de acontecimentos, levando à surdez permanente. A melhor estratégia passa pela prevenção, enquanto ao mesmo tempo se garante que a ação clínica não sofre atrasos. Desta forma, são necessários resultados rápidos, que demonstrem se a administração será segura ou não.

O objetivo deste trabalho, para ambas as doenças, é o desenvolvimento de um método de *screening*, caracterizado por uma abordagem rápida e fiável, usado para guiar a decisão clínica, particularmente na terapêutica.

Para a LHON, o método de *screening* é baseado em PCR em tempo-real com análise de *High-Resolution Melting* (HRM), para deteção das variantes

patogénicas TOP-3, avaliando as T_m dos *amplicons*. Neste caso, foram analisadas 94 amostras, incluindo doentes com suspeita de LHON, familiares, outros doentes com suspeita de outra doença mitocondrial e controlos saudáveis. Todas as amostras foram previamente classificadas por outro método, tendo sido sujeitas a anonimização antes da realização do trabalho.

Para a análise, a PCR em tempo-real foi realizada em triplicados, para permitir uma análise de HRM mais robusta. O software teve a capacidade de classificar amostras como diferentes variantes, ou seja, normal ou mutante. Esta informação foi cruzada com as classificações previamente existentes para avaliar o sucesso da classificação pelo software. As amostras foram corretamente classificadas.

Esta abordagem fornece resultados de forma rápida, podendo guiar a ação clínica em tempo útil. A presença de outros polimorfismos nos *amplicons* poderão obstruir a robustez dos resultados fornecidos por esta técnica e o seu efeito na classificação de variantes precisa de ser considerado. Por esta razão, foi realizada uma análise de previsão *in-silico*, considerando a presença de todas as variantes descritas. Nesse sentido, pode ser necessário um método complementar de análise para assegurar a especificidade dos resultados.

Para a Surdez mitocondrial não-sindrómica, o método de *screening* baseou-se também na PCR em tempo-real, mas foi realizada com *primers* de *Amplification-Refractory mutation system* (ARMS), desenhados para as variantes de sequência patogénicas associadas à MNSHL induzida por aminoglicosídeos, previamente descritas na literatura para esta doença. A discriminação de resultados foi feita com base na presença/ausência de amplificação para cada variante. Foram analisadas 32 amostras com esta abordagem, incluindo doentes com suspeita de MNSHL, seus familiares, doentes com suspeita de outra doença mitocondrial e controlos saudáveis, mas apenas foram obtidos resultados em tempo útil para a m.1555A>G. Todas as amostras tinham sido previamente classificadas por outro método, tendo sido anonimizadas antes da realização do trabalho.

Para a otimização, a PCR em tempo-real foi realizada em duplicados, aumentando a robustez da análise. O software de tempo-real mostrou quais as amostras que amplificaram como normais ou mutantes, permitindo a classificação das mesmas. Os dados foram comparados com as classificações previamente conhecidas, para avaliar o sucesso da abordagem em estudo. Todas as amostras em análise foram corretamente identificadas. No entanto, duas das três variantes patogénicas não foram implementadas em tempo útil para inclusão neste trabalho. Para a m.1494C>T e a m.7445A>G, a otimização não foi possível, e será necessário trabalho adicional no futuro, para a implementação da análise destas variantes.

Em conclusão, foi possível implementar um método da análise das variantes genéticas TOP-3 da LHON em 24h, o que representa um grande passo na medicina de precisão para diagnóstico desta doença.

Por outro lado, apesar de não ter sido concluída a implementação, iniciou-se uma abordagem semelhante para a MNSHL – que, quando for concluída, terá um enorme impacto para evitar a perda auditiva por exposição a aminoglicosídeos.

Este trabalho representa uma contribuição científica de alto impacto na investigação translacional reversa.

keywords

Mitochondrial disease, variant screening, High-Resolution Melting, ARMS, mitochondrial DNA, sequence variation.

abstract

Mitochondrial cytopathies are a set of diseases caused by a disturbance in the cell energy production. Mitochondrial dysfunction impairs efficiency of the mitochondrial respiratory chain (MRC) and ATP production, affecting the organism's energetic equilibrium. Pathogenic sequence variants in mitochondrial DNA (mtDNA) that lead to these pathologies are more frequent in tissues that need higher energy levels to function.

The presented work looks into two such diseases: Leber's Hereditary Optic Neuropathy and mitochondrial non-syndromic Hearing Loss (MNSHL).

LHON is characterized by presence of genetic alterations in mtDNA, with three main primary pathogenic sequence variants existing, which represent 90-95% of LHON cases with an identified genetic cause: m.3460G>A, in ND1 subunit gene; m.11778G>A, in ND4 subunit gene; and m.14484T>C, in ND6 subunit gene. All of these are subunits of the MRC's complex I. These mtDNA variations lead to mitochondrial dysfunction in complex I, creating ATP depletion, reactive oxygen species (ROS) increase and oxidative stress.

LHON is commonly characterized by a sequential vision loss and, within 1 year of symptoms starting, 97% of patients with vision loss in one eye develop loss in the second. Therapy administration yields good outcomes, if done in a short-time span after first vision loss. It is essential to quickly and reliably scan for pathogenic sequence variants, in order to act timely and rescue function.

Mitochondrial non-syndromic hearing loss and deafness (MNSHL) is characterized by sensorineural hearing loss (SNHL). This type of hearing loss, particularly when induced by aminoglycosides, has also three primary pathogenic sequence variants associated with ototoxicity: m.1494C>T and m.1555A>G, both in the *MTRNR1* gene, and m.7445A>G, in the *MTCO1* and *MTTS1* genes. These are responsible for ATP depletion, an increase of ROS and oxidative stress, due to alterations in the mitochondrial ribosome or tRNA.

In MNSHL, the cochlea is the affected tissue. With this disorder the principal modifier factor is the administration of aminoglycosides, a type of antibiotics, which trigger a cascade, that leads the individual permanently deaf. The best course of action is prevention, and to ensure clinical action is not dramatically slowed down, results that show whether administration is safe or not need to be quick.

The aim of this work, for both diseases, is the development of a screening method characterized by fast and reliable approach for genetic assessment, to be used for clinical guidance, particularly in therapeutics.

For LHON, the screening method is based on real-time PCR with High-Resolution Melting (HRM) analysis, for detection of the TOP-3 pathogenic sequence variants, by assessing the amplicon's T_m. In this case, 94 samples were analyzed, including LHON suspected patients, relatives, other mitochondrial disease patients and healthy controls. All samples were previously

classified by another method, having then been blinded before the performance of this work.

For analysis, Real-Time PCR was run in triplicates, to allow for a more robust HRM analysis. The software had the ability to classify samples as different variants, wild-type or mutant; information which was then crossed with the previous classification of the sample to assess the success of the software classification. Samples were correctly assigned.

This approach provides results in a quick fashion that guides clinical action in a timely fashion. The presence of other polymorphisms in the amplicons might be a hindrance to the robustness of the results provided by this technique and their effect on variant classification needs to be considered. For this, a predictive *in-silico* analysis was performed, regarding all described variants' presence in the sequences in analysis. Accordingly, an additional complementary method may be necessary for assurance of result's specificity.

For MNSHL, the screening method was also real-time PCR based, but this one was performed with Amplification-Refractory Mutation System (ARMS) primers, designed for the pathogenic sequence variants previously associated in literature for the MNSHL. Discrimination of results was done based on amplification in positive cases and lack of it in negative cases. This approach analyzed 32 samples, including MNSHL suspected patients, their relatives, other mitochondrial disease patients and healthy controls, but only results concerning the m.1555A>G were obtained timely. All samples were previously classified by another method, having then been blinded before performance of this work.

For optimization, Real-Time PCR was run in duplicates, to increase robustness of analysis. The Real-Time software showed if samples amplified as wild-type or mutant, with classification following. This data was crossed with previous known classification of the samples to assess the success of the approach. All analyzed samples were correctly identified with this approach. However, two of the three pathogenic sequence variants did not achieve implementation within the timeframe necessary for their inclusion, namely m.1494C>T and m.7445A>G. The optimization of their screening was not possible and further work is necessary to optimize and implement the approach concerning the analysis for these variants.

In conclusion, it was possible to implement an analysis method for LHON's TOP-3 pathogenic sequence variants within 24h, which represents a big step in precision medicine for diagnosis of this disease.

On the other hand, although the implementation was not concluded, a similar approach was started for MNSHL – that, when concluded, will have an enormous impact in preventing aminoglycoside induced HL.

This work represents a high impact scientific contribution in reverse translational research.

INDEX

ABBREVIATIONS

A: Nucleic Acid Adenosine

AAV: Adeno-associated vector

ADP: Adenosine diphosphate

AICAR: 5-Aminoimidazole-4-carboxamide ribonucleotide

ALCAR: Acetyl-L-carnitine

AmAn: Aminoglycoside Antibiotics

AMPK: AMP-activated protein kinase

Apaf-1: Apoptotic protease activating factor-1

ARMS: Amplification Refraction Mutation System

AS-PCR: Allele- directed specific Polymerase chain reaction

ATP: Adenosine triphosphate

B1: B1 vitamin; thiamine

B2: B2 vitamin; riboflavin

B3: B3 vitamin; niacin

B5: B5 vitamin; pantothenic acid

B6: B6 vitamin; pyridoxine

B7: B7 vitamin; biotin

B9: B9 vitamin; folate

B12: B12 vitamin; cobalamin

Bad: BCL2 associated agonist of cell death

Bak: Bcl-2 homologous antagonist/killer protein

Bax: Bcl-2-associated X protein

BCL2: B-cell lymphoma 2 gene

Bcl-2: B-cell lymphoma 2 protein

Bcl-X_L: B-cell lymphoma-extra-large protein

Bid: BH3 interacting-domain death agonist protein

Bim: Bcl-2-like protein 11 (BCL2L11)

BLAT: BLAST(Basic Local Alignment Search Tool)-Like Alignment Tool

bp: Base pair

C: Nucleic Acid Cytosine

Ca^{2+}: Calcium ion

CEP-1347: Inhibitor of JNK

CI: Complex I

CNV: Copy Number Variation

CoQ10: Coenzyme Q10

CT: Cycle Threshold

DMSO: Dimethyl sulfoxide

DNA: Deoxyribonucleic acid

dNTPs: Deoxyribonucleotide triphosphate

dsDNA: Double stranded DNA

E2F1: E2F transcription factor 1 gene

E2F1: E2F transcription factor 1

EPHX1: Epoxide hydrolase 1 gene

ER: Endoplasmatic Reticulum

G: Nucleic Acid Guanine

GJB2: Gap junction beta-2 gene

GJB2: Gap junction beta-2 protein

HL: Hearing Loss

HRM: High Resolution Melting

IHC: Inner Hair Cells

IMM: Inner mitochondrial membrane

IVF: *in-vitro* fertilization

JNK: c-Jun N-terminal kinases

LED: Light emitting diode

LHON: Leber's Hereditary Optic Neuropathy

L-strand: Light strand

M: Mutant

MAM: Mitochondrial-associated ER membrane

MC: Mitochondrial cytopathy

MCA: Melt curve analysis

MD: Mitochondrial disorder

MELAS: Mitochondrial eEcephalomyopathy, Lactic Acidosis, and Stroke-like episodes

MET: Mechanoelectrical transducer

Mg^{2+}: Magnesium ion

MitoQ: Mitoquinone

MNSHL: Mitochondrial non-syndromic hearing loss

MRC: Mitochondrial respiratory chain

mRNA: Messenger RNA

MTCO1: Mitochondrially encoded cytochrome c oxidase I gene

mtDNA: Mitochondrial DNA

MTND1: Mitochondrially encoded NADH dehydrogenase 1 gene

MTND4: Mitochondrially encoded NADH dehydrogenase 4 gene

MTND6: Mitochondrially encoded NADH dehydrogenase 6 gene

MTP-131: Mitochondria-targeted peptide 131

mtPTP: Mitochondrial permeability transition pore

MTRNR1: Mitochondrially encoded 12S RNA gene

MTS: Mitochondrial targeting signal

MTTS1: Mitochondrially encoded tRNA serine 1 (UCN) gene

NADH: Reduced form of NAD (Nicotinamide Adenine Dinucleotide)

NADPH: Reduced form of $NADP^+$ (Nicotinamide Adenine Dinucleotide Phosphate)

NCBI: National Center for Biotechnology Information

ND1: NADH dehydrogenase 1

ND4: NADH dehydrogenase 4

ND6: NADH dehydrogenase 6

nDNA: Nuclear DNA

Nfr2: Transcription nuclear factor erythroid 2-related factor 2

NGS: Next-Generation Sequencing

NTC: Non-Template Control

O_2: Oxygen molecule

ºC: degree Celsius

OPA1: OPA1 mitochondrial dynamin like GTPase gene

OXPHOS: Oxidative phosphorylation

PARL: Presenilin associated rhomboid like gene

PCR: Polymerase Chain Reaction

PD: Parkinson's Disease

PGC1α: PPAR gamma coactivator 1-alpha

PMB: Papillomacular bundle

POLRMT: RNA polymerase mitochondrial

PPAR: Peroxisome proliferator-activated receptor

qPCR: Quantitative Polymerase chain reaction

REDOX: Reduction-Oxidation

RFLP: Restriction Fragment Length Polymorphism

RGC: Retinal Ganglion Cells

RNA: Ribonucleic acid

RNFL: Retinal nerve fiber layer

ROS: Reactive oxygen species

RP103: Cysteamine Bitartrate Delayed-release Capsules

rRNA: Ribosomal RNA

SIRT1: Sirtuin 1 enzyme

SIRT3: Sirtuin 3 protein

SkQ-1: 10-(6′-plastoquinonyl) decyltriphenyl phosphonium cation

Smac/DIABLO: Second mitochondria-derived activator of caspases

SNHL: Sensorineural Hearing Loss

SNV: Single nucleotide variant

SOD2: Superoxide dismutase 2 gene

SOD2: Superoxide dismutase 2 protein

SRT1720: Selective activator of *Homo sapiens*' *SIRT1*

ssDNA: Single stranded DNA

T: Nucleic Acid Thymine

TE: Tris-EDTA buffer

TFB1M: Mitochondrial transcription factor B1 gene

TFB1M: Mitochondrial transcription factor B1 methyltransferase

Tm: Melting temperature

TP53: Tumor Protein p53 gene

TPP: Triphenylphosphonium

TRMU: tRNA 5-methylaminomethyl-2-thiouridylate methyltransferase gene

tRNA: Transfer RNA

tRNA$^{Ser(UCN)}$: tRNA serine 1 (UCN)

U: Uracil

UCSC: University of California, Santa Cruz

WT: Wild-type

INDEX OF FIGURES

INDEX OF TABLES

1. Introduction

1.1. The mitochondria

The cell is the basic unit of life, and it is powered by mitochondria, which are present in all nucleated cells. These organelles possess many forms, with variations on size, number and distribution throughout cells and their lifespan. These organelles are big enough to be seen in a microscope, but their structure requires a much more sensitive method, such as Transmission Electron Microscopy. On average, there are 3,000 to 5,000 mitochondria per cell, varying according to cell type. They are oval shaped, with length of 1-2μm and width of 0.5-1μm (1,2).

Mitochondria evolved from bacterial life, with this organism being absorbed and consequently creating an endosymbiotic relationship with another cell (1). This explains the ins and outs of the existence, function and workings of the mitochondrial genome. Mitochondria do not have all the necessary genetic material, with their genome and proteome being complemented by the nuclear genome (1). Bigenomic control, where both mitochondrial DNA (mtDNA) and nuclear DNA (nDNA) exert their effects, is connected to numerous aspects of mitochondrial action and function (3). Furthermore, as strong evidence of endosymbiosis, approximately 95% of the mitochondrial genome sequence is found in the nuclear genome – these sequences are termed pseudogenes (1,3).

Regarding replication, transcription and translation, mtDNA resembles more the bacterial genome (1–3). The Cambridge Consensus Sequence, completed in 1981 by Anderson *et al.* (4) and revised in 1999 (5), presents the mitochondrial genome as a double stranded circular DNA molecule of 16,568bp. The mtDNA contains 37 genes, encoding 13 peptides (2,3). The presence of their own genomic material makes the mitochondria, its interaction with the nuclear DNA and cell organelles, and its effects on the organism, particularly complex.

The mtDNA has some unique and distinctive characteristics, when compared to nDNA. The mtDNA is transmitted via maternal inheritance, escaping to Mendelian laws. During fertilization, only the female zygote's mitochondrial information prevails in the embryo (2).

Each mitochondrion contains two to 10 copies of mtDNA, while there are two copies of nDNA in each nucleus (1–3). This principle establishes another key feature of mtDNA: homo- and heteroplasmy. If all copies present in mitochondria are similar in sequence, it is defined as homoplasmy; if there are different copies, there is heteroplasmy, which happens at different percentages (depending on how many copies of each type exist) (3). Homo- and heteroplasmy are quite important in the event of variation. Due to the several-copy system, one copy presenting variation may not incite any substantial change in biochemical functioning and the phenotype will remain the same. However, the probability of phenotypical impact rises with the increase in heteroplasmy percentage (higher number of mutated copies) (3,6). This is referred to as the "threshold effect", by which, only after a certain percentage of heteroplasmy, the phenotypical change will be

noticeable. To further increase this complexity, up to 1,000 mitochondria exist per cell, equating up to 10^2-10^5 mtDNA copies per cell (2,3). The threshold effect occurs at different percentages for different pathogenic sequence variants, associating with varying degrees of disorder, with only some manifesting at homoplasmy (6).

The mtDNA is particularly susceptible to mutational effect, presenting high mutation rates, because of the combination of biochemical tasks performed in the mitochondria, which ultimately may lead to damage caused by reactive oxygen species (ROS), and its simpler nature – a lack of highly efficient repair or protection mechanisms, no histones, non-coding or intron regions, and a very compact structure (1–3,6,7).

With the migrations from out of Africa and human global colonization, just as nuclear genetic drift helped adaptation and thriving for certain populations, so did mtDNA variations, altering metabolism. Functional variants conferred an environment-related advantage, allowing population proliferation, creating haplogroups, that is populations with specific mtDNA haplotypes. However, besides adaptative variants, some maladaptive variants can be shared; or the adaptative variants can become malefic in another environment, by creating metabolic dysfunction. Hence, haplogroups can be adaptative and protective towards the environment or can predispose to disease, altering variant expression (3,8).

Another factor that must be considered is the affected tissue or organ – particularly the tissues that need higher levels of energy to perform, such as skeletal muscle or the brain (3,9). Pathogenic sequence variants in mtDNA are more noticeable in those tissues considering that they are usually accompanied by a depletion of ATP; this drop in energy production can be sustained by the cells that do not need much ATP to start with, but it will be critical in high energy demanding tissues, by disorder appearing first in these tissues or by being the most affected. Henceforth, mitochondrial disorders affect certain organs and tissues preferentially, according to their energy requirements (3,6,9). However, despite these hypotheses, and the specificities of disease mechanisms, the tissue specificity of mitochondrial cytopathies (MC) remains a mystery – why are not all high-demand tissues equally affected? More, why are only some, if not only one, affected?

Mitochondria regulate many cellular processes: oxidative phosphorylation (OXPHOS), production of ROS, regulation of cellular reduction-oxidation (REDOX) status, regulation of cellular Ca^{2+} concentration, control of cell death by activation of the mitochondrial permeability transition pore (mtPTP), and production of high energy intermediates that modulate cytosolic signal transduction or nuclear epigenomic pathways (2,3,8).

Mitochondria produce energy in the form of ATP, through the biochemical process known as OXPHOS. This process occurs at the mitochondrial respiratory chain (MRC), which locates at the inner mitochondrial membrane (IMM) (1–3). The MRC (Figure 1) includes 5 multi-enzymatic complexes: Complex I (or NADH dehydrogenase), Complex II (or succinate dehydrogenase), Complex III (coenzyme Q- cytochrome-c reductase), Complex IV (or cytochrome c oxidase), and Complex V (or ATP synthase or ATPase). Additionally, it has two intermediary transporters (Coenzyme Q10 (CoQ10)/ubiquinone and cytochrome-c) (3,6).

ATP synthesis' mechanism is based on the chemiosmotic theory proposed by Peter Mitchell in 1961 (10), stating that it is the ion concentration differences between the

mitochondrial matrix and intermediate space that drive ATP production at the MRC (1,3). Electrons are transferred from reducing equivalents (NADH, $FADH_2$) through complexes and transporters (CoQ10, iron-sulfur centers, cytochromes) to O_2, the final acceptor. This series of REDOX reactions create energy that is used towards a proton gradient (out of the mitochondria) and this combination creates a chemiosmotic gradient. The protons leave through the MCR complexes I, III and IV to the intermembrane space. The proton chemical gradient dissipates through complex V to the mitochondrial matrix. The gradient's energy allows ATP synthesis by ADP phosphorylation (1,6). If dysfunction happens in OXPHOS, and electrons leak to form free-radicals, by combining with O_2 molecules, forming ROS, which can lead to mitochondrial and cell damage and apoptosis, causing disease (3).

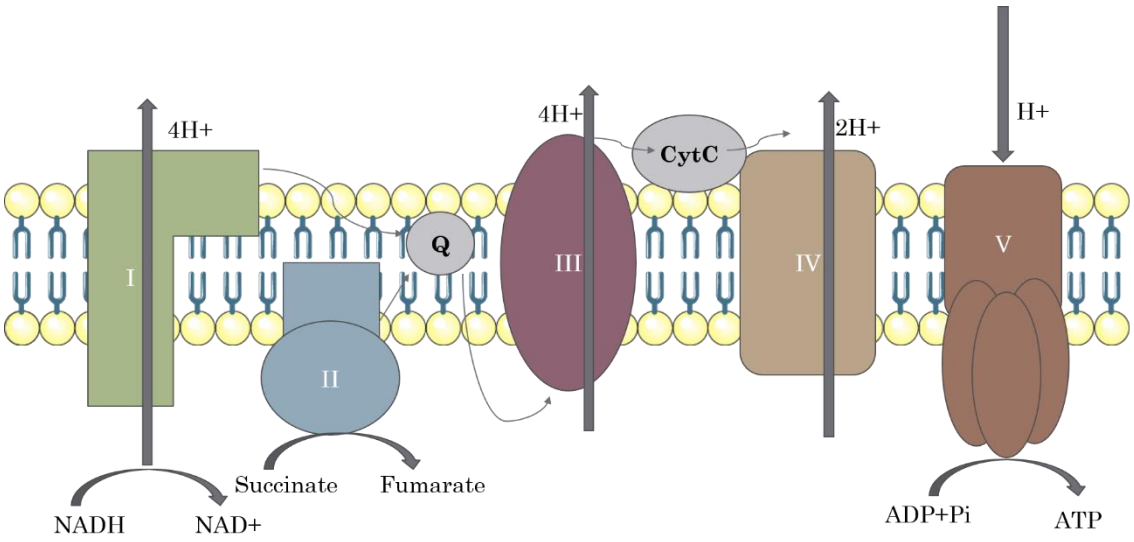

Figure 1. *Schematic representation of the MRC.*

One of the main roles of mitochondria, apart from producing ATP, is in apoptosis. They participate in the mitochondria-dependent or intrinsic apoptotic pathway, which is induced by DNA damage, binding of nuclear receptors by glucocorticoids, heat, radiation, nutrient deprivation, viral infection, hypoxia, and increased intracellular calcium concentration (11).

Apoptosis' morphological characteristics include chromatid condensation, DNA fragmentation, the nuclear membrane's disappearance, bleb formation (cytoplasmatic projections) and cell fragmentation into apoptotic bodies, which are degraded after phagocytosis (2). Apoptosis allows for elimination of unnecessary, damaged and malicious cells, and for regulation and repair of DNA damage, amongst control of other genomic, cell and molecular issues (7). Diminished apoptotic activity may lead to cancer, however over-apoptosis can lead to a variety of pathogenic situations, such as those found in Mitochondrial Disorders (MDs) (11).

Changes in the outer mitochondrial membrane lead to formation of pores and subsequent loss of membrane potential, releasing several factors from the intermembrane mitochondrial space to the cytosol. These lesions allow the transmission

of apoptotic signals. The signals are regulated by the BCL-2 family, with Bim, Bad, Bid, Bax, Bak and Smac/DIABLO being pro-apoptotic, and Bcl-2 and Bcl-X_L being anti-apoptotic molecules (2,7).

The apoptotic pathway starts when Bax forms homo-dimers in the presence of apoptotic signals, increasing membrane permeability and opening a channel that translocates cytochrome-c (a pro-apoptotic molecule) from the intermembrane space to the cytoplasm. The Bcl-2 interferes with Bax's function by forming a heterodimer with Bax, thus closing the channel and inhibiting cytochrome-c translocation. In the cytosol, cytochrome-c binds to Apaf-1 to form the apoptosome, which, in turn, recruits procaspase 9 and activates it to caspase 9, which will then activate executioner caspases 3, 6 and 7 (2,11).

1.1.1. Mitochondrial Cytopathies

The MCs are a set of diseases caused by a disturbance in OXPHOS (9). Efficiency of the MRC at electron transport for ATP production is a must for the organism's energetic equilibrium, ergo, mitochondrial dysfunction can result in serious damage to the individual. Although consensus has not yet been achieved, a threshold value below 40% of the mean control value normalized for citrate synthase activity seems a very good criterion to define a MRC deficiency (6).

MCs can be subdivided in three categories: i) primary mitochondrial disorders caused by variants in mitochondrial genes, ii) disorders with variants in nuclear genes involved in mitochondrial function, and iii) disorders that arise from issues in bigenomic interaction (12–15). Furthermore, considering other mitochondrial disorders, there are also secondary disorders that may arise from accumulation of mitochondrial damage over time, frequently involving neurodegenerative pathologies (16).

These diseases show clinical heterogeneity, reflecting the genetic complexity involved in these phenotypes. Firstly, they can be inherited from the maternal line, be sporadic, or have a Mendelian inheritance pattern. In addition, we can distinguish between genetic alterations directly affecting the MRC complexes and affecting intergenomic communication, causing mtDNA change. Furthermore, even when/if inherited, family members may not be affected or affected in a different way. The mtDNA has a different replication process from nDNA: i) mtDNA has continuous replication, leading to heteroplasmy levels changing in non-dividing tissues, if the variant and wild-type mtDNA have different replication rates, contributing to late onset of symptoms; and ii) mitochondria do not divide equally during division, resulting in non-uniform distribution of mutated mtDNA, with different levels of mutation between tissues or within the same tissue (9).

The MCs are multisystemic disorders and because they are so closely related with MRC damage, different tissues may be differently affected - the ones that require higher levels of energy suffer the most. Hence, there are different heteroplasmy thresholds effects for different cell types, with higher energy demand tissues showing a lower threshold. However, a heteroplasmic cell can maintain MRC functions if there is enough normal mtDNA to compensate the mutated mtDNA's effects (9).

1.2. Disorders investigated

The presented work is focused in two different disorders: Leber's Hereditary Optic Neuropathy (LHON) and Mitochondrial non-syndromic hearing loss and deafness (MNSHL). Albeit the different consequences and different pathologies/ clinical symptoms associated, the underlying problem for both is mutated mtDNA, with each one presenting three main mtDNA pathogenic sequence variants. Both conditions are related to loss of function in very high metabolism tissues: the cochlea and the optic nerve, that are linked to hearing and vision loss, respectively.

Next, the two disorders are presented, highlighting the etiopathogenicity and underlying mechanism, the epidemiology and prevention/therapy opportunities.

1.2.1. Leber's Hereditary Optic Neuropathy (LHON)

LHON was first described in 1871 by ophthalmologist Theodore Leber, and determined a MD in 1988 by Wallace (17), with the discovery of the first point mutation in mtDNA (m.11778G>A) (18,19). It is characterized by three main primary pathogenic sequence variants, which represent 90-95% of LHON cases: m.3460G>A, in the ND1 subunit gene; m.11778G>A, in the ND4 subunit gene; and m.14484T>C, in the ND6 subunit gene. All of these subunits belong to the complex I (CI) of the MRC (19). The m.11778G>A is the most prevalent in the populations of Europe, Far East Asia and Australia, with m.14484T>C having a reported founder effect in French Canada (20). The remaining cases are involved with other rarer variants; so far, LHON has been associated with 50 variants, in different ethnic populations (21).

1.2.1.1. Epidemiology

The prevalence of optic neuropathies is of 1/10,000 (20,22,23), with MDs having an incidence of 1/5,000 to 1/4,300 (8,20,24). The prevalence and incidence of variants and disease also vary according to population. While in the Netherlands incidence of LHON is 1/39,000 and in Finland 1/50,000 (19,20,25), in northeast UK there are reports of 1/31,000 (20,25) to 1/25,000 (19), with some places in Europe reporting 1/20,000 (26). However, 1/200 cord blood analysis show one of the ten most common mtDNA variants associated to LHON (8) and, in the UK, 1/350 neonates show one of the three primary LHON pathogenic sequence variants (20); according to literature, 1/8,500 of the general population carries a LHON pathogenic sequence variant (27). The overall populations' numbers vary between 1/40,000-50,000 (27) to 1/35,000-30,000 (23,28) for LHON incidence, with estimation of 1/14,000 in men (23).

1.2.1.2. Pathology

LHON presents as acute or sub-acute form and the visual acuity usually becomes 20/200 or worse, ranging from slightly subnormal to light perception (25,27). The visual loss in LHON is usually painless, with rare occasions of inflammation of the optic nerve causing

discomfort. Often, one eye is affected first with the second getting involved after within a few (six to eight) weeks to (six) months. Within 1 year, 97% of patients with vision loss in one eye develop blindness in the second eye (27). Afterwards, visual loss stabilizes, with either remaining permanent or with the patient experiencing spontaneous recovery (27). The resulting bilateral loss of vision causes significant to total blindness, perhaps reversible, with certain pathogenic sequence variants having higher recovery chances than others (19,25).

The symptoms are more prevalent in male carriers than female carriers, although maternally related; about 50% of male carriers develop LHON, while only 10% of female carriers are affected. The disease usually develops between the second and third decade of life (15-35 years old), and vision loss after 50 years old is very rare. The age-of-onset may also predict prognosis and recovery chances, with better probabilities for younger age (19,25,27,29). For homoplasmic LHON pathogenic variants, the penetrance of acute onset central scotoma is very variable, shifting according to pedigree. Furthermore, maternal relatives may show signs of visual impairment even if not progressing to subacute atrophy (8), or by possible structural plastic reorganization of the human visual cortex (30).

The disease can affect both eyes simultaneously (25%) or sequentially (75%), with vision deterioration being acute in both cases, and with retinal vascular engorgement, deformation of the optic nerve and edema of the retina. The underlying problem is mitochondrial dysfunction, which leads to cell death, particularly of neurons called retinal ganglion cells (RGCs) (19) (Figure 2).

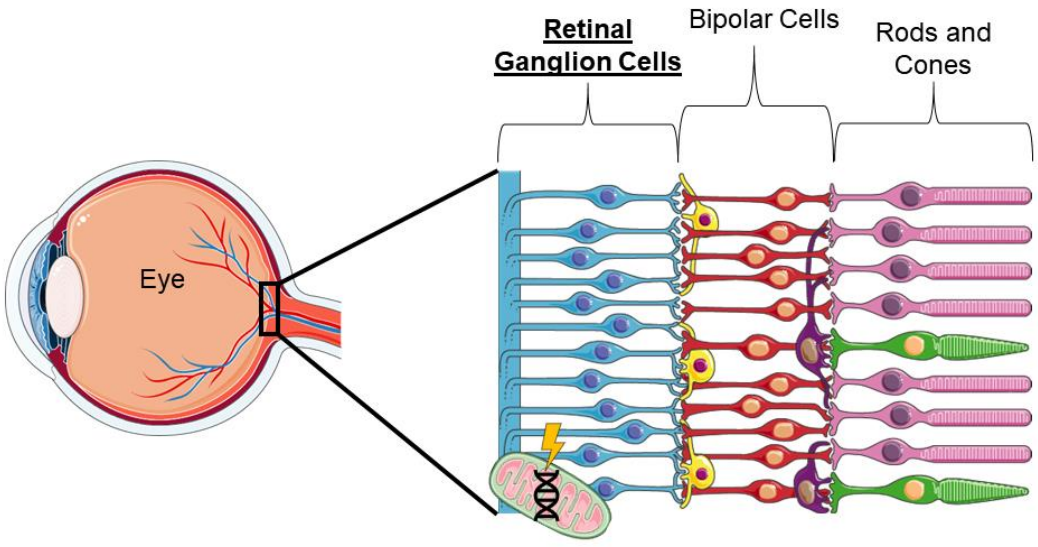

Figure 2. *Schematic representation of the structure of the inner retina.*

In classic clinical disclosures there is involvement of (mainly) the optic nerve, peripapillary telangiectatic blood vessels, vascular tortuosity, decreased visual acuity, dyschromatopsia and central scotomas (27). Dyschromatopsia appears early in disease

progression and visual field defects are central or cecocentral. Other features associated include swelling of the retinal nerve fiber layer (RNFL) around the optic disc (pseudoedema), hyperemia of the optic nerve head, circumpapillary telangiectasia, absence of disc leakage and engorged retinal vessels. Atypical findings are retinal and optic nerve hemorrhages, exudates, and retinal striations. In the chronic phase, the disc hyperemia, peripapillary telangiectasias, and pseudoedema resolve, with improvement of retinal vessels by the RNFL swelling subsiding (31), but appearing of optic nerve pallor (25,27).

The RGCs' death leads to a central scotoma, pseudoedema and RNFL loss, with the first of these enlarging into a larger central defect. The RNFL thickens with axonal swelling from impaired mitochondrial function and axonal transport. However, the retinal structure remains preserved (8,25,28). There is also optic disc pallor and cupping of the optic disc with RGCs' death (19).

In the chronic stage, both RNFL and macula become thinner. Here, only a thin covering of myelin is found in the remaining neurons, with demyelinating plaques within the brain's white matter and optic nerves, and marked vacuolation and cystic necrosis throughout the central nervous system (8,25,28). The optic nerve's blood-brain barrier is disrupted due to optic nerve degeneration and RGC loss (19).

Additionally, LHON can present as LHON plus, in which the phenotype includes impairment of other tissues, resulting in affected cardiac conduction, dystonia, movement disorders, brain lesions, encephalopathy episodes, and brainstem syndromes (28,32).

1.2.1.3. Genetic causes

LHON pathogenic sequence variants are usually homoplasmic, with 10-15% being heteroplasmic (19). LHON's variants that present milder phenotypes (m.11778G>A, m.14484T>C) are usually homoplasmic. The pathogenic sequence variants presenting severe phenotypes (m.3460G>A) cause atrophy when heteroplasmic and grimmer phenotypes when homoplasmic. Moreover, variants of higher severity are less frequent in the population. The milder variants are strongly affected by the haplogroup, which clarifies the highly variable frequencies of these pathogenic sequence variants between different populations (8).

The variants discussed in this work are located in genes that encode for CI (NADH dehydrogenase) subunits. The mtDNA genetic alteration results in a biochemical effect exerted there, and this dysfunction leads to impairment in the MRC, ultimately ending in ATP depletion and increase of ROS with subsequent oxidative stress.

In the case of m.3460G>A, it is located in *MTND1*, the *NADH ubiquinone oxireductase core subunit 1*, which forms the NADH dehydrogenase 1 protein. The nucleotide change leads to an amino acid change (from alanine to threonine). This pathogenic sequence variant reduces activity of the complex by 60-80% by "reducing the rotenone-sensitive and ubiquinone-dependent activity" (29) of MRC. Rotenone has been shown to be associated with the thinning of ganglion cell layers, nerve fibers and the inner plexiform layer, and to the loss of RGCs (29). This variant is the most severe, and the least frequent

of the TOP-3 trio. In European populations, there are frequencies of 22.6%, being lower in Chinese populations, with 1.1% (19).

The m.11778G>A is in *MTND4*, which produces the protein NADH hydrogenase 4, and occurs in 70% of LHON patients, with an incidence of 90% in Far East Asia countries (19,29), and 56.6% in Europe (19). Additionally, a founder effect of this variant in Brazil, from an Italian immigrant family, has been reported (19). There is an amino acid change (arginine to histidine), which modifies the polypeptide structure and alters its function. Variations in *MTND4* gene are associated with many other diseases involving mitochondria, such as Leigh syndrome, cardiomyopathy, MELAS, Parkinson's disease (PD), sporadic myopathy, acute myeloid leukemia and gastric, oral, blood and breast cancers; in addition, LHON female patients with *MTND4* pathogenic sequence variant can also show symptoms of Multiple Sclerosis (29). This pathogenic sequence variant seems to be the best contestant for gene therapy and some other therapies, as discussed later.

Finally, the m.14484T>C locates in *MTND6* (NADH hydrogenase 6 protein), and is the most frequent variant found in LHON, usually homoplasmic and the mildest one (19), with low penetrance. This pathogenic sequence variant presents a well-documented founder effect in French Canada. It creates a methionine to valine change; henceforth, CI becomes more sensitive to inhibitors that bind to the ubiquinone site (33,34), which results in affected neuronal activity. The frequency was reported as 24% in China by Manickam *et al.* (2017), but as 8.7% in the same population by Bi *et al*. (2016), who further report 20.8% as the frequency for European populations (19,29). Unlike the previous two genetic variants presented, this variant has been associated with epigenetic factors. The m.14484T>C is the best-case-scenario pathogenic sequence variant: usually associated with high-visual recovery, not only spontaneously but also in the context of novel therapies. Other diseases are also associated with *MTND6* alterations: autism, Leigh syndrome and cancer (29).

1.2.1.4. Biochemical Mechanism

The optic nerve consists of the projected axons from about 1.2 million RGCs, which are placed in the inner retina and are particularly susceptible to mitochondrial dysfunction in optic neuropathies, like LHON, having high energy consumption and low mitochondrial support (19).

The RGCs have i) high metabolic needs created by the characteristic spike activity, ii) near-constant exposure to light, which can induce cell damage, increasing exposure to glutamate and other cytotoxic compounds (28), iii) the sharp 90-degree bend of the axons at the *lamina cribrosa sclerae*, and, iv) mainly, the relatively long unmyelinated intraocular portion (which require a higher density of mitochondria to maintain efficient electrical potential and signal conduction). Due to those requirements, neuronal mitochondria: i) cluster at synapses so they can deliver sufficient ATP, ii) need to balance the fusion-fission process with the fluctuating bioenergetic demands, and iii) need to oversee the bidirectional transport along the dendrites and axons (19).

The rapid loss of RGCs in the acute phase of LHON is due to apoptosis, with early and preferential RGC loss in the Papillomacular Bundle (PMB). This happens due to the high

energy demand of the unmyelinated portion and the small axonal caliber (decreasing energy conduction, from greater surface area/volume ratio) of the PMB. These energy requirements, along with low energy production and slow axoplasmic transport, make the PMB susceptible to mitochondrial dysfunction (25,27,28,35,36). Spontaneous recovery of vision may be secondary to acutely dysfunctional RGCs, which possibly remain viable and can later achieve recovery (26).

Pathogenic sequence variants associate with a significant decrease of CI activity, respiratory rate and ATP levels, leading to a cascade of cell events: i) oxidative stress by OXPHOS dysfunction, ii) mitochondrial damage, iii) overload of mitophagy, iv) decrease of mitochondrial mass, v) inadequate ATP production and increased ROS, vi) apoptosis of RGCs in LHON (19,28).

One of the pathways that predispose to apoptosis starts with partial CI respiration defects, which reduce ATP production and impair excitatory glutamate transport. This leads to oxidative stress, thus increasing mitochondrial ROS production and predisposing the mtPTP to cascade into apoptosis of RGCs (8), resulting in the characteristic vision loss occurring in LHON. On the other hand, impairment in ATP production, problems in OXPHOS and mitochondrial ROS accumulation trigger a decrease in electrical potential, causing cytochrome-c leakage, which binds to Apaf-1, starting apoptosis of RGC (8,29,35).

Mitochondrial dysfunction also impairs calcium flow between organelles, hence, the crosstalk of endoplasmic reticulum (ER)-mitochondria. The mitochondrial-associated ER membrane (MAM) interface is compromised, as is mtDNA maintenance and mitophagy, affecting the RGC survival (19).

The involvement of the PMB leads to a cecocentral scotoma, with pupil‘s light reflexes staying intact due to melanopsin-containing RGCs’ survival, which are more resistant to metabolic impairment (19). These neurons are an evolutionary-ancient RGC subtype, that express the photopigment melanopsin, being highly specialized circadian-photoreceptors. Their preservation in LHON explains the maintenance of the pupillary light reflex even in patients with severe visual impairment, due to their relatively resistance to mitochondrial dysfunction (25,28).

1.2.1.5. Modifying Factors

The heterogeneity of clinical symptoms and thus “penetrance” of LHON comes from the many modifying factors’ impact on phenotype (Figure 3); haplogroup, other nuclear and/or mitochondrial variants, gender bias and many environmental factors have all been associated with and explain the variable “penetrance” and phenotypical expression of the disease. In addition, a heteroplasmy threshold of 60% has been proposed to associate with disease probability, that is, in heteroplasmy, when mutated copies are <60%, there is a lower probability of LHON. However, the effect may be modulated by the individual’s nuclear genome (19).

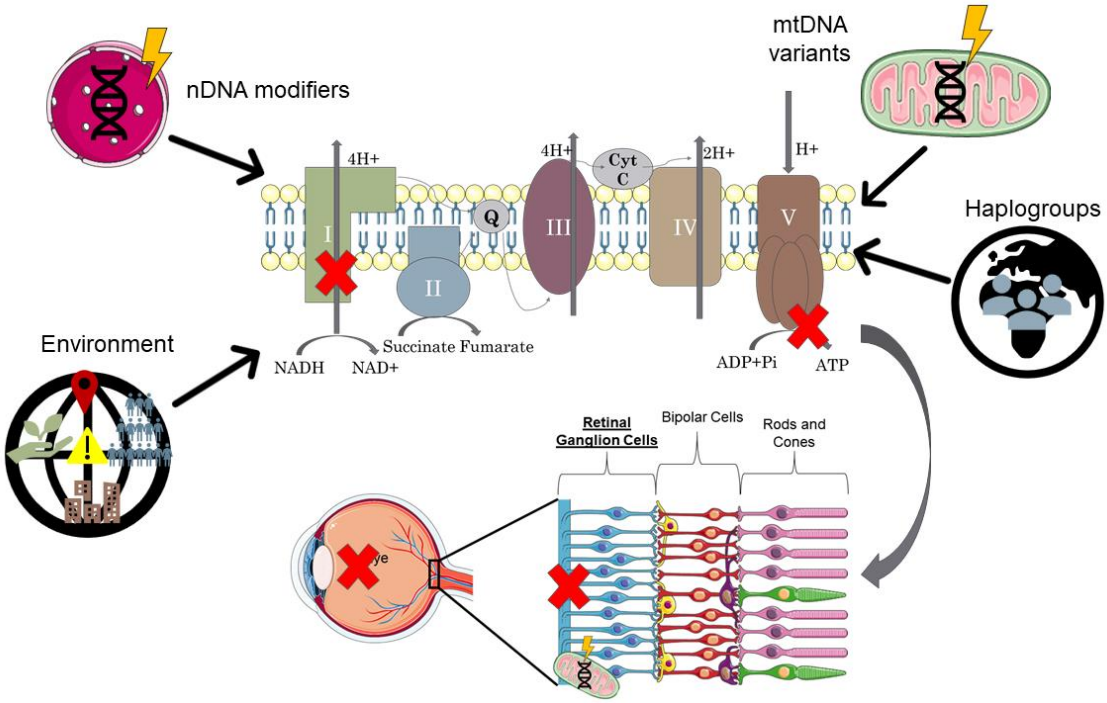

Figure 3. *Modifying factors for LHON.*

1.2.1.5.1. Genetic and Anatomical Modifiers

The mitochondrial haplotypes may influence disease due to benign sequence variants (commonly known as polymorphisms) that might act in synergy with LHON pathogenic sequence variants, by affecting complexes I and III (19,26,37). The role of the same variant may change drastically, considering different combinations of benign sequence variants, individual variants and the co-existing variants, and wherein (i.e. pathway) these act. The combination can lead to a protective or triggering effect, modulating disease expression and "penetrance", and changing the clinical phenotype (19,26,37). Haplogroup J was shown to increase "penetrance" of LHON in Caucasian/European populations, with m.11778G>A and m.14484T>C variants, particularly the J1c and J2b haplogroups (18,19,25,26,37). Haplogroup J, as well as haplogroup W, have both been shown to increase LHON risk in Iranian populations (19). Nonetheless, haplogroup J has been associated with a protective effect in aging, Parkinson Disease (PD), and lower cardiovascular risk (19,26). The "opposite" effect of haplogroup J for increasing risk of LHON and lowering it for the other disorders, comes from the uncoupling the mitochondria (26) and consequent biochemical effects. For m.3460G>A, haplogroup K increases "penetrance" (25,26). Haplogroup H3h has been associated to synergistic affect the pathogenic sequence variants (19). Haplogroup H and H8a have been shown to be protective for LHON (19,26). In Asian populations, haplogroup M7b1'2 increases "penetrance" with m.11778G>A, and for the same variant, haplogroup M8a decreases LHON risk (19,25).

In respect to the nuclear genome, both *TP53* and *EPHX1* have been associated with LHON, particularly regarding variability in age-of-onset (19,37). The chromosome region 3q26.2-3q28, in which genes *PARL* and *OPA1*, both involved in other optic neuropathies, are encoded, has also been associated with LHON (19).

These combinations of pathogenic sequence variants with other mtDNA or nDNA variants, tend to enhance “penetrance”, but without worsening or changing the phenotype (26). Despite this tendency, this is not always the case, as stated above.

The anatomy of the optic nerve conformation should also been considered, since that small optic discs with high fiber concentration are associated with disease (37).

Research to explain gender bias has focused on X-chromosome linkage and hormonal differences. While X-linkage studies have mostly landed flat (18,26,37), hormonal action seems a good candidate for gender bias’s cause. Estrogens were demonstrated to have a protective effect against mitochondrial dysfunction and disease, by activating mitochondrial biogenesis and creating a compensatory effect (18,25,37). The increase in biogenesis and its marker, mtDNA copy number, lessen dysfunction and their interaction with mitochondrial dysfunction modulates “penetrance” (37). Furthermore, it was shown that 17β-estradiol led to biogenesis activation, increased SOD2 activity, decreased ROS and ultimately, reduced apoptosis; the estrogen β-receptor is very abundant in RGCs and their RNFL neurons (25). Additionally, when “penetrance” is reduced, only males stay affected, since “penetrance” variability follows the same gender ratio within the same LHON pedigree (18).

As previously mentioned, another factor for LHON’s variable “penetrance” is the observation that unaffected carriers have higher mtDNA copy numbers, higher mitochondrial mass and can activate mitochondrial biogenesis according to the metabolic needs, and this increased biogenesis may be able to overcome the variants’ pathogenicity (37). The correlation between unaffected carriers presenting higher levels of mtDNA and affected individuals having lower amounts of mtDNA has been described (19,37).

1.2.1.5.2. Environmental Modifiers

Many environmental factors have been associated with LHON. Smoking, as well as alcohol, have both been significantly associated with LHON expression. Besides worsening symptoms in more susceptible individuals, they can lead to disease expression in patients that could have been unaffected carriers, albeit these develop the pathology quite later in life than usual (over 35-40 years old) (37). Cigarette smoke conflicts with biogenesis, reducing mtDNA copy number (37), and allowing the mitochondrial dysfunction’s effect to increase “penetrance”.

Many medications have been associated with LHON: antidepressants, anticonvulsants, anxiety medications, antipsychotics, barbiturates, cholesterol reduction drugs, inflammatory/analgesic medications, anti-arrhythmic medications, β-blockers, antivirals, chemotherapeutics and sugar lowering substances (35,38).

Nutritional deficiencies are another main environmental modifier with low levels of vitamins B_1, B_2, B_6, B_9 and B_{12} associating with disease (25,35).

Additional environmental factors include head trauma or other physical injury (18,25,26), industrial toxins or infection/exposure to toxic factors (25,26), psychological stress (26) or non-controlled diabetes (18).

1.2.1.6. Prevention and Therapy

1.2.1.6.1. Prevention and Classic symptom management

Prevention and management comes in the forms of baseline vision testing and genetic analysis to rule out the disease, with follow-ups every 4-6 weeks (35). Some drugs, which will be discussed next, could be used in LHON patients with identified pathogenic mtDNA sequence variants or carriers in risk of developing the disease as a prevention strategy, mostly in a combined therapy-prevention manner and in cases of loss of vision in one eye (39).

Classic treatments are based on symptomatic and supportive treatments, namely low vision aids and rehabilitation, as well as occupational therapy, psychological support and knowledge, and avoiding (environmental) risk factors and toxins (23,25,27,28,35). Genetical counseling is also recommended for family members, as well as prenatal testing (23,28,29,35).

1.2.1.6.2. Nutritional and Pharmacological Treatments

Vitamins (E, C (22), B_2, B_{12} (19), B_3, B_5, B_7, B_9 (24)), minerals, and co-factors such as α-lipoic acid, L-carnitine, creatine, L-arginine, thiamine, menadiol, dichloroacetate, cyclosporine, minocycline and cysteine (22,24,25,27) can be used as supplements to prevent or ameliorate and treat symptoms. Exercise and caloric restriction have also been pointed out as possible options, due to neuroprotective effects of these lifestyles choices, related mainly to SIRT3 activation (24).

Furthermore, antioxidants can help against mitochondrial dysfunction, as is the case with Szeto-Schiller peptides (also known as Bendavia/Ocluvia or MTP-131) (24), which act on cardiolipin, thus improving mitochondrial plasticity and enhance electron transport (29,35,40). Other REDOX compounds, like curcumin, methylene blue, RP103 and exogenous glutathione (24,40) can also be used for the same purpose. Moreover, antiapoptotic compounds can combat mitochondrial dysfunction – corticosteroids and cyclosporine A are immunosuppressants, and the latter is also a mtPTP modifier (23,27,40); brimonidine purite, an α-2 agonist, inhibits excitotoxicity induced by glutamate transport, by favoring uptake from the synaptic cleft (8,24,25,27). Mitophagy can be targeted with rapamycin, which ameliorates mitochondrial dysfunction (24).

Drugs that would act on mitochondrial biogenesis and mtDNA levels are under research (39) – bezafibrate, rosiglitazone, estrogen-like molecules, AICAR, ALCAR, fenofibrate, thiazolidinediones, pioglitazone, activators of the PPAR-PGC1α axis, agonists of AMPK, resveratrol, metformin, agonists of Nrf2, triterpenoids and *Bacopa monnieri*, or triggering factors of SIRT1, SRT1720, quercetin, and isoflavone-derived compounds (19,22–25,40). Estrogens/estradiol are of particular interest due to the gender bias observed in LHON (8,24,39).

Therapeutic photobiomodulation or far-red/ near-infrared therapy (18,40) would increase complex IV activity and ATP production. The use of growth-promoting compounds for neuronal regeneration (18) has also been considered.

Research work frequently looks into using ubiquinone analogues for compensatory therapy, in which the electrons would be transported directly to complex II, bypassing CI dysfunction (18,19,22,25). The analogues studied are Coenzyme Q10 (CoQ10), idebenone and EPI-743 (18,23,24,27–29,35,40,41). In literature, idebenone has produced the best results and is now approved for treatment, but EPI-743 may also be of interest (22,24), both having antioxidant activity (19,22). Other analogues – mitoquinone (MitoQ), SkQ-1 and triphenylphosphonium (TPP) – directly target the mitochondria (24,35,40) and have been investigated.

Idebenone is a particularly relevant compound; it is a synthetic shorter-chain analogue of CoQ10 with a less lipophilic side chain than CoQ10 (35,40). Due to these more balanced lipophilic properties, its oral administration is more readily delivered into mitochondria (35), presents rapid uptake by the eye (40) and also enables an easier transfer between cytoplasm and mitochondria (27). Furthermore, it is more potent than CoQ10, presenting antioxidative properties (19,24,40) and reduces ROS production, limiting oxidative cell damage and lipid peroxidation (22). It acts as an electron transporter and, unlike CoQ10, it participates in REDOX reactions outside the mitochondria (40) and acts as an electron transporter directly to the complex III of the MRC, bypassing CI dysfunction and improving ATP generation (19,22,24,40–42). The reactivation of ATP synthesis results from the reactivation of the electron flow by bypass of CI (Figure 4). This activity also induces a metabolic shift away from CI dependent respiration, towards alternative metabolic pathways (24), namely stimulating complex II function and the glycerol-phosphate shuttle (40).

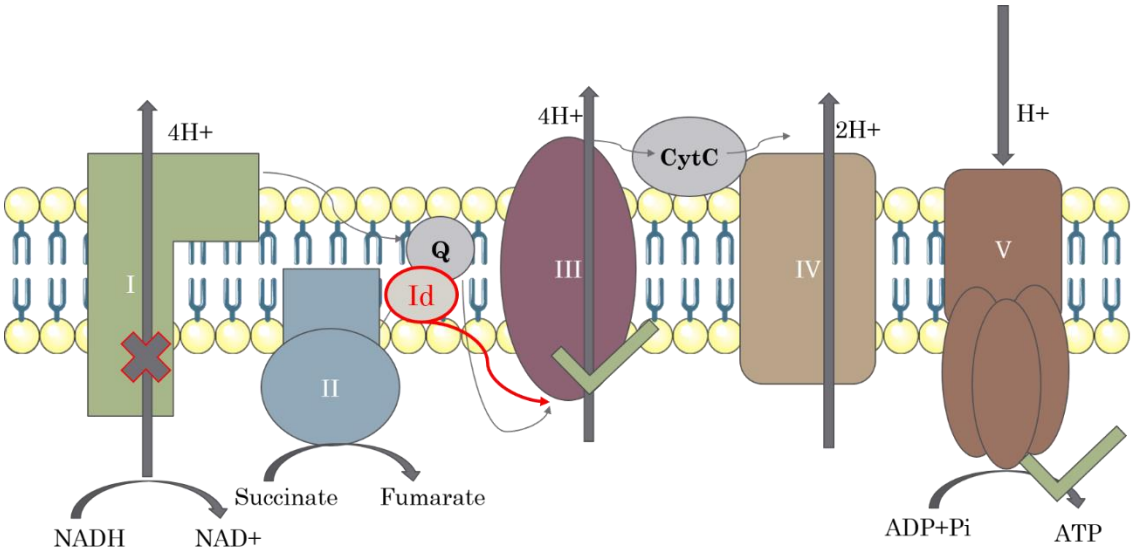

Figure 4. *Schematic representation of the action of idebenone (Id), represented in red, on the MRC.*

Idebenone was approved in September 2015 by the European Medicines Agency (EMA) (24,35,40,41), based on results of human trials conducted in the last decade and lack of adverse reactions in those studies (22,23). In both of the main studies, the biggest take

away is that there is a window of opportunity for treatment: as soon as onset of vision loss happens.

In the randomized trial (43,44), idebenone presented a positive trend away from further vision loss in the group treated with idebenone, seemingly protecting against further vision loss. In the same study, patients with unequal acuity, that is, in earlier stages (acute stage), were more likely to benefit from treatment (22–24,27,35,40). Furthermore, these beneficial effects seemed to prevail and remain stable after discontinuation of idebenone (22,23,35). Models in mice have shown that idebenone may protect against loss of RGCs (19,41).

The retrospective study (45) presented a trend in visual recovery in patients using idebenone. This study was performed with patients with <1 year of onset of disease; results showed a trend in earlier visual recovery for those in treatment than those untreated. Results showed a significant delay in involvement of the second eye, but after involvement of both there was no significant difference to overall visual outcome between groups. Earlier start of treatment (discordant visual acuity) and longer therapy duration were predictive factors for vision recovery (22–24,27,35). The patients presenting the highest and best recovery were those affected with m.11778G>A (23,27,35); the patients affected with m.3460G>A presented worse responses (35).

This analogue can be administered alone or in combination with supplements, being possible that its administration with vitamins C and B_2 (46) accelerates onset of visual recovery (19,24,27). Improved color vision from idebenone administration has also been reported (24,41).

1.2.1.6.3. Gene Therapies

Gene therapy attempts to restore mutation by inactivating the gene in question, replacing it with a WT copy, or introducing a new gene to counteract and prevent disease (24,29).

Some challenges need to be accounted for: i) the therapeutic agent needs to be capable of bypassing blood-brain barrier for achieving a high enough drug concentration, ii) there is a limited therapeutic window (massive early loss of RGCs), iii) limited availability of sensitive optic nerve biomarkers and iv) limited financial resources. Furthermore, v) the double membrane of the mitochondria (25), and particularly the inner mitochondrial membrane (IMM), is impermeable and requires a highly efficient vector to transfect enough therapeutic agent per mitochondria per cell in order to restore function (22,23). Thus, gene insertion would prove difficult (29), but some methods have been designed to bypass this difficulty.

The eye is a good tissue for gene therapy since it is an accessible organ for direct surgical interventions (particularly the RGC layer (25)), and it benefits from relative immune privilege (28), making LHON an excellent candidate. Furthermore, since it is the easiest organ to submit to the procedure, it would have a higher success chance.

Gene therapy in LHON aims i) to increase respiratory activity and ATP synthesis, ii) to stop excessive ROS accumulation, and iii) to diminish/inhibit the apoptotic cascade (18). All three of these goals should be implemented at disease onset (when only one eye is

affected), taking advantage of the window of opportunity before the second eye loses vision (18).

One model was prepared with transfection of cells with *Saccharomyces cerevisiae*'s gene, with viral transduction delivery of a single polypeptide of CI of *S. cerevisiae* into the optic layer. This restored mitochondrial activity by gene integration in the nuclear genome, protein expression and transport to mitochondria, where it is incorporated in the mitochondrial machinery assembly (8,18). This therapy would bypass the CI mutation and/or reduce ROS toxicity (8).

Administration of adeno-associated virus (AAV) vector-mediated gene therapy may vary. It can involve both gene replacement and gene addition approaches, the retinal injection can be performed in different sites and the promoter, doses, volumes and administration frequency all shift. This would deliver a gene product into the affected retina, restoring function (16,22,25,29,40,47).

Allotropic expression is a very promising model, with reported positive results concerning *MTND4* gene (16,22,25,35). Here, a mtDNA gene is recoded and engineered to be introduced into nDNA, adding nuclear gene expression elements and a mitochondrial targeting peptide (8). When expressed, the gene creates a WT cytoplasmic-translated protein, which is targeted to mitochondria and assembled into IMM, where it competes with the mutant copy, thus restoring function (23,27–29,35). Once the protein is present at the MRC, it salvages OXPHOS efficiency by rescuing function of complex I or V (47). This method does not fully repair the mtDNA damage, but it shifts it below the pathogenic threshold, due to the competition of the new proteins with the mutated ones (18,47).

This insertion happens with the help of an AAV vector via intra-vitreous injection (18,41), and, for import and translocation, a mitochondrial targeting signal (MTS) is added to the nucleotide sequence (22,25,27,41,47). The AAV vector is the most appropriated for allotropic expression, since it can penetrate the nuclear membrane (41).

Specifically for LHON, the plasmid with the transducing virus and normal gene is injected into the vitreous of the eye, entering mitochondria of the RGCs; the plasmid is then uncoated, with translation of gene, restoring the defect and curing disease (8). Function restoration is seen with mitochondrial biogenesis increase and rescue of RGCs, improving visual function (23,40). This can be optimized by targeting mRNAs to the mitochondrial surface, coupling translation and translocation (47).

Besides the expression of *MTND4*, the overexpression of *SOD2* has also been demonstrated when packaged with AAV vector, *SOD2* contributing to suppress apoptosis and prevent RGC death (25,27,41).

It has been proposed the modification of an AAV construct, in order to carry a gene coding for a product with neuroprotective capacity, enhancing survival of dysfunctional neurons (28).

The above discussed allotropic expression can be called allotropic protein expression (8), since there is also allotropic mRNA expression. The advantage with the latter is that mtDNA-encoded mRNAs are degraded by the cell when found in cytoplasm, so this technique uses natural mechanisms to prevent toxicity, since mRNAs would not accumulate, while in allotropic protein expression, there is accumulation of the cytosolic-

translated mtDNA protein in cytosol, due to it not being degraded, causing toxicity. The disadvantage of this technique is the low uptake of mRNA molecules into mitochondria, but the low levels of heteroplasmy observed could be sufficient to restore function (8).

Direct delivery attempts to deliver the WT gene with an AAV vector directly into the mitochondria (8,40,41), bypassing nucleus, cytoplasm, and the need for a MTS. Here, a modified AAV with a MTS is injected intraocularly (40). Delivery of the entire circular mtDNA directly into mitochondria, named “protofection” (27), showed restoration of respiration and ATP production (35).

Another mechanism for gene therapy in MCs is heteroplasmy shifting (8,16) since phenotypic expression is influenced by mtDNA variant levels. This can be achieved by modulation of mutant/WT mtDNA ratio, targeting mutant copies for degradation, metabolic-induced shifting or, as with gene therapy, delivery of WT mtDNA genomes with AAV vectors (16).

A different type of gene therapy is the prevention of germline transmission, by creating a “three-parent embryo” or “mitochondrial donation”: *in vitro* fertilization of a donor cytoblast with mtDNA in which the parental nuclear DNA is implanted, or transplantation of maternal DNA into the donor oocyte, and then performing IVF (16,23,24,27,28,41). With this, the progeny would carry the parents nDNA, but not the mutant parental mtDNA, having instead the healthy mtDNA of the donor.

1.2.1.6.4. Stem cell Therapy

Recently, stem cell therapy has also been considered for application in LHON, focusing on the importance of optic nerve function in RGCs, by transplantation of RGCs or by generating trophic factors that promote RGC survival (23–25,28,41). The strategies in development are not mutually exclusive and all aim to improve optic nerve function in RGCs (23).

Mesenchymal stem cells (from bone marrow) were studied regarding the production of neurotrophic factors that can promote RGC survival (24,25,41). Since some LHON patients experience spontaneous visual recovery, it follows that some RGCs survive despite the mitochondrial dysfunction and oxidative stress they are submitted to (25). These cells provide paracrine support to damaged RGCs with the release of neurotrophic factors (platelet-derived growth factor) and anti-inflammatory cytokines (24,25). Their neuroprotective effect has been reported in animal models for optic nerve damage and is currently in experimental stage in humans, where it has reported increased RGC survival, improved visual acuity and enlargement of the optic nerve area (24,25).

Embryonic stem cells were in study for cellular transplantation, with some successful results with rod and cone photoreceptors transplantation in humans (24). However, transplantation of RGCs, with their generation and purification, is still in its experimental stages (23–25,41). There have been successful reports from CRISPR-Cas9 gene editing in *in vitro* and *in vivo* models (24,48). Moreover, these transplanted cells would need to correctly migrate and perform all necessary neuronal connections (23–25). This approach can be used for disease modeling, using stem cells to study pathogenesis, and for experimental models that would facilitate validation of therapies for optic

neuropathies, such as LHON (23–25). The induced pluripotent stem cells particularly allow for patient-specific neuronal populations (28), which could help in what concerns the integration/rejection of stem cells by the eye (24).

1.2.1.7. Challenges in LHON management

As said before, LHON affects one eye first and there is a short timeframe until the second eye is involved. As mentioned, there are many prevention and treatment therapies. Regardless of approach, the moment of administration matters in all therapeutics, with best results being obtained when administration happens as soon as initial vision loss in the first eye, with tremendous difference in recovery after loss in the second eye (18,47). The timeframe between vision loss of one eye to the other, is critical for clinical action. However, the variant must also be considered when choosing a therapeutic method, since some methods (such as idebenone and gene therapy) show different results with different pathogenic sequence variants. Thus, it is essential to quickly and reliably scan for genetic alterations, in order to act timely and rescue function. Hence, a diagnostic tool that provides unequivocal results in a fast pace serves a very sought-after purpose. There are other methods available for genetic testing of the disease, but there are limitations associated with them, whether in terms of the time necessary until the final diagnosis or the cost, amongst other factors. The rapid genetic screening of LHON has been referred to as necessary in literature.

1.2.2. Mitochondrial Non-Syndromic Hearing Loss and aminoglycoside-induced deafness

Hearing Loss (HL) can be genetic or non-genetic, and either post-lingual or pre-lingual (49). Several variants have been associated with genetic HL, with different sets of genetic alterations associated with different subcategories. The HL can be categorized into Conductive Hearing Loss and Sensorineural Hearing Loss (SNHL). SNHL can be syndromic (30%) or non-syndromic HL (70%), the latter divided further into non-ototoxic or ototoxic HL (50).

Focusing on ototoxic SNHL, there are three pathogenic sequence variants associated to this type of HL: m.1494C>T, m.1555A>G and m.7445A>G; with both m.1494C>T and m.1555A>G encoded on the *MTRNR1* gene, while m.7445A>G is located in *MTCO1* and is a precursor of *MTTS1*. The *MTRNR1* encodes for the A-spot of the 12S rRNA of mitochondria, being linked with bilateral SNHL at high frequencies but with no apparent vestibular dysfunction. The *MTCO1* gene encodes for the mitochondrial $tRNA^{Ser(UCN)}$, associating with different levels of hearing impairment and variable age-of-onset. According to Jacobs *et al.* (2011), these variants are considered pathogenic due to i) their absence from unaffected families, ii) producing a biochemical phenotype in cell models and iii) the demonstration of effects on mitochondrial protein synthesis (51).

1.2.2.1. Pathology

Matrilineal relatives with a primary pathogenic sequence variant show variable "penetrance", severity and age-of-onset (usually from 5 to 30 years old) of HL, presenting itself alongside other symptoms. However, there are some common features of matrilineal HL/SNHL: bilateral, sensorineural HL with loss of high frequencies and no apparent vestibular dysfunction (49). The HL may arise from damage to ear tissues (i.e. ototoxicity), which disrupt sound transmission after the cochlea. This matrilineal HL will be referred as the Mitochondrial Non-syndromic Hearing Loss (MNSHL).

The cochlear and vestibular apparatus tissues present a high metabolism rate and require high levels of ATP. Thus, as aforementioned, facing severe consequences when affected by mtDNA pathogenic sequence variants. Mitochondria are primary targets in cochlear dysfunction induced by noise, age or ototoxic drugs, through calcium dysregulation, mtDNA deletions and targeting of the mitochondrial ribosomes (52).

All these pathogenic sequence variants are usually present in homoplasmy; therefore, this disease presents a high threshold for pathogenicity (50,53). Moreover, a strong correlation between degree of heteroplasmy and phenotype has been drawn, for both Asian and Spanish/European populations (54). In addition, homo/heteroplasmy levels seem to be associated with the maternal inheritance: above threshold levels in the mother, higher mutant levels or homoplasmy arise in offspring, while below threshold levels influences the offspring to have lowered, close to normal, variant load (54).

1.2.2.2. Epidemiology

The incidence of ototoxicity is reported to be 2-45% in adults and 0-2% in infants (55,56). Meanwhile, prevalence of HL is of 3% in Japan and 0.5-2.4% in Europe (57).

The frequency of genetic variants is complex, varying according to the combination of pathogenic variant and population, and values fluctuate in literature, mainly due to the combination of factors like variant, HL type, aminoglycosides' antibiotics (AmAn) administration and other environmental modifiers, as well as familial mitochondrial or nuclear genetic variants. For example, HL "penetrance" varied from 3.2% to 62.5% when AmAn-induced HL was included, creating an average of 29.5% of HL incidence; when AmAn was excluded the "penetrance" varied 0-50%, averaging at 17.6% (58). In another study, the frequency of patients with m.1555A>G ranged from 0-47.8% (avg 17.6%) in a Chinese pedigree; while in an Arab-Israeli family and Spanish population it was, respectively, 65.4% and 54.1%. With m.1494C>T, values with inclusion of AmAn were 31.7% and of 17.5% with exclusion. Moreover, in Chinese families age-of-onset was 5 to 30 years, while in Spanish families it was 1-65 years (58).

The *MTRNR1* pathogenic sequence variants (m.1555A>G and m.1494C>T) account for more than 17% of MNSHL cases. The m.1494C>T pathogenic sequence variant presents much lower frequencies and seems to be limited to Chinese and Spanish populations (49). For m.1555A>G, the most frequent pathogenic sequence variant, an incidence of 33% was reported in Japan, 13-5% in China and 17% in Caucasian (USA

and Spain) cohorts. In SNHL, m.1555A>G has an incidence of 0.3-2.5% in Caucasian populations, and 0.9-5.3% in Asian populations (49). Europeans show 0.5-5%, while Spanish cohorts specifically show frequencies of 15-20% (59). Some reports present frequencies as high as 25%, in Spain, compared with 7.5% of UK or 4.2% in Italy (51). In Asian populations, m.1555A>G has been reported with frequencies of 3% in Japan, 5.3% in Indonesia, 2.9% in Chinese populations and 8.35% in Northern Chinese populations.

1.2.2.3. Genetic Causes and Aminoglycosides

The pathogenic sequence variants discussed previously induce sequence changes (57) that ultimately end up altering the secondary and tertiary structure of the mitochondrial RNA, reducing RNA and mRNA steady-state levels, and causing tRNA modification (50). The mtDNA is quite similar to the bacterial genome and the mutational variations induce higher similarity and, thus, higher probability of causing excessive interaction with AmAn.

The trigger for ototoxicity and AmAn-induced HL is the combination of the mutated mitochondrial ribosome resembling the one in bacteria (52,60) plus AmAn administration. If the mutational change induces a bacterial-like ribosomal structure, it creates the possibility for AmAn to bind to mtDNA and, consequently, exert an effect in the mitochondria. Thus, it is essential to consider the action of AmAn, as the variants are risk factors to HL, although environmental and nuclear modifiers may be involved to produce disease phenotype.

Aminoglycoside is an antibacterial drug (Figure 5), used against infections caused by Gram-negative bacteria, particularly in the hospital environment (55), and with vast use in less developed countries (49). However, they also work on Gram-positive bacteria and *Mycobacteria*, which, along with low cost, makes their use compelling (61).

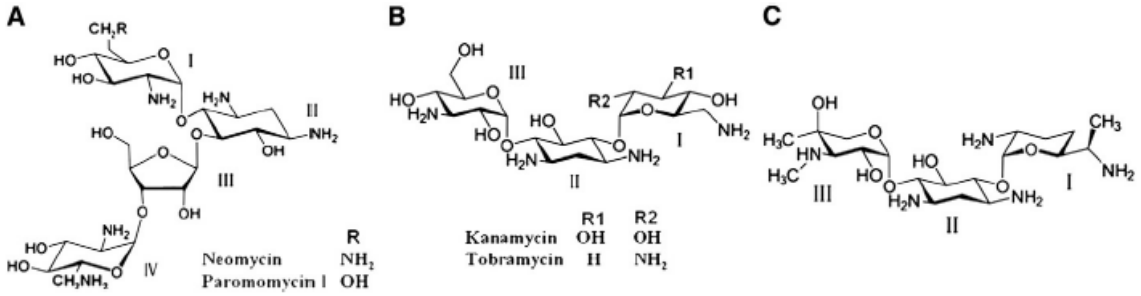

Figure 5. *Aminoglycoside structure. "(A) Neomycin-class antibiotics with a 2-deoxystreptamine (ring II), distributed at positions 4 (ring I) and 5 (rings III and IV). (B) Kanamycin-class antibiotics and (C) Gentamicin C1A with substitutions at positions 4 (ring I) and 6 (ring III)." This image was published in Mitochondrion, 11, Guan MX, Mitochondrial 12S rRNA pathogenic sequence variants associated with aminoglycoside ototoxicity, 237-245, Copyright © Elsevier (2011). Use has been authorized by the publisher.*

The AmAn have been synthetized to target the bacterial molecules to halt their infection via binding to ribosomal RNA (16SrRNA in the bacterial 30S subunit), affecting protein synthesis by codon misreading and inhibition of tRNA (49,52,60). These drugs have been linked with nephrotoxicity, ototoxicity and vestibular toxicity, and while nephrotoxicity is reversible, the other two are not. Glomerular filtration clears AmAn out from most tissues, but they concentrate in renal tubular cells, and in perilymph and endolymph of the inner ear (49).

Without these drugs' administration, the prevalence of ototoxicity diminishes, because they do not exert their effect on the pathogenic variants; the association of ototoxicity with AmAn administration comes from the lack of reported nefarious phenotype until after contact with this drug, or, on the other hand, MNSHL that is not AmAn-induced is not as pronounced and/or has a later age-of-onset (49,55). Patients treated with AmAn exhibit a high frequency of SNHL, often permanent and bilateral (49,50). The type and doses of AmAn, length of administration and age of patient all mold MNSHL severity (49).

AmAn ototoxicity can derive from genetic etiology or predisposition with autosomal dominant, autosomal recessive, X-linked or mitochondrial patterns of inheritance (49). *MTRNR1* pathogenic sequence variants increase drug susceptibility by 4- to 16-fold, by combination of increased drug binding to mitochondrial RNA and exacerbation of the mutants' deficiency in ribosomal production (60). The genetic alterations lead to a hypersensitivity to AmAn, meaning that drug administration can induce or aggravate MNSHL in matrilineal relatives, on accounts of phenotype severity and age-of-onset (55).

The mitochondria-bacteria resemblance becomes a danger: the drug can bind to the A-site of the mutated mitochondrial 12S rRNA (a highly conserved region of mtDNA and a mutation hotspot (62)), which resembles the bind location of the bacterial A-site of 16S rRNA. m.1555A>G is equivalent to the 1491 position of *E. coli*'s 16S rRNA and forms a similar secondary structure to bacteria; the new G-C pair creates the AmAn binding-site in mitochondria. The m.1494C>T creates the same issue, since it binds to nucleotide 1555 in the 12S rRNA stem-loop (49,55,63). These variants create a U1494-1555A or a C1494-1555G base pair at the 12S stem-loop; this mutated U-A or G-C base pair removes the stem-loop, and facilitates AmAn binding, by tertiary structure change (49,53) (Figure 6). Thus, the pathogenic sequence variants of *MTRNR1* gene facilitate the binding of AmAn to the 12S ribosomal subunit, causing mistranslation or premature termination of protein synthesis (49,50,63), creating the attack on mitochondria and its dysfunction. The 12S subunit, like the 16S, is crucial for RNA-protein or RNA-RNA interaction (49,50).

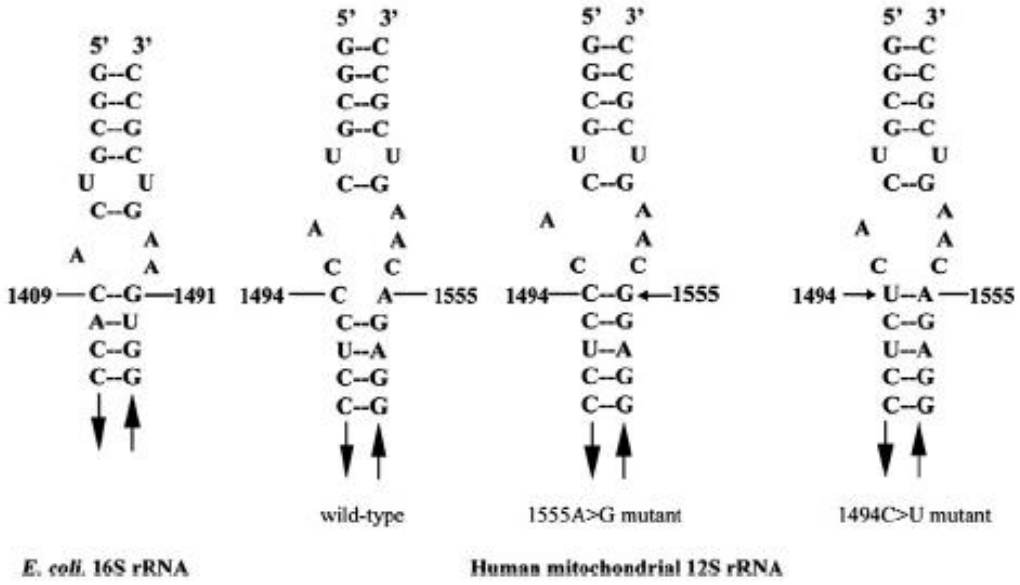

Figure 6. *Comparison between bacterial 16S rRNA and human 12S rRNA stem-loop. This image was published in Mitochondrion, 11, Guan MX, Mitochondrial 12S rRNA variants associated with aminoglycoside ototoxicity, 237-245, Copyright © Elsevier (2011). Use has been authorized by the publisher.*

In addition, m.1494C>T, in the absence of AmAn, shows late-onset and progressive deafness, with varying severity and age-of-onset, with AmAn administration inducing or worsening MNSHL (49).

The m.7445A>G reduces metabolism of mitochondrial tRNA, like other variants coding for tRNA (63), leading to failure in tRNA metabolism, altering translation and mitochondrial respiration (50). m.7445A>G locates at the stop codon, and while the A>G change has no structural effects, it does affect the processing rate of the L-strand $tRNA^{Ser(UCN)}$ precursor, resulting in reduction of the tRNA steady-state levels and thus reducing the amount of ND6 mRNA (50,64). In addition, this mutation can carry additional symptoms, namely palmoplantar keratoderma (59).

In the end, this change halts the correct operation of the mitochondria, disrupting protein synthesis (reduced by 30-40% (49,53)) as it impacts accuracy and efficiency of translation, decreasing it by 28-50% (49). Protein synthesis decreases more than 50% is noted as the threshold for dysfunction, decreasing cellular respiration and growth (49,63).

By themselves these three variants are not able to create a phenotype (49,53,63), but the action of AmAn contributes to an additional 30% decrease in protein synthesis and subsequent ATP loss and ROS gain, making translational rate fall below threshold (49). Mitochondria damage ensues, with loss of their basic function and structure, elevating ROS' concentration and ATP depletion (which one comes first is still a point of dispute), ending in mitochondria apoptosis. This loss of mitochondria in ear tissues, in HL, starts with the cochlea and continues to the apex (55).

1.2.2.4. Mechanism for Pathology

As is the case with LHON and many other mitochondrial disorders, the loss of mitochondria has a higher impact in high energy-demand tissues. In HL, the problematic tissue is the cochlear apparatus and the inner hair cells (IHC); the human cochlea has about 5000 hair cells, which cannot be replaced.

Mitochondrial dysfunction – ROS accumulation and depletion of ATP – creates IHC damage, due to accumulation of AmAn in the perilymph and endolymph of the inner ear, causing ototoxicity because they are difficult to metabolize (49). Another way that AmAn can induce deafness is by interference with the auditory nerve (55). Apoptosis of IHCs makes transmission of sound impossible, once it cuts the chain of sensory transport and the brain cannot receive the auditory input, ergo HL occurs (Figure 7).

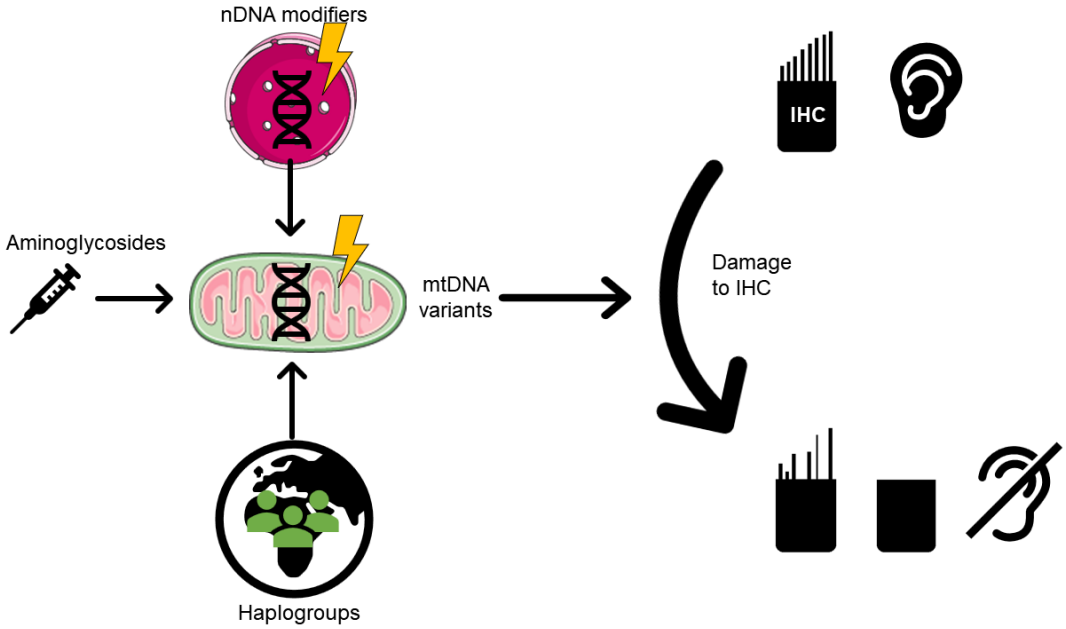

Figure 7. *Schematic representation of different factors that influence mtDNA variants that cause IHC damage and thus HL.*

AmAn cross the blood-endolymph barrier, moving to the apical membrane of hair cells via the mechanoelectrical transducer (MET) channel and other cationic channels (63). This channel opens unidirectionally upon noise, creating a concentration of AmAn in hair cells' cytosol, unable to retreat into the endolymph. There, AmAn interact with the 12S subunit, causing inaccurate translation of mitochondrial proteins and finalizing in cell apoptosis (63). The progression in hair cells' death goes from the basal turn to the apical turn of the cochlea, in line with deafness onset, since high frequency loss happens first. ROS accumulation too plays a major role, with causal relationships in both drug-induced and noise-induced HL, and with administration of antioxidants ameliorating the phenotype. Further, ROS leak out of the cochlear tissues, impacting the surrounding structures (52).

The AmAn molecule needs the REDOX capacity of a transition metal ion to induce ototoxicity, forming an iron-aminoglycoside complex, with enzymatic reactions catalyzed by nitric oxide synthase or NADPH oxidase (52,56). It can act directly on mitochondrial membrane proteins hindering their correct function, or indirectly by their abnormal synthesis (52). Furthermore, the complex chelates metal ions from biomolecules, producing chelated metal complexes (i.e. arachidonic acid), which are REDOX-active and create ROS, which by turn induce oxidative damage in biomolecules. Ergo, treatment with iron chelators is a possibility for protection from AmAn (56).

Mitochondria and ROS are involved in signal transduction pathways, such as AMPK (62), with ROS-dependent activation of AMPK regulating the pro-apoptotic function of E2F1 (65). This process can be activated by *MTRNR1*'s pathogenic sequence variants – that directly inhibit the ribosome assembly – or by overexpression of TFB1M methyltransferase – TFB1M binds to POLRMT to promote 12S methylation and alters ribosome biogenesis and activity, increasing ROS (56,58,65). Hence, mitochondrial stress leads to tissue-specific apoptotic signaling in the stria vascularis and spiral ganglion neurons. No HL occurs with mutated *TFB1M* and reduced *E2F1*; however, with m.1555A>G, there is an increase in *E2F1* expression, activation of caspase-3 in the strial epithelium and of AMPK in the spiral ligament (56,58). Ergo, asymptomatic carriers of *MTRNR1* pathogenic sequence variants may lose their hearing later by natural disease progression or in response to stressors (AmAn or noise), which activate the ROS-AMPK-*E2F1* pathway (65).

1.2.2.5. Modifying Factors

While the three variants are definitely involved in mitochondrial dysfunction, AmAn-hypersensitivity and HL, by themselves, produce only milder phenotypes. The phenotype is aggravated when the primary variants act in tandem with AmAn or other toxins, secondary genetic modifiers (nuclear or mitochondrial genes) (50,58) and haplogroup (55), that contribute to phenotypical expression (53,64,66,67). Even hetero-/homoplasmy correlates with penetrance and severity of phenotype – the variability in penetrance of Spanish families may be due to the heteroplasmy of m.1555A>G (66).

Modifiers in the nuclear genome can be associated with worsening of the phenotype. Genetic alterations in the *TRMU* gene have been indicated as such one possibility, by creating problems on tRNA metabolism (63), having been detected in European and Arab-Israeli populations (58). *GJB2* is another nuclear variant often referred to in literature as a modifier factor for MNSHL (67), linked by its regulation of the endolymph ion concentration (63). A number of mitochondrial secondary variants (not haplogroup associated) have been shown to alter tRNAs metabolism (50). In addition, deletions, which inhibit protein synthesis in the mitochondria and alter copy number, can be associated with the MNSHL phenotype (50).

Considering haplogroups that may modify MNSHL, J's specific variants increase penetrance when associated with variants in $tRNA^{Ser(UCN)}$, like m.7445A>G (58,65). The L1b haplotype has been associated with higher penetrance in African families (65). The M7b1 haplotype enhances penetrance and severity of MNSHL when 12S variants are

coupled with AmAn administration (66), with haplogroup B showing an increase in Chinese patients with m.1555A>G, and haplogroup D likewise being involved in higher frequency of m.1555A>G (51,60). The H haplogroup has been associated with higher incidence in Spain cohorts (49,58), with the HV cluster showing patients with early-onset post-lingual HL (51). Penetrance of MNSHL has an higher incidence in C, Y and F2 haplogroups as well (49).

1.2.2.6. Prevention and Therapy

For prevention of MNSHL by AmAn ototoxicity, assessing pedigree by genetic variant screening is advised prior to administration (55,63), as well as examination of family history for MNSHL combined with the molecular analysis (49). The use of audiometry screening is also recommended (63), although genetic variant screenings have some important advantages – i) this disease affects infants, whom are unable to indicate their loss of hearing; ii) the loss of high frequencies (4.0-8.0 kHz) comes first, which may be less or not-at-all noticeable to the patient (68). With the results from these analysis, it is possible to identify people at risk; this is an important concern for public health, because pathogenic sequence variant carriers should avoid using this antibiotic, to reduce their risk for ototoxicity (55).

Surpassing prevention, although it is the main goal, some therapies have been proposed and in development, as will now be described.

When it is not possible to screen and avoid administration, it is necessary to protect the inner ear, by administration of antioxidants alongside AmAn (55,63) which will fight back the increase in ROS production, as well as some other supplements to relieve oxidative stress. Another method would be to inhibit the transporter that uptakes and accumulates AmAn in the inner ear (55).

The MET channel, necessary for the biochemical mechanism of AmAn ototoxicity, has a 1.25nm pore size, which allows AmAn passage; as such, an increase of the AmAn molecule's size has been proposed. This would mean that only one compound was administrated, unlike the AmAn-antioxidants combination (63).

Substances for otoprotection should likewise be considered. For example, salicylate, such as aspirin (57), which acts as an iron-chelator and antioxidant. The use of ethacrynic acid would disrupt the hemo-labyrinth (endolymph is a labyrinthine fluid) barrier, reducing AmAn concentrations in the endolymph by opening the barrier and allowing it to flow back to the bloodstream. Dexamethasone, a glucocorticoid, can modulate ion transport and immune response in the inner ear. These treatments will also confer vestibular protection. The cochlear neurons can be protected by administration of 4-methylcatchol (inducer of nerve growth factor synthesis), or of α-lipodoic acid (a free radical scavenger) (56). Another way to protect hair cells is by stopping apoptosis; this can be done with CEP-1347, which blocks the JNK pathway, reducing hair cell fragmentation and loss (69).

Moreover, precision medicine is considered for the diagnosis and/or cure of this disease in the future (55).

Overall, strategies for ameliorating symptoms are scarce and underdeveloped, and the main concern with MNSHL is to avoid their use on in-risk patients. Therefore, it is necessary to create a method that identifies that group sensibly, reliably and quickly, because their administration only occurs in the event of infections, and obviously that means a fast response is a must, to ensure survival.

2. Fundamentals of Methodology

For the screening of LHON variants it was opted for a Real-Time Polymerase Chain Reaction (PCR) with High-Resolution Melting (HRM). Initially, it was considered to have both diseases follow the same method, however, due to HL's variants' characteristics, for this analysis, it was opted for a Real-Time PCR with Amplification-Refractory Mutation System (ARMS) primers. Here, an introduction to the techniques used in this dissertation is presented.

2.1. Real-Time Polymerase Chain Reaction

Polymerase Chain Reaction is a technique developed by Kary Mullis's group in 1983, and a Nobel-awarded technique in 1993. The desired DNA sequence is amplified many times by an enzyme (i.e. *Taq* polymerase), with the help of primers, which denominate the sequence area, dNTPs, for sequence amplification, and Mg^{2+} and buffer, to allow for the proper reaction.

Real-Time PCR is described by the Saunders Comprehensive Veterinary Dictionary (70) as "a method for the detection and quantification of an amplified PCR product based on incorporation of a fluorescent reporter dye". This technique was first developed around 1993, by Higuchi *et al*. (71), a decade after Mullis' conventional PCR. Unlike conventional PCR, with Real-Time PCR we can monitor amplification "in real-time", by bioinformatically seeing the increase in fluorescent signal cycle by cycle, and, moreover, identifying the products by quantification or qualitatively. Quantitative PCR is used for allelic discrimination and genotyping (72), amongst other applications.

The fluorescence increase happens in direct proportion to the number of double-stranded DNA molecules in the reaction, that is, the PCR product increase. It is this relationship that allows quantification of nucleic acids and determination of sequences' presence/absence. The PCR cycle number at which signal can be discriminated is represented by the Cycle Threshold (C_T). Furthermore, the greater the amount of starting template, the sooner the C_T is reached and the lower that value is (73).

The Real-Time PCR instruments are composed of a thermal cycler with an integrated excitation light source (lamps, LED or lasers), a fluorescence detection system and its software, which performs the quantitative fluorescence analysis. Energy emitted at discrete wavelengths by fluorophores is monitored in detectors, with filters or channels being used to detect shorter wavelength ranges. After, the software simplifies data, with results in graph form, where amplification curves show starting DNA quantity, whereas dissociation curves show PCR product purity (72).

For Real-Time PCR, product needs to be smaller in size than the usual PCR procedure, as to comply with the higher specificity and sensitivity of this technique. Here, the product should be 50-200bp long, which can be extended to 400bp (74). For dyes, double-stranded DNA (dsDNA) intercalating dyes (Figure 8) detect both specific and non-specific (non-specific products and primer-dimers) amplifications; on the other hand, fluorophores attached to oligonucleotides only detect specific products. The cheaper

option are intercalating dyes, which bind to the minor groove of dsDNA, increasing fluorescence and measuring it in the extension phase of qPCR cycle (72).

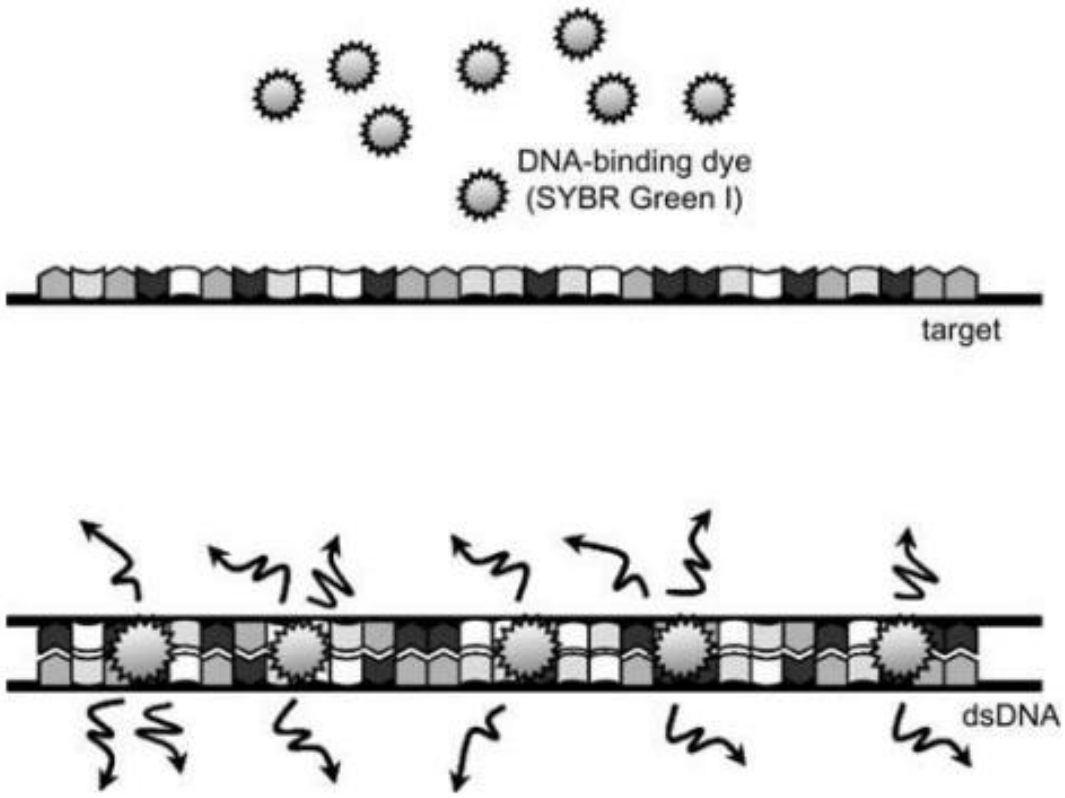

Figure 8. *Schematic of SYBR® Green I fluorescence. This image was published in Molecular Diagnostics, 2nd edition, Patrinos, G. & Ansorge, W., Page 89, Copyright © Elsevier Books (2011). Use has been authorized by the publisher.*

For variant detection we can use i) Polymorphic or mutant allele-directed specific (AS-PCR) analysis, which detects known variants, using primers specific for the single nucleotide variant (SNV) and identification of it is confirmed by presence of the PCR amplicon; or ii) Melting curve analysis (MCA), used for known or unknown variants, being able to detect the presence of the SNV and identify the type of nucleotide substitution. Both are based on the conversion of dsDNA into single-stranded DNA (ssDNA) due to heat denaturation, with shift in dsDNA-binding dye fluorescence being tracked with temperature change (75).

2.2. High-Resolution Melting

In 1997, five years after the Real-Time PCR technique is developed, Wittwer *et al*. (76) develop the LightCycler® machine, and with it the HRM technique (73), directing melting analysis with dsDNA dyes or dual hybridization probes (75). That same year, Ririe *et al.*

(77) differentiated PCR products by MCA, with plots of fluorescence as function of temperature (75). Both techniques of MCA and melting temperature (T_m) analysis are based on the fundamental thermodynamic properties of DNA (75).

In 2003, Gundry *et al.* (78) performed HRM in a dedicated instrument, and at the same time, Wittwer *et al.* (79) developed HRM with LCGreen® (dsDNA saturation dye), in a closed tube system without labeled oligonucleotides, and genotyping and detecting variants. Alongside it, they introduced the melting curve subtraction and fluorescence difference as methods to differentiate genotypes – a change in melting curve identifies heterozygotes and a change in T_m shows different homozygotes (75).

When using dsDNA dyes, MCA is performed to check specificity. HRM starts with amplification of the sequence with dsDNA-binding dye (Figure 8). The combination of sequence plus dye denaturates on a temperature gradient (50-95ºC), with dsDNA melting into ssDNA by temperature increase, fluorescence being monitored throughout this process. Because the fluorescence happens when the dye is bounded, with temperature of DNA denaturation a sharp decrease in fluorescence is detected by the optical system due to dye dissociation (72).

The fluorescence-reading equipment captures the fluorescent data points per change in temperature. The software (for data normalization, curve shape comparison and genotype clustering) takes the readings and increases melting curve quality, detecting small sequences differences in PCR products (73). The result is a melt curve profile of the amplicon. For analysis, the T_m point, when there is 50% of dsDNA and 50% ssDNA, and the curve's inflection point, is used. For easier visualization, the negative derivatives are plotted: T_m values appear as peaks in derivative plots (Figure 9). PCR products of different length/nucleotide content show distinct peaks on the derivative plot because they denature at different temperatures. Here, nonspecific products can be detected as lower temperature/intensity, allowing assessment of PCR purity (72). HRM's algorithms and plots scale the data, showing small differences, creating high specificity of the technique.

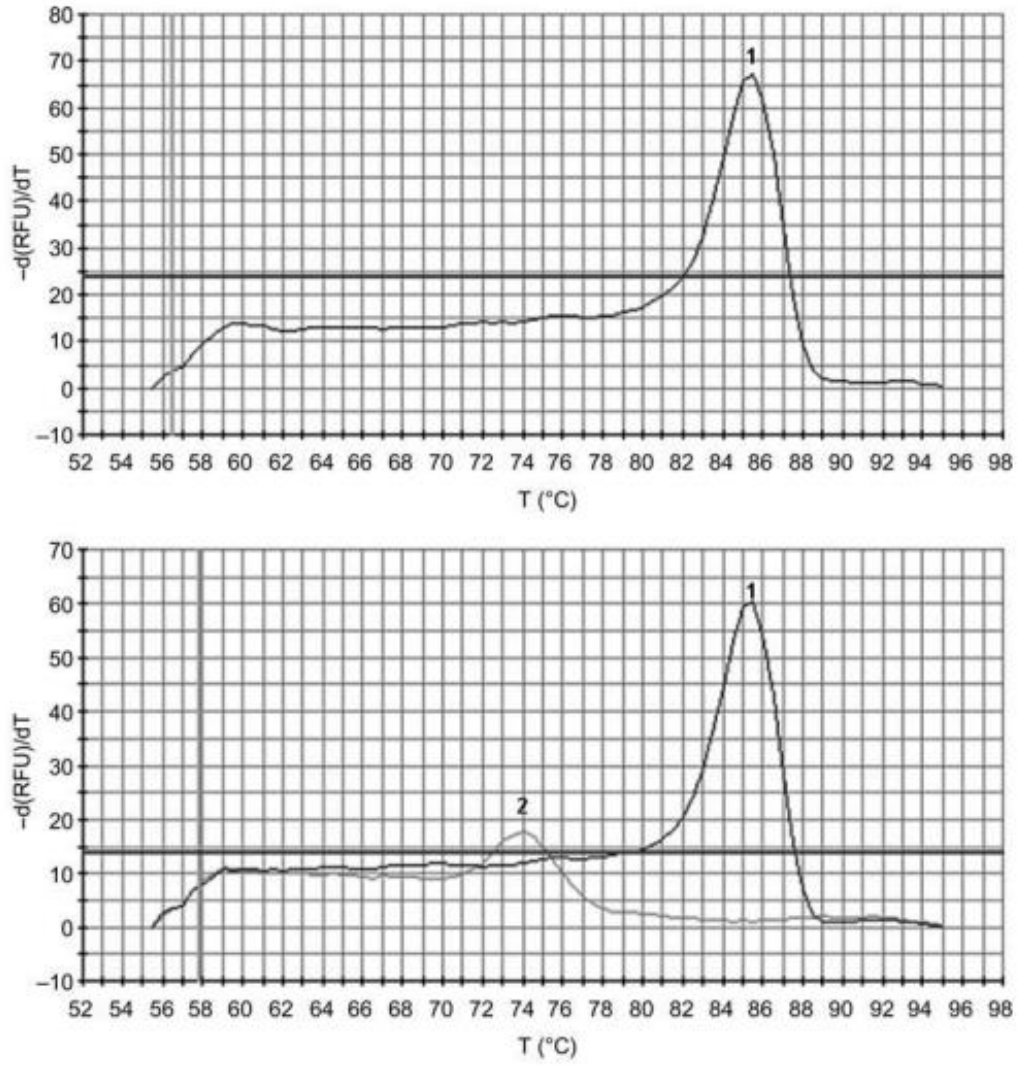

Figure 9. *Melting curve analysis, by derivative curve. This image was published in Molecular Diagnostics, 2nd edition, Patrinos, G. & Ansorge, W., Page 90, Copyright © Elsevier Books (2011). Use has been authorized by the publisher.*

PCR products should be short so differences between genotypes, which are assigned based on small T_m differences, are more distinguishable; furthermore, they allow for very rapid PCR due to reducing denaturation temperature (74). Better discrimination is obtained with lower length, and the T_m difference between variants needs to be >0.3ºC. Amplicon length should be 100-300bp, to allow for SNVs, inversions, insertions and deletions analysis. The short length avoids detection of SNV outside the region of interest, but too small amplicons may not produce enough fluorescence.

HRM is used to identify genetic variation (genotyping SNVs, evaluate methylation and copy number variation) (75). This method is simple, fast and based on PCR melting curve techniques, with identification of genetic variants by differences in T_m of amplicons (Figure 10). HRM can discriminate sequences based on composition, length, GC% content, heterozygosity, or strand complementarity (73). Because the melting step occurs after amplification, on the same thermal cycler, the opportunities for processing errors and contamination are minimized (80). HRM is appropriate for diagnostic due to

its high sensitivity, specificity, not labor-intensive (no manual post-PCR processing), with rapid turn-around and closed-tube format (75), and low reaction cost. In a similar standing to HRM we have AS-PCR and exonuclease assays (73). HRM meets the needs of a more and more automated clinical laboratory, which requires rapid attainment of genetic information for quick but still reliable clinical decision (80).

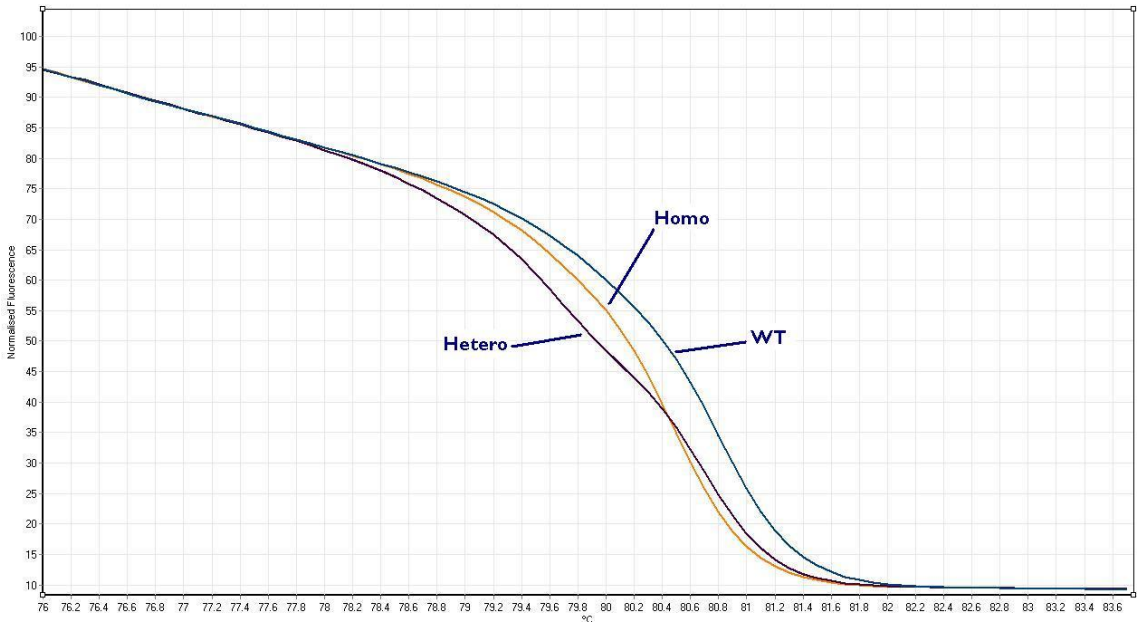

Figure 10. *Aligned Melt Curves in HRM variant calling. This image is available in the public domain.*

2.3. Amplification-Refractory Mutation System

AS-PCR was developed in 1989, with use of specific primers where the 3'-terminal base of the primer matched to the WT or mutant template, resulting in specific amplification – this is based on the inefficiency of DNA amplification when a mismatch occurs between template and the 3'-terminal nucleotide of the primer, where extension will not be efficient when the mutant is present, and only efficient with the WT template, and vice-versa. That is, the target sequence is preferentially amplified when in presence of the perfect-match primer and poorly amplified when with a mismatched primer (75) (Figure 11).

Newton *et al.* (81) developed ARMS, the sequence specific PCR amplification, where, in addition to the 3'-terminal mismatch, they introduced an additional deliberate mismatch near the 3'-terminal (the 2nd or 3rd from the 3' end). Because the first mismatch destabilizes the primer-template duplex, this addition reduces false positives, enhancing the reaction. ARMS is used for the analysis of point genetic variants and allows for specific PCR, as we pretended, and it can determine heteroplasmy levels (75).

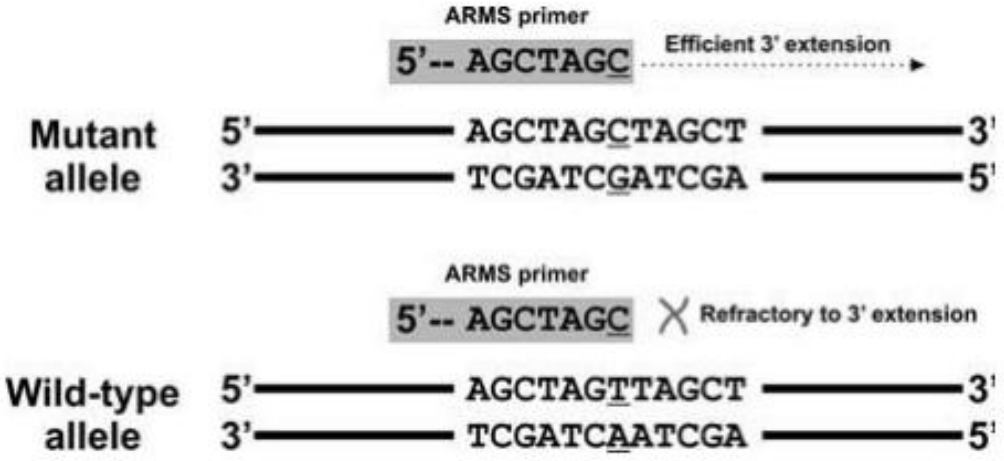

Figure 11. *Schematic of ARMS primers. This image was published in Molecular Diagnostics, 2nd edition, Patrinos, G. & Ansorge, W., Page 16, Copyright © Elsevier Books (2011). Use has been authorized by the publisher.*

ARMS primers design and characteristics differ some from HRM primers, differences which allow us to create more specific primers. Software, like *Primer1* or *WASP*, can be used to design primers since they support the design of variant specific primers, including the deliberate mismatch (75).

Mismatches are made based on the nucleotide variation – when the nucleotide change creates a strong mismatch, it needs to be balanced with a second, user-made, weak mismatch, or vice-versa. Base pair changes of GA, CT, TT have maximum mismatch strength, with CC being a strong mismatch; AA and GG are of medium strength; CA, GT are weak mismatches, and finally, AT and GC mismatches have no strength.

3. Aims of the Study

Concerning LHON, an early diagnosis is essential for timely treatment of the disease, which should be administered as soon as possible after vision loss in the first eye starts, in order to guarantee the best recovery percentage, since the therapy is most effective before the aggravation of clinical symptoms. The type of pathogenic sequence variant is also relevant, and needs to be pinpointed, since different pathogenic sequence variants show differences in treatment requirement, in order to obtain the best recovery chance.

A quick genetic study is necessary when AmAn's administration is considered, since these have been demonstrated to be a phenotypical/clinical modifier, causing or aggravating the phenotype of ototoxic HL. Thus, the development of a quick diagnostic tool may prevent the AmAn toxicity without prohibiting fast clinical action or furthering the development and spread of infection. Also, in this case, the type of pathogenic sequence variant is relevant, as it represents a predictability factor for how severe the hearing loss by AmAn can be.

The aim of the work presented henceforth is the development of two quick, easy to perform and to interpret diagnostic tools, namely screening genetic tests, for top primary pathogenic sequence variants, for rapid diagnosis of LHON and for MNSHL. The final goal is to create a reliable, easy and quick tool to be used in clinical setting, which will provide strong results in less than 24 hours after sample collection.

For LHON, it is aimed to investigate the TOP-3 pathogenic mtDNA variants: m.3460G>A, m.11778G>A, m.14484T>C, by Real-Time quantitative PCR with High-Resolution Melting curve analysis.

For MNSHL, it is aimed to identify the three pathogenic mtDNA variants: m.1494C>T, m.1555A>G, m.7445A>G, by Real-Time quantitative PCR with Amplification-Refractory Mutation System.

The results will allow accurate clinical diagnostic and, consequently, support clinical decision of the best next step. For LHON, it will help the decision concerning the therapeutic approach to perform, with the best recovery chance both in terms of time and variant. For ototoxic HL, ideally it will prevent MNSHL by avoiding the AmAn administration, using another antibiotic for treatment.

.

4. LHON

4.1. A 24h screening test for top three LHON pathogenic sequence variants to be used in clinical setting and treatment assessment (A Scientific Paper)

Sara Martins[1,2,3], Maria João Santos[1,2,4], Márcia Teixeira[1,2], Luísa Diogo[1,2,4,5], Maria do Carmo Macário[1,2,4,5], João Pedro Marques[5], Pedro Fonseca[4,5], **Manuela Grazina*** [1,2,4]

1. CIBB - Center for Innovative Biomedicine and Biotechnology (https://www.cibb.uc.pt/);
2. Laboratory of Mitochondrial Biomedicine and Theranostics, CNC - Center for Neuroscience and Cell Biology, University of Coimbra, Portugal;
3. Biology Department, University of Aveiro, Portugal;
4. FMUC - Faculty of Medicine, University of Coimbra, Portugal;
5. CHUC - Coimbra University Hospitals EPE, Portugal

*To whom correspondence should be addressed. Tel: (+351)239-480040; Email: mgrazina.fmuc@gmail.com. Present Address: Faculty of Medicine, University of Coimbra, Pólo III – Subunit I, Azinhaga de Sta. Comba, Celas, PT–3000-354 Coimbra (Portugal)

4.1.1. Abstract

Diagnostic of Leber's Hereditary Optic Neuropathy (LHON) has been mainly based on the presence of one of three mitochondrial DNA variants: m.3460G>A, m.11778G>A, and m.14484T>C. The disease results in progressive vision loss, sequentially on both eyes within eight weeks to six months. Recently, a treatment became available and its success may vary according to presence and type of pathogenic sequence variant, being influenced by onset.

The aim of this work was to develop a screening method, offering a quick and reliable genetic assessment of TOP-3 pathogenic sequence variants, to be used for guidance in clinical decision, particularly therapeutics.

The screening method is based on real-time PCR with High Resolution Melting (HRM) analysis, for detecting the TOP-3 pathogenic sequence variants, by assessing amplicon's T_m. The variant classification is made using HRM Software. Ninety-four samples were analyzed, including LHON suspected patients, relatives, other mitochondrial disease patients and healthy controls.

A new Real-Time PCR/HRM screening method is described to detect TOP-3 LHON pathogenic sequence variants. This is a simple, robust and easy test, performed in a cost-efficient and quick manner. Therefore, this is a better alternative to other existing methods, since it allows an earlier clinical decision, including therapeutics, with possible rescuing of the visual function.

Keywords: LHON, mtDNA variant, real-time PCR, High resolution melting, variant screening

4.1.2. Introduction

Mitochondria produce energy (ATP) through oxidative phosphorylation (OXPHOS) at the mitochondrial respiratory chain (MRC) enzymatic system. Tissues with higher energy requirements are more affected by mitochondrial dysfunction, since they cannot sustain the ATP depletion (9). Due to multiple copies of mitochondrial DNA (mtDNA), creating a threshold effect, disease usually appears above a certain percentage of heteroplasmy, with some exceptions for pathogenic sequence variants occurring in homoplasmy, such as m.11778G>A. Another key-role of mitochondria is in the intrinsic apoptotic pathway, which can lead to pathogenicity if over-done (1,7,11).

The optic nerve consists of about 1.2 million retinal ganglion cells (RGCs) particularly susceptible to mitochondrial dysfunction, having high energy consumption (19,28). Causative variants have been associated with a significant decrease of complex I (CI) activity, respiratory rate and ATP levels, leading to a cascade of cell events: i) increased ROS and oxidative stress, ii) mitochondrial damage, iii) mitophagy impairment, iv) mitochondrial mass loss, v) inadequate ATP production and vi) apoptosis of RGCs (19,28).

Leber's Hereditary Optic Neuropathy (LHON) has been genetically characterized by three main primary mtDNA variants, which represent 90-95% of total pathogenic sequence variants identified in LHON cases: m.3460G>A (*MTND1* gene, ND1 subunit); m.11778G>A (*MTND4* gene, ND4 subunit); and m.14484T>C (*MTND6* gene, ND6 subunit) (Table 1) – all encoding subunits of CI of the MRC (20). The m.3460G>A is the most severe and less frequent (19). The m.11778G>A is present in 70% of LHON patients, being the most prevalent (19,20,29). Finally, m.14484T>C has the mildest effect (19), with low penetrance, and variable incidence (19,29). The LHON variants are usually homoplasmic, with 10-15% being heteroplasmic (19). From the TOP-3 pathogenic sequence variants, the milder variants (m.11778G>A, m.14484T>C) tend to present in homoplasmy, and may be influenced by haplogroup, explaining population variability. However, severe pathogenic variants (m.3460G>A) in heteroplasmy cause atrophy and grimmer phenotypes when homoplasmic (8). The mtDNA alterations have a biochemical effect, and the dysfunction affects MRC, ultimately ending in a depletion of ATP production and subsequent increased ROS content and oxidative stress (18,19,28,38).

Genetic modifiers may include haplogroups (J, W, K, H and M) or nuclear genetic alterations (*TP53*, *EPHX1*, 3q26.2-3q28) (18,19,25,26,37,82). Other modifiers can be hormonal (estrogens) (18,25,37), or related with copy number and mitochondrial biogenesis (19,37). Smoking, alcohol, drugs, nutritional deficiencies (B-complex vitamins), physical injury, exposure to toxic factors, psychological stress or non-controlled diabetes have all been linked to LHON etiology (18,25,26,35,37,38).

LHON is a rare maternally inherited disorder and it is clinically characterized by bilateral and painless vision loss, either simultaneously (25%) or sequentially (75%) (19). Usually the second eye becomes affected after six/eight weeks to six months (27), and, within one year, 97% of patients with loss in one eye develop blindness in the second eye (27). The vision loss is significant, but spontaneous recovery may occur, particularly associated with m.14484T>C (27). The symptoms develop between 15-35 years of age, with higher prevalence in men (83) (Table 1); 50% of male carriers develop LHON, while only 10% of female carriers are affected (19,25,27,29). Although typical LHON is

restricted to the optic nerve atrophy, other symptoms, including neurological manifestations, may also occur (32).

Table 1. *Prevalence of LHON's TOP-3 pathogenic sequence variants.*

	TOP-3	**Relative %**	**Prevalence Men:Women**
TOP-3 *	m.3460G>A	8-25	3:1
	m.11778G>A	50-70	6:1
	m.14484T>C	10-15	8:1
TOP-16	m.3376G>A	Rare	N/A
	m.3635G>A		
	m.3697G>A		
	m.3700G>A		
	m.3733G>A		
	m.4171C>A		
	m.10197G>A		
	m.10663T>C		
	m.13051G>A		
	m.13094T>C		
	m.14459G>A		
	m.14482C>A		
	m.14482C>G		
	m.14495A>G		
	m.14502T>C		
	m.14568C>T		

*Data from Abu-Amero, 2011(83).

There are many forms of symptom management (23,25,27–29,35); therapies, such as gene therapy or pharmacological approaches, have been developed in recent years (8,19,22–25,27,29,35,40). A contender that works specially in patients harboring m.11778G>A is idebenone, an ubiquinone analogue that acts by a compensatory mechanism that restores bioenergetic capacity (18,19,41,22–24,27–29,35,40).

The timeframe is critical for clinical action, since the identification of the pathogenic variant is mandatory to delineate treatment. It is essential to quickly and reliably scan for genetic alteration, in order to act timely and rescue function.

Our aim was the development of a quick, reliable and easy to perform and interpret diagnostic tool, for detecting TOP-3 pathogenic LHON pathogenic sequence variants. The goal is to present a test for clinical implementation, providing strong results in less than 24 hours after sample collection. The three mtDNA genetic variants m.3460G>A, m.11778G>A and m.14484T>C, were investigated by Real-Time PCR with High Resolution Melting (HRM) curve analysis. The results allow for accurate genetic

diagnostic and, consequently, support the clinical decision for therapeutic approach, with the best recovery chance, both in terms of time and variant.

4.1.3. Materials & Methods

4.1.3.1. Study Design and Sample Collection

The sample population included 94 subjects: ten samples of non-LHON patients (patients with suspicion of other MC), 20 healthy controls, 14 LHON patients and 35 non-affected relatives, with another 15 samples from individuals with suspected LHON but negative for these variants. Total DNA was previously extracted from several tissues according to standard protocols (84). All samples were previously analyzed and confirmed by at least one additional method (Sanger, Next Generation Sequencing or PCR-RFLP), for diagnosis purpose. All samples were identified, allowing for result comparison and confirmation of the true/false status of HRM results.

This study was included within a broader project with approvals by the local Ethical Committee (#CE-071/2013 and #CE-032/2014) and National Committee of Data Protection (authorization #5484/2018), and informed consent was obtained, following the Tenets of the Helsinki Declaration. Control samples of healthy individuals in this study were completely anonymized, accordingly to the European Union General Data Protection Regulation (Regulation (EU) 2016/679) and to Portuguese Law (DL 58/2019 and DL 59/2019).

4.1.3.2. Primer Design

The principal role of the genetic alterations in study was confirmed in literature and bioinformatic records. The genes in which the variants are located were assigned in *MITOMAP*; the gene sequences were obtained for *Homo sapiens* in *NCBI Gene* (genes *MTND1*: ID 4535; *MTND4*: ID 4538; *MTND6*: ID 4541), which were used for primer design.

The requirements for primer design were i) sensitivity of reaction, ii) specificity of reaction, iii) size of products (70-300 bp in length), iv) the different amplicons (with, without pathogenic variant and possible nuclear product) had to be distinct in size and temperature, v) different variants had to be distinguishable between each other. Moreover, the T_m difference between variants needed to be >0.3ºC in order to be differentiated by the HRM software analysis. Short amplicon length allows for detection of SNVs, inversions, insertions and deletions, while avoiding detection of other variants. However, if the products are too small, they cannot produce enough fluorescence for detection.

The primers were custom made with a primer design bioinformatic/*in-silico* tool, namely *Primer3Plus* (http://www.bioinformatics.nl/primer3plus) for m.3460G>A and *WASP* (http://bioinfo.biotec.or.th/WASP) for m.11778G>A and m.14484T>C. The *WASP* primers were slightly modified, to make them more suitable for the purpose of this work.

The confirmation of primers' specificity and difference of amplicons was conducted using the bioinformatic tools *USCS In-Silico* (https://genome.ucsc.edu/cgi-bin/hgPcr) and *USCS BLAT* (https://genome.ucsc.edu/cgi-bin/hgBlat).

The specificity of the primer pair was verified by checking the predicted PCR product(s).

The amplicon sequence obtained by *USCS In-Silico* tool was then processed by *USCS BLAT*, which screens whole gene for similar DNA sequences, that is, it shows how unique or identical the amplicon sequence is within the human genome. It also provides detailed information about the most similar sequences, and how similar (%) they are. Ideally the amplicon would be unique, but values lower or near 90% are acceptable, and span of sequence was also considered. In practice, it is aimed to obtain a prediction of HRM results, showing that the desired amplicon and undesired/nuclear alternative products were different enough to allow discrimination, if necessary.

In addition, *EndMemo - DNA Melting Temperature (Tm) Calculator* (http://endmemo.com/bio/tm.php) was used, allowing prediction of T_m values. This bioinformatic tool allowed to compare the T_m of different products (wild-type (WT), mutated and similar nuclear pseudogenes) and to understand if they were distinct enough to allow discrimination by the HRM software (>0.3ºC between each other).

Each pair of primers identifies only one of the three variants at a time. The position of amplicons in the *Homo sapiens* mitochondrial genome is as unique from pseudogenes as possible, but it might carry some SNVs.

The sequences of primers, annealing temperature values, site of amplicons and similarity are presented in Table 2 (further information upon request).

Table 2. *Primers used for LHON's TOP-3 genetic variation detection, in Real-Time PCR HRM.*

Name	# bp	Predicted Annealing Temperature	Product size (bp)	Highest Similarity
3460F	21	58.3ºC	73	None found
3460R	21	63.2ºC		
11778F	19	55.8ºC	53	92.5% with chromosome 5
11778R	21	52.9ºC		
14484F	17	45.8ºC	96	93.6% with chromosome 5
14484R	21	54.7ºC		

* **R:** Reverse primer, **F**: Forward primer; **bp**: base pair

4.1.3.3. Primer Preparation

The primers were obtained by *in-silico* tools, namely *Primer3Plus* and *WASP*, adapted as necessary. They were run by bioinformatic tools to confirm their specificity, their product and its T_m.

The information on primers used is on Table 2. Solutions were prepared to 50µM (final concentration) with TE (1:10) and further dilutions were made with TE (1:10). This step was performed in a sterilized PCR workstation for preventing contamination.

4.1.3.4. Real-Time PCR and HRM

The HRM analysis has been used to identify genetic variation (75). This method is simple, fast and based on melting curve techniques, with identification of genetic variants by differences in T_m of amplicons (73). The opportunities for processing errors and contamination are minimized due to the closed-tube analysis of Real-Time PCR/HRM (80). This technique is appropriated for diagnostic due to its high sensitivity, specificity, not labor-intensive, with rapid turn-around and closed-tube format (75) and low reaction cost.

The reaction was prepared inside a sterile PCR workstation that was pre-treated under UV-light for 15 minutes. The MeltDoctor™ HRM Master Mix (Applied Biosystems), featuring SYTO®9 dye, was used. The reactions were prepared according to manufacturer's recommendations: 10µL of MeltDoctor™ HRM Master Mix, 0.3 µM of each primer, 20ng/µL of genomic DNA; for a final volume of 20µL per well. The DNA samples and primers were diluted as necessary with deionized water and TE (1:10), respectively, in sterile conditions.

The reaction was run in the Applied Biosystems™ 7500 Fast Real-Time PCR equipment, using the 7500 Software v2.0.6. The experiment's conditions were programmed following manufacturer's instructions, except for the annealing temperature, which was optimized for the specific primers used in this work, namely at 55ºC. The PCR run set-up specifications are described in Table 3.

Table 3. *PCR run set-up conditions used for detection of LHON's TOP-3 pathogenic sequence variants*

Stage	**Step**	**Temperature**	**Time**
Holding	Enzyme Activation	95ºC	10min
Cycling (40 cycles)	Denature	95ºC	15s
	Anneal/extend	55ºC	1min
Melt curve /dissociation	Denature	95ºC	10s
	Anneal	55ºC	1min
	HRM	95ºC	15s
	Anneal	55ºC	15s

Optimization was developed based on three positive controls (one for each variant), one negative control, one non-template control (NTC) and a random patient sample.

Screening was conducted after optimization and included 41 positive samples, 53 negative samples and one NTC, to assess the three variants; all samples were analyzed in triplicates.

The analysis of the samples was performed blindly, relatively to presence/absence of pathogenic variant.

4.1.3.5. HRM Analysis

Results were analyzed using 7500 Software v2.0.6 and HRM v2.0.1. The amplification plot was observed, along with C_T values, as well as the normalized and derivative plots, to check for overall results. By checking the normalized and derivative curves it was necessary to confirm if the results of triplicates were similar. Furthermore, for assurance of quality in analysis assessment, slopes in normalized curves shall appear as a sharp drop and T_m peaks in the derivative curves must be unique, to allow for the specific identification of T_m by the software, and thus its specific identification of the variant in each sample.

The HRM software discriminates each well into a variant according to specific T_m and the corresponding confidence value is calculated.

After identification of the variants by HRM Software, the results were compared with previous sequencing and PCR-RFLP data.

4.1.4. Results

Samples were also assessed by other, previously established, techniques (Sanger Sequencing, NGS, RFLP) and the samples in study were identified as: 53 negative samples, 34 positive samples for m.11778G>A, six positive samples for m.14484T>C and one positive sample for m.3460G>A.

The samples were then analyzed by the Real-Time PCR method presented, with a confirmation run.

Data obtained showed sensitivity=1, specificity=1, Positive Predictive Value=1 and Negative Predictive Value=1.

Primers were found to be specific and the derived products have high dissimilarity. Optimization revealed 55ºC (Supplementary Figures 1-3; Table 3) as the correct annealing temperature, with good amplification of all targets and all samples (Supplementary Figures 1, 2). The amplification products present good C_T values for all targets, achieving plateau and emitting enough fluorescence for detection. NTCs show some late fluorescence due to primer-dimers, without interference in the assay. Both positive and negative controls achieved the quality parameters, both in the implementation process and in amplification or HRM analysis.

As seen in Table 4, the T_m between WT amplicon and mutant amplicon are distinguishable enough for easy identification by HRM Software (>0.3ºC apart). The Positive Control (PC) and the Negative Control (NC) have the T_m specified, resulting from averaging the observed T_m in the software (the negative control samples averaged into the NC value, and the positives into the PC values).

Table 4. *Comparison of T_m values for each variant (WT vs mutant) of the TOP-3 LHON pathogenic sequence variants.*

TARGET	**PC/NC**	**average T_m (ºC)**
m.3460G>A	PC	79.21
	NC	79.80
m.11778G>A	PC	74.31
	NC	76.55
m.14484T>C	PC	72.34
	NC	71.89

PC: positive control; **NC:** negative control; **T_m:** Melting temperature.

Supplementary Figure 2 presents the optimization's normalized and derivative melt curves. In the derivative curves (Supplementary 2B), the peaks, which represent the T_m value of the product, show that the targets are distinguishable between each other. The very early peaks at 55ºC are from primer-dimers, and can be ignored, not affecting the HRM analysis or results.

Obtained normalized (Figure 12B) and derivative (Figure 12C) curves were as expected. Normalized curves showed a slope with a sharp drop, samples aggregated according to target (similar T_m), and, finally, individual peaks were present in derivative curves. The normalized curves show definition (separation by target), and the slope is of good quality, allowing for correct identification by the HRM software. The derivative curves show good separation by target, with only one peak per sample.

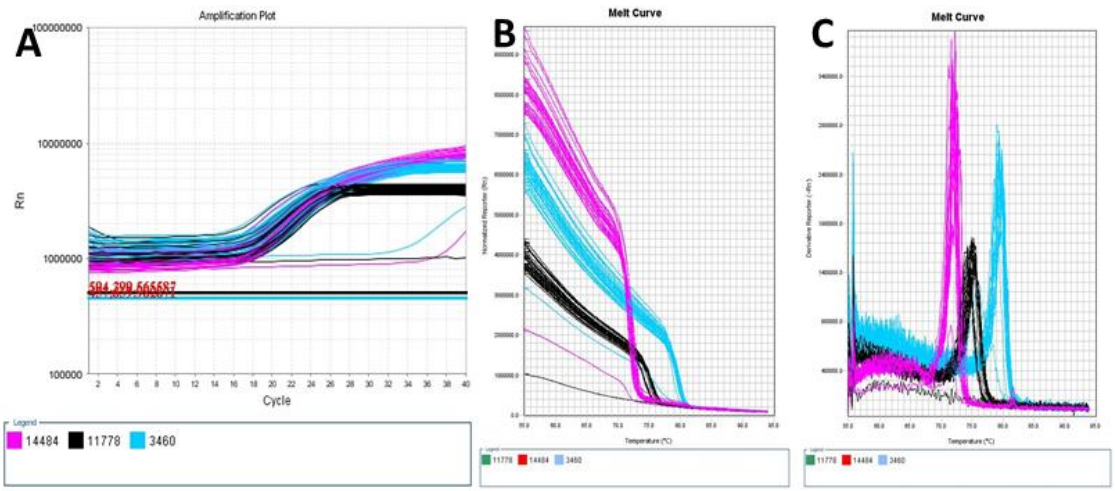

Figure 12. *For a complete Real-Time PCR plate: (A) Amplification Plots; (B) Normative Melt Curve; (C) Derivative Melt Curve.*

The positive genetic variants are distinguishable from controls (Supplementary Figure 3). The aligned melt curves are produced by the HRM software, automatically adjusted for the region of analysis interest, as seen in Figure 13. There is a clear distinction between negative and positive results, as evidenced by the clear grouping of the two colors. In the amplification analysis, the presence of a lower plateau in fluorescence affected variant identification, since the HRM software identified it as another variant than that of the remaining triplicates.

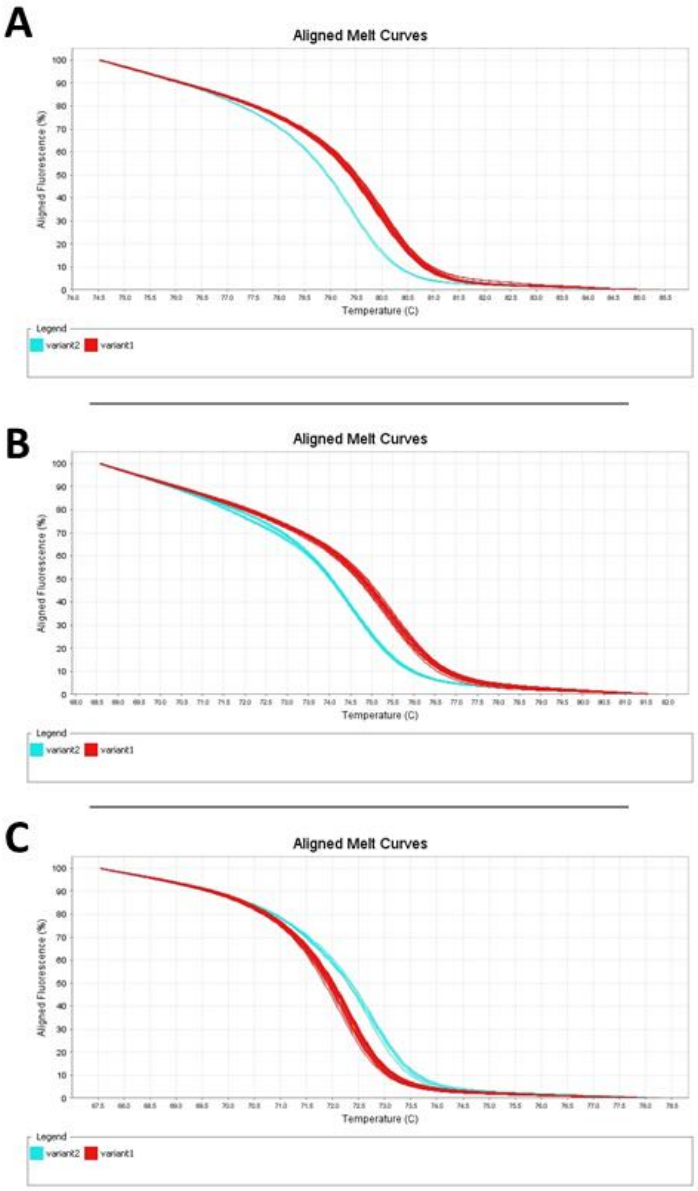

Figure 13. *Aligned Melt Curves, from the HRM Software, with variant calling (discriminated by color), for a complete plate. Representation per target: (A) m.3460G>A; (B) m.11778G>A; (C) m.14484T>C.*

4.1.5. Discussion

This approach presents as an easier and faster method to identify the TOP-3 LHON genetic variants, with the software resolving much of the identification process, providing the variant identification and its confidence value.

The use of triplicates is recommended, for any cases in which well omission is necessary or preferred. Well omission occurs when issues on the amplification curve, that could disrupt the software variant classification, are seen: elevated starting fluorescence, absent or late amplification (absence of plateau stage), and low amplification (distinctly

lower plateau). These problematic factors could create results that the HRM software considers different variants, confounding the deductive process.

According to results presented in Figure 13, if triplicates would show different variants, one of two things could happen: i) the confidence value on one of the wells would be much lower, which would exclude it; ii) there was low or no amplification, which could be seen in amplification curves or with very high C_T values. These variants would be discarded, considering the remaining triplicates' variant as the true result.

The average time of preparation is 90 minutes, with further 135 minutes of Real-Time PCR run time, each run allowing the assessment of eight samples in triplicate.

This technique easily allows for two different runs in one 8-hour workday. This second run can be used for a different set of samples, allowing the screening of a total of 16 samples per day, or, if seen as necessary to confirm or clarify results and boost their robustness, screen eight samples and their confirmation run.

The confirmation runs showed that the hardware and software have the capacity to correctly assign all samples, since all the results were correct.

The variants in study comprise 95% of all pathogenic variants found in LHON cases, thus being useful in a considerable number of cases. If the result is negative, other methods, such as NGS, can be used to search for other rare LHON variants (85), indicated in Table 1.

Given the fact that the amplified sequence may contain other sequence variants (benign or pathogenic SNVs), it is possible that it will translate in HRM analysis as a third variant (different from positive and negative controls) or as a false (positive or negative) result. Since HRM is based on the sample's T_m value, and this is obtained from the G+C/A+T ratio, the possibilities were analyzed in detail and can be classified as follows:

i. The third variant comes from any nucleotide change that is different from the one in screening, since it alters T_m by making the value either too high or too low in comparison to the values expected.
ii. False positives have the same T_m as the mutant sample, which can happen if WT samples have the same nucleotide change in another nucleotide. Other changes in WT can also alter the T_m to mutant values; any other nucleotide change that establishes the same GC/AT content that is seen in the mutant sample will then lead to a T_m that closely resembles the one of the mutant sample, creating a false positive (Tables 6-8).
iii. False negatives might happen when mutant samples have the reverse change (if the variant is G>A, then it would need a simultaneous A>G). As with false positives, false negatives can happen from other nucleotide changes, if they occur simultaneously with the pathogenic variant. These differences are related with GC/AT content (Tables 6-8).

This can happen for any SNVs located in that amplicon span; below, on Tables 6, 7 and 8, the possible nucleotide changes that can be found in these amplicons are presented, although *de novo* variants may also occur.

The tables 5-8 summarize which nucleotide changes are relevant for each pathogenic variant.

Table 5. *Nucleotide changes that HRM would indicate as false negatives or positives in the TOP-3 LHON pathogenic sequence variants' genetic screening.*

	m.3460G>A & m.11778G>A	**m.14484T>C**
false negative	A>G	C>T
	T>C	G>A
	G>T	G>T
	A>C	C>A
false positive	G>A	T>C
	C>T	A>G
	G>T	A>C
	C>A	T>G

Table 6. *List of SNVs that could originate a false positive or false negative HRM result, for m.3460G>A analysis.*

	Nucleotide change	**Nucleotide**	**Frequency (%)**	**Associated diseases**
false negative	A>C	3468	ND (1 r.c.)	
	A>G	3463	ND (2 r.c.)	
		3465	ND (5 r.c.)	
		3468	ND (4 r.c.)	
		3480	3.9	Somatic Variation (Tumor)
	T>C	3456	0.1	
		3470	ND	Somatic Variation (Tumor)
		3472	ND (5 r.c.)	LHON (Reported); Polymorphism
		3473	ND (1 r.c.)	
false positive	C>A	3471	ND (2 r.c.)	
	C>T	3459	ND (5 r.c.)	
		3462	ND (6 r.c.)	
		3469	ND (1 r.c.)	
		3471	ND (1 r.c.)	
		3474	ND (6 r.c.)	
	G>A	3481	ND	MELAS (Reported)
		3483	0.4	
third variant	A>T	3465	ND (2 r.c.)	
	G>C	3483	ND (2 r.c.)	

r.c.: reported cases

Table 7. *List of SNVs that could originate a false positive or false negative HRM result, for m.11778G>A analysis.*

	Nucleotide change	**Nucleotide**	**Frequency (%)**	**Associated diseases**
false negative	A>G	11785	ND (1 r.c.)	
	T>C	11781	ND	Somatic Variation (Tumor)
false positive	C>T	11779	ND (9 r.c.)	
		11782	0.1	
		11788	0.1	

r.c.: reported cases

Table 8. *List of SNVs that could originate a false positive HRM result, for m.14484T>C analysis.*

	Nucleotide change	**Nucleotide**	**Frequency (%)**	**Associated diseases**
false positive	A>G	14495	ND (2 r.c.)	LHON (Confirmed); TOP-19
		14497	ND (21 r.c.)	
		14500	ND (22 r.c.)	
		14501	ND (9 r.c.)	
		14506	ND (2 r.c.)	
		14509	ND (9 r.c.)	
		14513	ND (1 r.c.)	
		14517	ND (9 r.c.)	
		14518	0.1	
		14524	ND (11 r.c.)	
		14526	ND (3 r.c.)	
		14527	0.4	
		14536	ND (4 r.c.)	
		14539	ND (6 r.c.)	
	T>C	14487	ND	Leigh (Confirmed)
		14488	0.1	
		14494	ND (17 r.c.)	
		14498	ND	LHON (Reported); Polymorphism
		14502	0.4	LHON (Reported); TOP-19
		14503	ND (6 r.c.)	
		14512	ND (17 r.c.)	
		14514	ND (20 r.c.)	
		14515	ND (17 r.c.)	
		14530	0.1	
		14540	ND (11 r.c.)	
	T>G	14530	ND (1 r.c.)	

r.c.: reported cases

Table 9. *List of SNVs that could originate a false negative or third variant HRM result, for m.14484T>C analysis.*

	Nucleotide change	Nucleotide	Frequency (%)	Associated diseases
false negative	C>A	14491	ND (1 r.c.)	
		14533	ND (5 r.c.)	
	C>T	14485	ND (15 r.c.)	
		14491	ND (12 r.c.)	Somatic Variation (Tumor)
		14521	ND (3 r.c.)	
		14529	ND (1 r.c.)	
		14533	ND (11 r.c.)	
third variant	T>A	14498	ND	Somatic Variation (Tumor)
		14512	ND (2 r.c.)	
	A>T	14496	ND	
		14527	ND	
	C>CC	14536	ND	DMDF (Reported)
	C>G	14520	ND	

r.c.: reported cases

The variant m.3480G defines the haplogroup K, associated with high frequencies in populations originating in Europe and Near East, particularly in the Ashkenazi Jewish ethnicity. Accordingly, the screening of the TOP-3 pathogenic variants is predicted to be a challenge in different populations.

In order to assure the maximum specificity of the test in a timeless screening, as presented, an additional method may be required to improve quality control, since all techniques have limitations.

This shows that older methods may still have an important role in genetic analysis and deserve to be rehabilitated. If it is the case, the samples may be also analyzed alongside PCR-RFLP. The combination of the advantages of that method and of this approach would enable the attainment of a robust result, while still keeping to the 24-hour period, without significantly increasing the costs.

The approach presented here is robust for genetic variant analysis. The development of this screening was centered around the aim of ameliorating the conditions presented by other techniques (RFLP, pyrosequencing, other PCRs, Sanger sequencing and NGS (80,85)), comparing time/cost/labor; particularly time, since this is an essential issue for starting therapy. Techniques like RFLP are surpassed in terms of robustness and time, although still important as a complementary method. Sequencing techniques give robust

and accurate results, but they take much longer due to the arduous task of data analysis and present higher costs. Considering the month-long wait for NGS data analysis, this 24-hour turn-around method is extremely helpful in creating faster clinical action, including therapeutic decision. Furthermore, it presents less labor than that associated with all techniques mentioned (73,75,80,82,85). The developed approach can be implemented by any laboratory with access to a real-time PCR machine capable of detecting the SYTO®9 dye (dsDNA binding dyes) and with HRM settings.

A few other similar techniques have been developed, relying on ARMS primers (82,85), or TaqMan® probes (86). But here, by using normal primers, an easier and less costly method is created; having less optimization issues, because it does not inevitably require multiplex analysis, as is the case of ARMS, and, furthermore, not increasing costs, as TaqMan® probes would. Multiplex is not necessarily obligatory for ARMS primers, but without it, more wells will be used, which means that, to maintain triplicates, the number of samples being analyzed per plate must be reduced, thus compromising the in-mass quickness, as well as increasing the cost. The primers used in the present study have a very high level of specificity, as verified by bioinformatics' tools.

4.1.6. Conclusions and Future Perspectives

The developed and presented approach allows for the detection of LHON TOP-3 genetic variants, distinguishing between a wild-type and a pathogenic sequence variant, with minor differences in amplicon. These variants comprise about 95% of all genetic positive LHON cases, thus being very useful in a clinical setting.

The method is robust, simple, of easy-analysis, fast and cost-efficient. This detection is reliable enough to inform the medical decision on diagnosis and therapeutics, and its implementation would allow timely action, which is essential for recovery of eye function and vision, if possible.

This is a pioneering study with a notable contribution to make personalized and precision medicine a reality, which is closer to the patients' needs, who will benefit from this study worldwide.

4.1.7. Acknowledgements

The authors are grateful to the patients for their contribute to this work and wish to acknowledge Doctors Paula Garcia, Teresa Kay, Helder Simões, Marta Zegre Amorim, Joana Patrícia Ferreira, Cristina Camilo, Sara Martins, Ana Gaspar, Ana Berta Sousa, Joaquim Murta and Rufino Silva for additional contributions to this work, concerning patient managements.

4.1.8. Funding

This work was financed by the European Regional Development Fund (ERDF) funds through the COMPETE 2020 - Operational Programme for Competitiveness and Internationalisation (Strategic project POCI-01-0145-FEDER-007440;

HealthyAging2020 CENTRO-01-0145-FEDER-000012-N2323) and Portuguese National Funds via FCT – Fundação para a Ciência e a Tecnologia, through the strategic plan UID/NEU/04539/2019, the project Pest-C/SAU/LA0001/2013e2014 and a Doctoral grant FCT-SFRH/BD/86622/2012; Portugal. The LBioMiT is also financed by Santhera Pharmaceuticals, allowing the implementation of the national project “Investigação Translacional Epidemiológica, Bigenómica e Funcional nas Atrofias Ópticas” (PI Professor Manuela Grazina).

4.1.9. Conflicts of Interest

The authors declare no conflicts of interest.

5. Hearing Loss

5.1. Development of a screening method for detection of TOP-3 mitochondrial pathogenic sequence variants associated to Aminoglycoside-induced Hearing Loss

5.1.1. Materials & Methods

5.1.1.1. Study Design and Sample Collection

The population in study included 32 samples: ten non-HL patients (with suspicion of other MC), ten healthy controls, seven samples of patients with suspected MNSHL and five non-affected relatives. Total DNA was previously extracted from several tissues including whole blood, muscle homogenate (from biopsy, usually from deltoid) and amniocytes (from amniocentesis) according to standard protocols, in the scope of diagnostic investigation.

The samples were analyzed for the m.1555A>G pathogenic sequence variant. Three additional samples were used: a synthetic positive control for m.1494C>T, a positive control for m.7445A>G (negative control for m.1555A>G), and a negative control sample. All samples have been previously analyzed and genotyped by at least one additional method (Sanger, NGS or PCR-RFLP), for diagnostic purposes. All samples were identified, allowing for result comparison and confirmation of the true/false status of ARMS Real-Time PCR amplification results.

Control samples of healthy individuals in this study were completely anonymized, accordingly to the European Union General Data Protection Regulation (Regulation (EU) 2016/679) and to Portuguese Law (DL no. 58/2019 and no. 59/2019). Patient samples were obtained for diagnosis with informed consent, accordingly to DL no. 12/2005, no. 131/2014 and the Norm 015/2013 of the Directorate-General of Health, following the Tenets of the Helsinki Declaration.

5.1.1.2. Primer Design

The variants were chosen considering literature and bioinformatic records, being reported as the three mtDNA pathogenic sequence variants with a primary role in non-syndromic, ototoxic HL. The gene of each variant in study was localized in *MITOMAP*, then searched for *Homo sapiens* sequence in *NCBI Gene*. The sequences of those genes (*MTRNR1*: ID 4549; *MTCO1*: ID 4512; *MTTS1*: ID 4574) were used to design the primers. Due to the fact that m.7445A>G is the last nucleotide of *MTCO1*, and is behind the first nucleotide of *MTTS1*, both genes were used for the design.

As explained previously, ARMS is based on the amplification inefficiency by specific primers, in which the target sequence is preferentially amplified in the presence of the perfect-match primer and poorly amplified when annealing to a mismatched primer (75); featuring the introduction of an additional mismatch (75) based on the nucleotide change.

The requirements for primer design were i) sensitivity, ii) specificity of reaction, iii) products' size (70-300 bp in length), iv) only one sequence variant per amplicon, v) products should be dissimilar from possible unspecific amplification of pseudogenes. Short amplicon length allows for detection of sequence variants, inversions, insertions and deletions, while avoiding detection of other variants. However, if PCR products are too small, they cannot produce enough fluorescence for detection.

Primer design was performed using bioinformatic/*in-silico* tools, namely *Primer3Plus* (http://www.bioinformatics.nl/primer3plus), *WASP* (http://bioinfo.biotec.or.th/WASP), *PrimerBLAST* (https://www.ncbi.nlm.nih.gov/tools/primer-blast/) and *Primer1* (http://primer1.soton.ac.uk/primer1.html).

Each primer pair obtained was processed by bioinformatic tools, namely *USCS In-Silico* (https://genome.ucsc.edu/cgi-bin/hgPcr) and *USCS BLAT* (https://genome.ucsc.edu/cgi-bin/hgBlat). Firstly, the specificity of primers pairs was checked by assessing which PCR products the pair produced. The obtained amplicon sequence in *USCS In-Silico* was then assessed by *USCS BLAT* for evaluating its similarity in the mitochondrial and nuclear human genomes, the latter of which contains pseudogenes. The *USCS BLAT* screens whole gene for similar DNA sequences in comparison to the introduced amplicon, that is, it shows how unique or identical the amplicon sequence is within the human genome. It also provides detailed information about the most similar sequences, and how similar (%) they are. Values nearing 90% were considered acceptable; the similarity percentage and the span of the sequence were both considered.

For HL, primer design with bioinformatic tools was unsuccessful, pertaining to both primer specificity and amplicon similarity to pseudogenes. Thus, primers for the MNSHL approach were hand-designed, to obtain primer pairs and subsequent products that obeyed the parameters described above.

The start-off point was the variant's placement, since one of the primers would need to overlap that nucleotide on the 3'-terminal. A length of 18-23bp was used for a framework. From there, different options were analyzed, while considering annealing temperature, GC% content and other parameters named above. The second primer was designed taking into account these parameters, as well as the resulting amplicon and its properties.

Furthermore, the mitochondrial gene regions were aligned with NCBI's *BLAST* tool (*blastn*, *megablast*), allowing comparison with the nuclear chromosomes, assessing pseudogenes, and the best way to avoid their amplification. With the *MTRNR1* gene (SNVs 1494 and 1555) it was necessary to account for the chromosomes 11, 5 and 17. The *MTCO1* and *MTTS1* genes had pseudogenes in the chromosomes 1, 5, 3 and 17. The alignment was analyzed for SNV differences between the two genomes, trying to gather as many nucleotide differences between nuclear and mitochondrial product as possible, while also having the product's length short enough for real-time PCR.

Moreover, regions with nucleotide differences were used as primer locations, in order to create even more mismatches, and thus more specificity.

These primers were then submitted to the *in-silico* analysis as above described. Results are presented at Table 9.

Since no combination of set-up conditions were satisfactorily obtained for considering the experiment optimized, other primer pairs were later designed. These primers agreed to the same conventions stated above, with differences pertaining to primer placement (the specificity occurring in the reverse rather than in the forward primer for m.7445A>G) and the location or nature of the extra-mismatch nucleotide (the mismatch could take place in the 3rd to last nucleotide instead of the 2nd to last, or the mismatch could be represented by another mismatched nucleotide).

Each pair of primers identifies only one of the three variants at a time. The position of amplicons in the *Homo sapiens* mtDNA is as unique from pseudogenes as possible, but it might carry some other mtDNA SNVs.

5.1.1.3. Primer Preparation

The primers used are described in Table 9 (further information available upon request). The primers were resuspended into a 50μM (final concentration) solution with Tris-EDTA buffer (TE) (1:10), and vortexed to ensure homogenization. Further dilutions were made with TE (1:10). This was done in a sterilized PCR workstation, to prevent contamination of the original stock or the diluted primer solutions.

Table 10. *Real-Time PCR ARMS primers for MNSHL variants*

Name	# bp	Product size (bp)	Highest Similarity (sequence span)
1494F	22	145	97.2% with chr 5 & 11 (140/145)
1494R-WT	24		
1494R-M	24		
1555F-WT	24	190	95.8% with chr 5 (624/190) & 97.2% with chr 11 (176/190)
1555F-M	24		
1555R	23		
1555F_WT_2	23	189 (with 1555R)	95.8% with chr 5 (624/190) & 97.2% with chr 11 (176/190)
1555F_M_2	22		
1555C^{-}	24	189 (with 1555R)	96.4% with chr 5 & 97.8% with chr 11 (176/190)
1555MT	23		95.3% with chr 5 & 96.6% with chr 11 (176/190)
1555smut	26		95.8% with chr 5 & 97.2% with chr 11 (176/190)
7445F-WT	24	103	98.1% with chr 1 & 88.4% with chr 5 (103/103)
7445F-M	24		
7445R	23		
7445F	21	229	98.7% with chr 1 & 97.4% with chr 17 (230/230)
7445R_WT_2	22		
7445R_M_2	22		
7445R_WT_3	22	230 (with 7445F)	98.7% with chr 1 & 97.4% with chr 17 (230/230)
7445MT	23		98.3% with chr 1 & 97% with chr 17 (230/230)
7445smut	25		98.7% with chr 1 & 97.4% with chr 17 (230/230)
7445C^{-}	25		99.2% with chr 1 & 97.9% with chr 17 (230/230)

5.1.1.4. Optimization of MNSHL protocol

The reaction was prepared inside a sterile PCR workstation that was pre-treated under UV-light for 15 minutes. The iTaq™ Universal SYBR® Green Supermix (BioRad), featuring SYBR® Green I dye, was used.

The reaction was run in the Applied Biosystems™ 7500 Fast Real-Time PCR, with the 7500 Software v2.0.6.

Optimization was conducted with three positive samples (one for each variant), one negative control and one NTC. The protocol of the dye manufacturer was followed

considering both set-up and reaction mix, with variables of those being altered as necessary for the specificity of the experiment.

First, annealing temperature was setup at 55ºC, 60ºC, 65ºC and 62.5ºC, with the latter presenting the best results. However, unspecific products (primer-dimers) and the unwanted target continued to amplify; therefore, to increase specificity, the reaction mix was modified. There was introduction of DMSO, primer concentration was fluctuated, and DNA concentration was decreased (from 20ng/µL to 10ng/µL). However, the problems persisted for m.1555A>G and for m.7445A>G detection, with both having amplification of mutant and WT samples in WT target, and m.7445A>G presented unspecific amplification (see 5.1.2.).

Since no combination of set-up conditions were satisfactorily achieved, other primer pairs were designed. This redesign is described in 5.1.1.2. As previously, several conditions were experimented for optimization: DNA was diluted in 20ng/µL, 10ng/µL and 5ng/µL; primers were tried at 500nM, 300nM, 200nM and 100nM concentrations; and DMSO was used at concentrations 5%, 4.5%, 4%, 3.5%, 3%, 2.5% and 2%. The annealing temperature was maintained at 62.5ºC.

In the end, m.1555A>G partial optimization occurred with 10ng/µL, 100nM of primer concentration and, for the WT target (where wild-type samples would specifically amplify) reaction set-up, 4% of DMSO was added to the mixture, while, for the mutant target, 4.5% of DMSO was added.

At the deadline for finishing the laboratory work for the present thesis, the optimization of the screening for m.7445A>G and m.1494C>T was considered unsuccessful, and the implementation was achieved only for the analysis of the m.1555A>G variant, although improvements are still necessary.

5.1.1.5. Implementation

The implementation proceeded for the m.1555A>G variant analysis, using 32 samples, ten of which were healthy controls, ten patients with other MCs, and 12 samples positive for m.1555A>G, seven of which were of patients and five from carriers. The seven patient samples were obtained from five patients, with two of them providing two samples each; the same happened with one relative, who provided two samples. These duplicate samples were obtained from different tissues. The effect on results is discussed in 5.1.3.

All samples were prepared inside a sterile PCR workstation that was pre-treated with UV light for 15 minutes. The iTaq™ Universal SYBR® Green Supermix (BioRad), featuring SYBR® Green I dye, was used. The experiments were run according to the best optimization conditions for the 1555WT target, the reaction mix included 5µL of Supermix, 100nM of each primer, 10ng of genomic DNA and 4% of DMSO; and for the 1555M target, the reaction mix had 4.5% of DMSO; both for a final volume of 10µL per well. Samples were analyzed in duplicates.

The reactions were run at the Applied Biosystems™ 7500 Fast Real-Time PCR, with the 7500 Software v2.0.6. The program set-up used is described in Table 10.

Table 11. *PCR run set-up conditions*

Stage	Step	Temperature	Time
Holding	Enzyme Activation	95ºC	2-5min
Cycling (40 cycles)	Denature	95ºC	15s
	Anneal/extend	62.5ºC	60s
Melt curve Analysis		60ºC-95ºC	0.5ºC increment at 2.5s/step

Variant calling was performed by assessing the amplification of the samples in WT and mutant targets. A WT sample should be amplified in the WT target and non-amplified in the mutant target and conversely. Variant calling was then crossed with the previously known identification, performed in a single-blind manner.

5.1.2. Results

Samples were also assessed by other, previously established, techniques (Sanger sequencing, NGS, PCR-RFLP), being identified as positive or negative for the variants in study.

Some of the first primer pairs did not produce the expected result as necessary, showing unspecific products. New pairs were designed for the screening of m.1555A>G and m.7445A>G, which solved that problem. The first primer pair for m.1494C>T analysis did not produce any unspecific products.

The unspecific amplification, in the first primer pair for m.7445A>G analysis, was a primer-dimer that presented with a T_m=68ºC; the primer pair had a possible overlap area (composed of five T/A), which, considering all possible primer pairings, could create a product of 27 to 36 nucleotides. The possible sequences were run for *in-silico* analysis with *EndMemo - DNA Melting Temperature (Tm) Calculator*, and the predicted value of T_m was 67ºC, close to the observed value.

Partial optimization was possible for the m.1555A>G variant screening (Figure 14), presenting very good amplification results for positive (mutant) samples (Figure 15A) and reasonable amplification for the negative (WT) samples (Figure 15B). Implementation was performed in 32 samples, 12 of which were positive and 20 were negative. Amplification products presented good C_T values for all targets, achieving plateau and emitting enough fluorescence for detection.

While mutant samples are well identified, with amplification appearing only in 1555M target, this was not the case with wild-type samples, which presented amplification in both targets. Accordingly, this assay still needs improvement to be considered optimized.

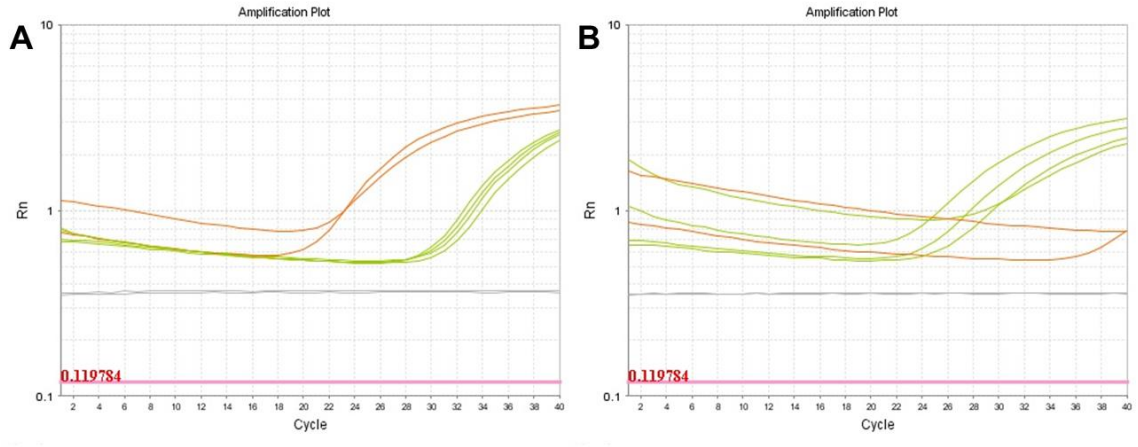

Figure 14. *(A) Positive and negative samples in the 1555 mutant target mix; (B) negative and positive controls in 1555 WT target reaction. Green represents the positive/mutant samples, and the orange the negative/wild-type samples.*

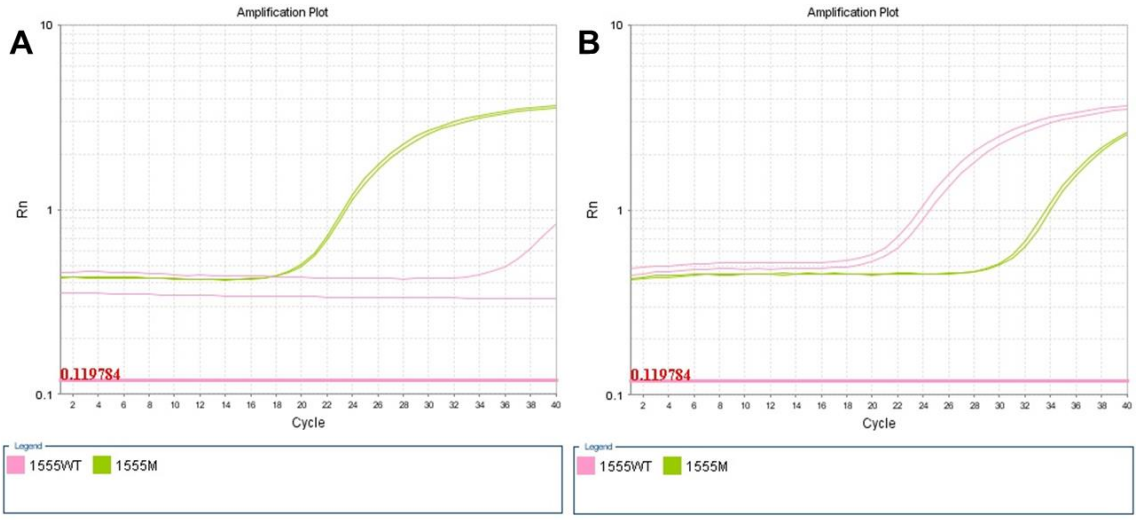

Figure 15. *(A) Example of the screening of a mutant sample. (B) example of the screening for a wild-type sample.*

As referenced before (in 5.1.1.5.), six samples were coupled, with three individuals (two patients and one relative) providing two positive samples each. After variant calling and confirmation (all correctly assigned), the pairs were compared to see if results differed. It was observed that DNA extracted from muscle (two of the three pairs) (Figure 16) presented earlier amplification in both the WT and mutant targets, and that the levels of fluorescence detected could sometimes be more elevated in the plateau stage. The C_T difference (values of average of duplicates) is related in Table 11. The other pair had DNA extracted from whole-blood (lymphocytes) and DNA extracted from amniocytes (Figure 17A and 17B), where amplification and C_T values was similar, with amniocytes amplifying only slightly earlier (Table 11). The amplification profile of these lymphocyte

samples was average, since they were very similar to the profiles of other lymphocyte samples (Figure 17C and 17D), meaning that the observed differences between tissues are relevant. However, the differences in amplification profile did not affect variant calling or the difficulty in doing so.

Table 12. *Comparison of C_T values between different types of tissues, by pair.*

	Lymphocyte pair 1	**Muscle pair 1**	**Lymphocyte pair 2**	**Muscle pair 2**	**Lymphocyte pair 3**	**Amniocyte pair 3**
M	19.83	16.125	19.235	16.31	19.12	17.96
WT	37+undt	28.365	31+undt	32.87	33.745	33.225

undt: undetermined (= no amplification = no C_T).

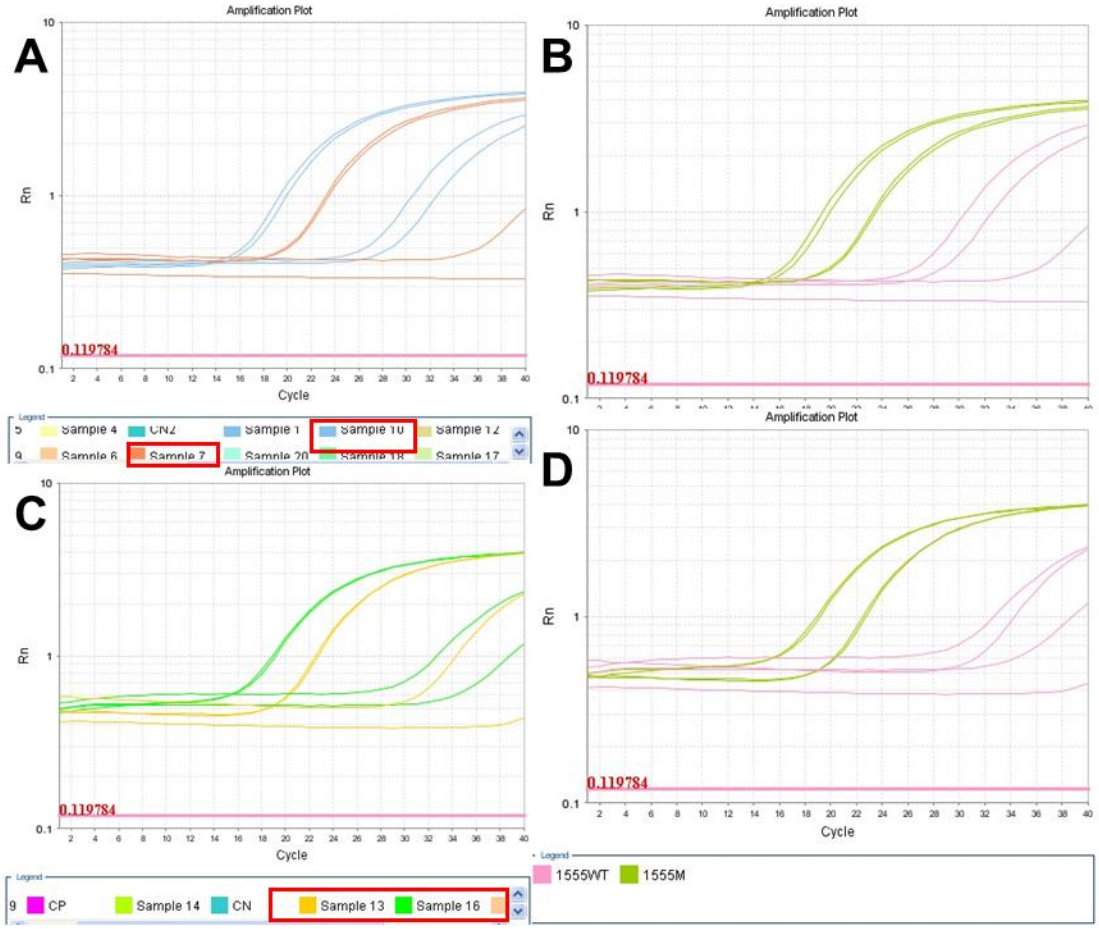

Figure 16. *Comparison between lymphocyte samples and muscle samples. (A) Amplification comparison between lymphocyte (Sample 7, in orange) and muscle (Sample 10, in blue) and (B) Amplification comparison of the same pair but differentiated by target. (C) Amplification comparison between lymphocyte (Sample 13, in yellow) and muscle (Sample 16, in green) and (D) amplification comparison of the same pair but differentiated by target.*

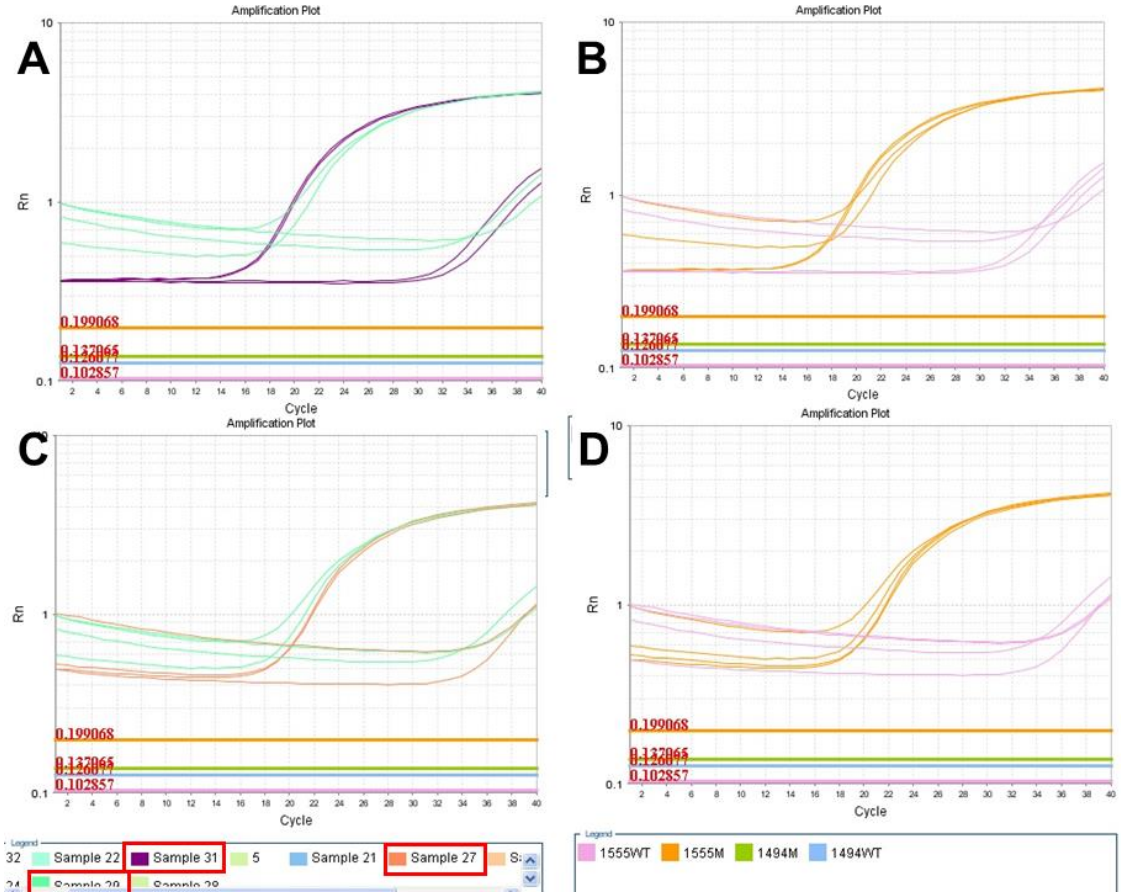

Figure 17. *Amplification comparison between samples. (A) Amplification comparison between lymphocyte (Sample 29, in green) and amniocyte (Sample 31, in purple) and (B) amplification comparison of the same pair but differentiated by target. (C) Amplification comparison between lymphocyte (Sample 29, in green) and another lymphocyte (Sample 27, in orange) and (D) amplification comparison of the same pair but differentiated by target.*

Concerning the detection of the pathogenic variant m.1555A>G, all of the 32 samples were correctly identified as positive or negative, with identification and confirmation performed with a single-blind analysis, presenting no false positives or false negatives. Accordingly, sensitivity, specificity, negative predictive and positive predictive values all equal 1.

Optimization of m.1494C>T (Figure 18) analysis was possible for the mutated target, but the WT target still displayed amplification of both WT and mutated variants; thus, implementation was not possible. Furthermore, implementation of the screening of this pathogenic variant would have uniquely negative results, because no positive samples were easily accessible.

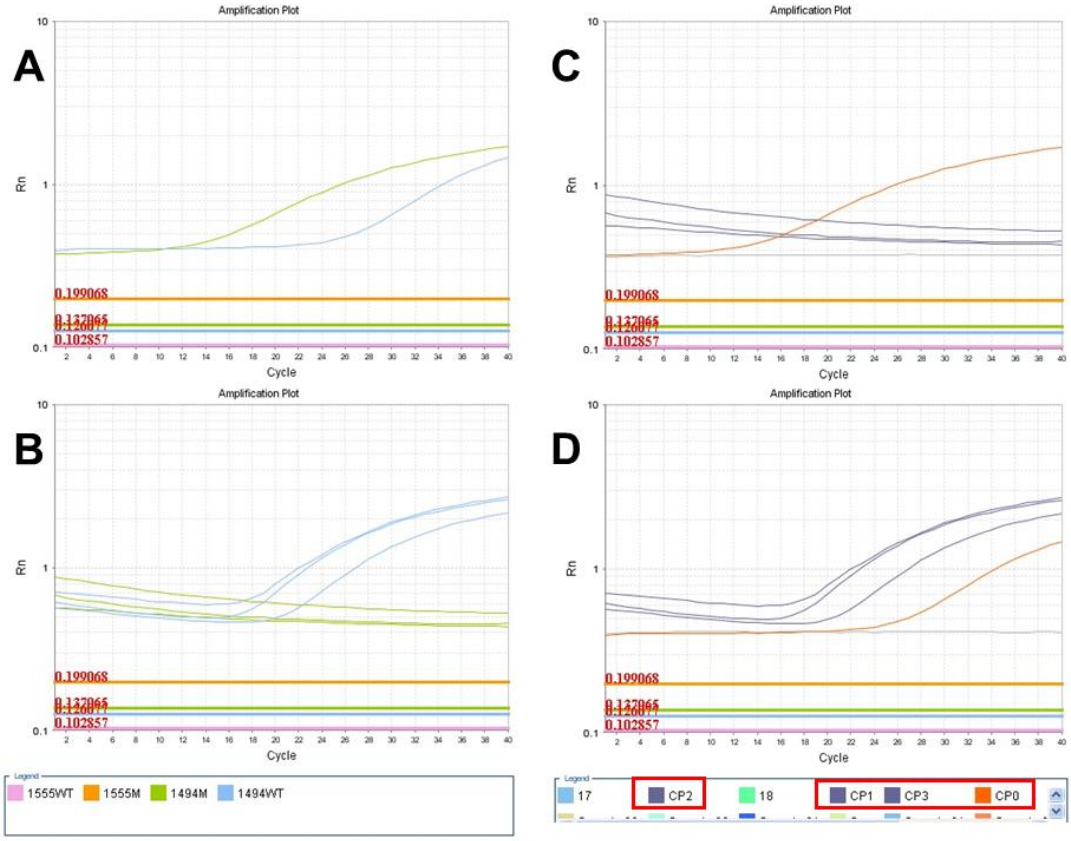

Figure 18. *Optimization of screening for m.1494C>T. (A) Mutant control and (B) WT control analyzed by target. (C) Positive and negative controls in the mutant target reaction and (D) controls in the WT target reaction. Controls in blue are wild-type, and the orange is the mutant.*

Optimization of m.7445A>G (Figure 19) screening was not possible for WT target, with amplification of both WT and mutant samples happening. Optimization for the mutant target was possible, but unable to be implemented without the WT target.

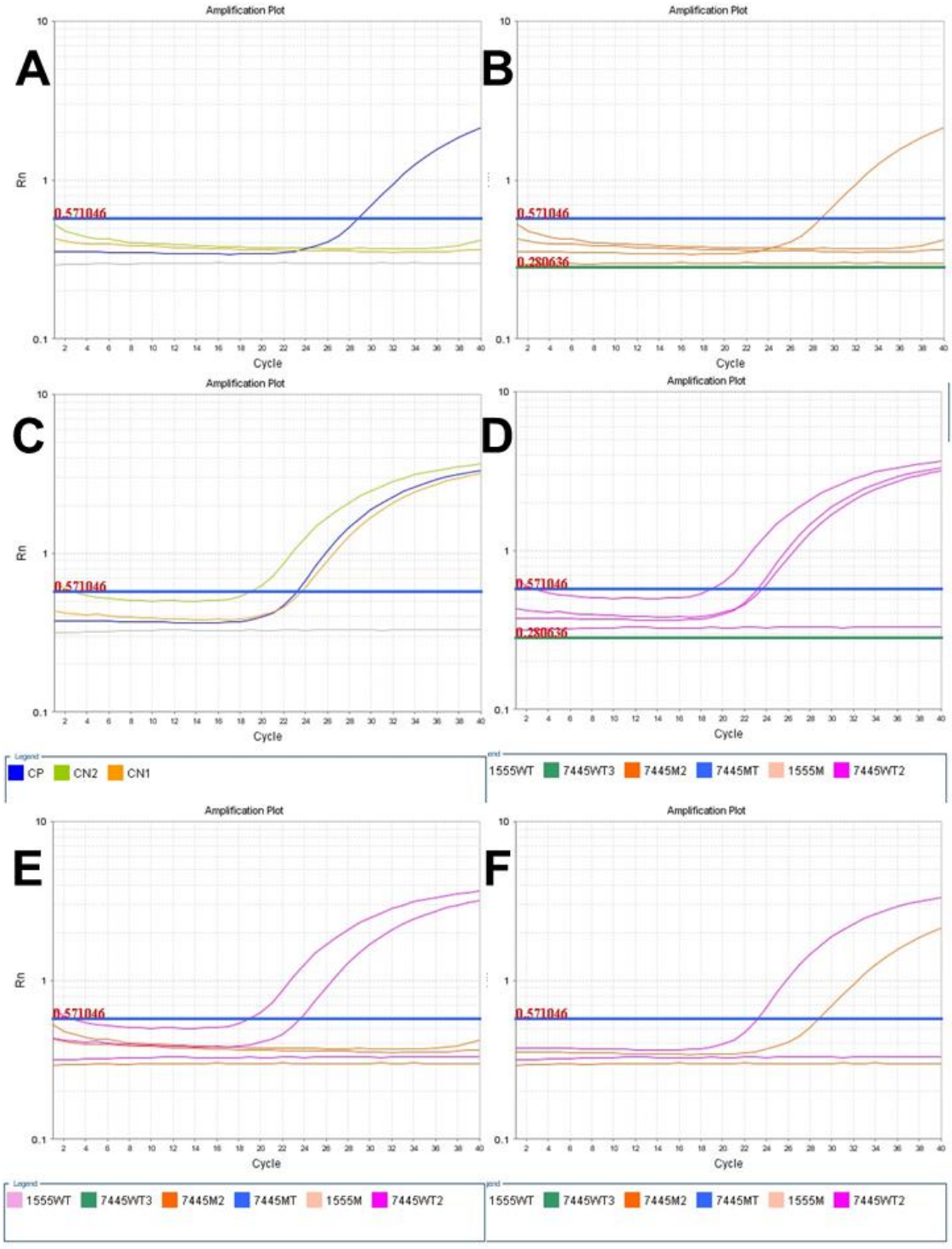

Figure 19. *Optimization of screening for m.7445G>A. (A) The mutant target reaction with positive and negative controls, discriminated by target and (B) by sample, in which the single amplification is of the mutant sample. (C) The WT target reaction with positive and negative controls, by sample and (D) by target. CN1 and CN2 are WT samples; CP is the mutant sample. (E) WT control and (F) mutant control analyzed by target.*

Double amplification also occurs in 1555M target, but the unspecific amplification is residual, with big differences in C_T between the two variants.

The 7445WT and the 1494WT targets present similar amplifications in both wild-type and mutant control samples; the difference is in the fact of being possible to distinguish 1555 targets, but not the targets for the other M/WT sequence variants.

5.1.3. Discussion

Optimization was only possible for the analysis of m.1555A>G, although improvements can be made, and further optimization of m.1494C>T and m.7445A> screening is necessary. The PCR set-up could be adjusted in order to obtain the best conditions for the non-optimized targets, or, if that ultimately fails, an approach with TaqMan® probes could be used instead. These probes generate fluorescence only when they hybridize with target sequences, increasing specificity (87). However, it is more expensive.

For m.1555A>G analysis implementation, WT samples still presented amplification in both mutant and WT targets, making it less intuitive to make a variant call. However, there are two possibilities to distinguish and identify samples: i) if there is WT target amplification, it should be a WT sample, because otherwise no amplification would have occurred and it would be higher than the 1555M; moreover, in mutant samples there is only amplification in the mutant target, or residual 1555WT target amplification; ii) according to description (section 5.1.2.), it is possible to perform an identification by the differences in amplification profiles/C_Ts; that is, with the WT sample, 1555WT target amplification would present earlier (lower C_T) than 1555M and with higher fluorescence. This state is not ideal, but it allowed for correct calling of all samples in a preliminary phase of the screening set-up.

All samples tested were homoplasmic; but the question arises of what would be the result if the sample tested was heteroplasmic. In theory, amplification would only occur in one target with homoplasmy, and the occurrence of both target amplifications would occur in a heteroplasmic situation. However, as this happens in WT samples already, this type of thought process becomes hindered and the call of heteroplasmy/homoplasmy is not possible as of now.

Another observed variation involved the type of tissue from which DNA was extracted. In the three pairs of samples, there were differences in amplification between muscle and lymphocytes (Figure 16), with the former presenting higher levels of fluorescence and lower C_T values. This is justified by the higher mtDNA copy number present in muscle in comparison to blood (88–90). Lymphocytes and amniocytes (Figure 17A and 17B) do not present significantly different amplification profiles, but it is still possible to see an earlier C_T in amniocytes, but these differences are lesser compared to other lymphocytes (Figure 17C and 17D) than to muscle. Thus, the type of tissue from which DNA was extracted should be considered in analysis. For example, muscle samples are much more susceptible to amplify both targets, regardless of mtDNA variant. Furthermore, differences in amplification profile did not affect variant calling, so the only potential problem would be the heteroplasmy identification. Moreover, since the aim of the screening is a quick screening, the sample collection for analysis favors the whole blood, since it is a much more accessible tissue.

The approach planned presents an easier and faster method for identifying the genetic variant, being a closed-tube analysis, with easily readable results of a Yes/No profile. This type of technique has been used by others in other MCs (82,85). It has also been used for HL, but without including the trio of variants (91,92), usually with m.7445A>G being left out. The use of duplicates or triplicates is recommended, to better assess if sample's amplification or the quality of the result.

Other techniques for MNSHL screening have been developed, but they usually do not include this trio of pathogenic sequence variants, usually excluding the m.7445A>G variant (93–95) and often only including the m.1555A>G variant (96). This might be explained with the population's variant frequency shifting across the globe, and some variants become less interesting to assess in the populations investigated by other groups. Wang *et al.* (2017) (97), presented a method with multiplexed fluorescent (dual-labeled self-quenched) probes to detect the three variants in study and one other (m.7444G>A). The detection was performed with MCA with three different detection probes. The impact of other SNVs in the analysis was not addressed by the authors. Analysis of the sequences presented high *BLAT* values for the amplicon having m.1494C>T and m.1555A>G (98.7%); the primer pair for the m.7445A>G-containing sequence presented unspecific amplification, of both mtDNA and chromosome 1, a pseudogene with 99.6% similarity with the mtDNA amplicon (difference of only one nucleotide with mtDNA).

The present approach was developed with the intent of ameliorating the conditions that other screening techniques (NGS, pyrosequencing, PCR-RFLP, Sanger sequencing (80,85)) present, particularly in terms of time when this is an essential issue for preventing AmAn-induced MNSHL, but also considering cost and labor. Techniques such like RFLP are capable of screening genetic variants relatively quickly (98), even if sometimes surpassed in terms of robustness and time, they remain important as a complementary method. Sequencing techniques give robust and accurate results, but they take much longer due to the arduous task of data analysis and present higher costs. Furthermore, the setting proposed involves less labor compared with other techniques mentioned (73,75,80,82,85).

The use of AmAn is restricted, but their use is still widespread in some regions of the globe and in certain conditions. Their broad-spectrum and rapid acting profile (99) makes them appealing for clinical use, particularly with hospital infections, as they are often used, due to antibiotic-resistant bacteria (99).

5.1.4. Conclusions

The aim of this setting could not be reached within the timeframe of this work and genetic screening was optimized and implemented for only one of the three variants in study, although requiring improvement. However, the successfully implemented analysis of m.1555A>G is the most common of the three pathogenic variants; thus, although the optimization of this approach was not fully materialized, the performance of the screening was possible for the most common of the variants associated with MNSHL.

Further optimization is necessary, in order to include the screening for m.7445A>G and m.1494C>T variants. For this to happen, new primers for these variants would need to be designed and submitted to the optimization process. Those primers could have a different mismatch or TaqMan® probes could also be used. These probes are more specific but also more costly than the ARMS primers or HRM. Since some problems continue to occur with the screening for m.1555A>G, the strategy used for this approach should be switched, and custom-made primers employed.

Multiplex analysis would also be of interest if possible, since it would allow for less Real-Time plate wells to be used, and thus more samples could be assessed in the same plate, reducing costs and obtaining an in-mass quickness in the analysis, which has a high clinical impact.

The development of such an approach for MNSHL is of the utmost importance because the hearing loss due to AmAn administration is so sudden and so easily preventable. The most pressing issue in this scenario is to assess quickly, since the treatment of infection needs to be handled as fast as possible to prevent complications and assure efficient treatment.

References

1. Alberts B, Johnson A, Lewis J, Morgan D, Raff M, Roberts K, et al., editors. Energy Conversion: Mitochondria and Chloroplasts. In: Molecular Biology of the Cell. 6th edition. New York City, NY, USA: Garland Science; 2015. p. 735–812.

2. Azevedo C, & Sunkel CE. Biologia Celular e Molecular. 5th ed. Lidel, editor. Lisboa: Lidel; 2012. 656 p.

3. Grazina MMM. Genoma Mitocondrial e Défice Energético no Diagnóstico das Doenças da Cadeia Respiratória Mitocondrial. Universidade de Coimbra; 2004.

4. Anderson S, Bankier AT, Barrell BG, De Bruijn MHL, Coulson AR, Drouin J, et al. Sequence and organization of the human mitochondrial genome. Nature. 1981;290(5806):457–65. DOI: 10.1038/290457a0

5. Andrews RM, Kubacka I, Chinnery PF, Lightowlers RN, Turnbull DM, & Howell N. Reanalysis and revision of the Cambridge reference sequence for human mitochondrial DNA. Nat Genet. 1999 Oct;23(2):147. DOI: 10.1038/13779

6. Grazina MM. Mitochondrial Respiratory Chain: Biochemical Analysis and Criterion for Deficiency in Diagnosis. In: Wong L-JC, editor. Mitochondrial Disorders: Biochemical and Molecular Analysis. Springer Science-Business Media; 2012. p. 73–91. DOI: 10.1007/978-1-61779-504-6_6

7. Alberts B, Johnson A, Lewis J, Morgan D, Raff M, Roberts K, et al., editors. Cell Death. In: Molecular Biology of the Cell. 6th edition. New York City, NY, USA: Garland Science; 2015. p. 1021–34.

8. Wallace DC, & Lott MT. Leber Hereditary Optic Neuropathy: Exemplar of an mtDNA Disease. In: Singh H, Sheu S, editors. Pharmacology of Mitochondria Handbook of Experimental Pharmacology, vol 240. Spring, Charm; 2017. p. 339–76. DOI: 10.1007/164

9. Schmiedel J, Jackson S, Schäfer J, & Reichmann H. Mitochondrial cytopathies. Cell Calcium. 2003;250:267–77. DOI: 10.1007/s00415-003-0978-3

10. Mitchell P. Coupling of phosphorylation to electron and hydrogen transfer by a chemi-osmotic type of mechanism. Nature. 1961;191(4784):144–8. DOI: 10.1038/191144a0

11. Berdanier CD. Mitochondria in health and disease. 1st ed. Berdanier CD, editor. Boca Raton, FL: Taylor & Francis/CRC Press; 2005. 619 p.

12. Thompson K, Collier JJ, Glasgow RIC, Robertson FM, Pyle A, Blakely EL, et al. Recent advances in understanding the molecular genetic basis of mitochondrial disease. J Inherit Metab Dis. 2019;(January):1–15. DOI: 10.1002/jimd.12104

13. Boggan RM, Lim A, Taylor RW, McFarland R, & Pickett SJ. Resolving complexity in mitochondrial disease: Towards precision medicine. Mol Genet Metab. 2019;(July):1–11. DOI: 10.1016/j.ymgme.2019.09.003

14. Gorman GS, Chinnery PF, DiMauro S, Hirano M, Koga Y, McFarland R, et al. Mitochondrial diseases. Nat Rev Dis Prim. 2016 Dec 20;2(1):16080. DOI:

10.1038/nrdp.2016.80

15. Alston CL, Rocha MC, Lax NZ, Turnbull DM, & Taylor RW. The genetics and pathology of mitochondrial disease. J Pathol. 2017;241(2):236–50. DOI: 10.1002/path.4809

16. Farrar GJ, Chadderton N, Kenna PF, & Millington-Ward S. Mitochondrial disorders: Aetiologies, models systems, and candidate therapies. Trends Genet. 2013;29(8):488–97. DOI: 10.1016/j.tig.2013.05.005

17. Wallace DC, Singh G, Lott MT, Hodge JA, Schurr TG, Lezza AMS, et al. Mitochondrial DNA mutation associated with Leber's hereditary optic neuropathy. Science (80-). 1988;242(4884):1427–30. DOI: 10.1126/science.3201231

18. Carelli V, Ross-Cisneros FN, & Sadun AA. Mitochondrial dysfunction as a cause of optic neuropathies. Prog Retin Eye Res. 2004;23(1):53–89. DOI: 10.1016/j.preteyeres.2003.10.003

19. Bi R, Logan I, & Yao Y-G. Leber Hereditary Optic Neuropathy: A Mitochondrial Disease Unique in Many Ways. In: Singh H, Sheu S, editors. Pharmacology of Mitochondria Handbook of Experimental Pharmacology, vol 240. Springer, Cham; 2016. p. 309–36. DOI: 10.1007/164_2016_1

20. Yu-Wai-Man P, Griffiths PG, & Chinnery PF. Mitochondrial optic neuropathies - Disease mechanisms and therapeutic strategies. Prog Retin Eye Res. 2011;30(2):81–114. DOI: 10.1016/j.preteyeres.2010.11.002

21. Cai W, Fu Q, Zhou X, Qu J, Tong Y, & Guan MX. Mitochondrial variants may influence the phenotypic manifestation of Leber's hereditary optic neuropathy-associated ND4 G11778A mutation. J Genet Genomics. 2008;35(11):649–55. DOI: 10.1016/S1673-8527(08)60086-7

22. Chun BY, & Rizzo JF. Dominant Optic Atrophy and Leber's Hereditary Optic Neuropathy: Update on Clinical Features and Current Therapeutic Approaches. Semin Pediatr Neurol. 2017;24(2):129–34. DOI: 10.1016/j.spen.2017.06.001

23. Yu-Wai-Man P. Therapeutic Approaches to Inherited Optic Neuropathies. Semin Neurol. 2015;35(5):578–86. DOI: 10.1055/s-0035-1563574

24. Lopez-Sanchez MIG, Crowston JG, Mackey DA, & Trounce IA. Emerging Mitochondrial Therapeutic Targets in Optic Neuropathies. Pharmacol Ther. 2016;165:132–52. DOI: 10.1016/j.pharmthera.2016.06.004

25. McClelland C, Meyerson C, & Van Stavern G. Leber hereditary optic neuropathy: current perspectives. Clin Ophthalmol. 2015;9:1165–76. DOI: 10.2147/OPTH.S62021

26. Tońska K, Kodroń A, & Bartnik E. Genotype-phenotype correlations in Leber hereditary optic neuropathy. Biochim Biophys Acta - Bioenerg. 2010;1797(6–7):1119–23. DOI: 10.1016/j.bbabio.2010.02.032

27. Rasool N, Lessell S, & Cestari DM. Leber hereditary optic neuropathy: Bringing the lab to the clinic. Semin Ophthalmol. 2016;31(1–2):107–16. DOI: 10.3109/08820538.2015.1115251

28. Yu-Wai-Man P, Votruba M, Burté F, La Morgia C, Barboni P, & Carelli V. A

neurodegenerative perspective on mitochondrial optic neuropathies. Acta Neuropathol. 2016;132(6):789–806. DOI: 10.1007/s00401-016-1625-2

29. Manickam AH, Michael MJ, & Ramasamy S. Mitochondrial genetics and therapeutic overview of Leber's hereditary optic neuropathy. Indian J Ophthalmol. 2017;65(11):1087–92. DOI: 10.4103/ijo.IJO

30. d'Almeida OC, Mateus C, Reis A, Grazina MM, & Castelo-Branco M. Long term cortical plasticity in visual retinotopic areas in humans with silent retinal ganglion cell loss. Neuroimage. 2013;81:222–30. DOI: 10.1016/j.neuroimage.2013.05.032

31. Theodorou-Kanakari A, Karampitianis S, Karageorgou V, Kampourelli E, Kapasakis E, Theodossiadis P, et al. Current and Emerging Treatment Modalities for Leber's Hereditary Optic Neuropathy: A Review of the Literature. Vol. 35, Advances in Therapy. Springer Healthcare; 2018. p. 1510–8. DOI: 10.1007/s12325-018-0776-z

32. Grazina MM, Diogo LM, Garcia PC, Silva ED, Garcia TD, Robalo CB, et al. Atypical presentation of Leber's hereditary optic neuropathy associated to mtDNA 11778G>A point mutation-A case report. Eur J Paediatr Neurol. 2007;11(2):115–8. DOI: 10.1016/j.ejpn.2006.11.015

33. Carelli V, Ghelli A, Bucchi L, Montagna P, De Negri A, Leuzzi V, et al. Biochemical features of mtDNA 14484 (ND6/m64V) point mutation associated with Leber's hereditary optic neuropathy. Ann Neurol. 1999 Mar 1;45(3):320–8. DOI: 10.1002/1531-8249(199903)45:3<320::AID-ANA7>3.0.CO;2-L

34. Ravn K, Wibrand F, Hansen FJ, Horn N, Rosenberg T, & Schwartz M. An mtDNA mutation, 14453G→A, in the NADH dehydrogenase subunit 6 associated with severe MELAS syndrome. Eur J Hum Genet. 2001 Oct 19;9(10):805–9. DOI: 10.1038/sj.ejhg.5200712

35. Pilz YL, Bass SJ, & Sherman J. Revisión de las neuropatías ópticas mitocondriales: de las formas hereditarias a las adquiridas. J Optom. 2017;10(4):205–14. DOI: 10.1016/j.optom.2016.09.003

36. Khan NA, Govindaraj P, Meena AK, & Thangaraj K. Mitochondrial disorders: challenges in diagnosis & treatment. Indian J Med Res. 2015;141(1):13–26. DOI: 10.4103/0971-5916.154489

37. Caporali L, Maresca A, Capristo M, Del Dotto V, Tagliavini F, Valentino ML, et al. Incomplete penetrance in mitochondrial optic neuropathies. Mitochondrion. 2017;36(August 2016):130–7. DOI: 10.1016/j.mito.2017.07.004

38. Kogachi K, Ter-Zakarian A, Asanad S, Sadun A, & Karanjia R. Toxic medications in Leber's hereditary optic neuropathy. Mitochondrion. 2019;46(May):270–7. DOI: 10.1016/j.mito.2018.07.007

39. Ruiz-Pesini E, Emperador S, López-Gallardo E, Hernández-Ainsa C, & Montoya J. Increasing mtDNA levels as therapy for mitochondrial optic neuropathies. Drug Discov Today. 2018;23(3):493–8. DOI: 10.1016/j.drudis.2018.01.031

40. Gueven N, Nadikudi M, Daniel A, & Chhetri J. Targeting mitochondrial function to treat optic neuropathy. Mitochondrion. 2017;36:7–14. DOI: 10.1016/j.mito.2016.07.013

41. Finsterer J, Mancuso M, Pareyson D, Burgunder JM, & Klopstock T. Mitochondrial disorders of the retinal ganglion cells and the optic nerve. Mitochondrion. 2018;42(October 2017):1–10. DOI: 10.1016/j.mito.2017.10.003

42. Lyseng-Williamson KA. Idebenone: A Review in Leber's Hereditary Optic Neuropathy. Drugs. 2016;76(7):805–13. DOI: 10.1007/s40265-016-0574-3

43. Klopstock T, Yu-Wai-Man P, Dimitriadis K, Rouleau J, Heck S, Bailie M, et al. A randomized placebo-controlled trial of idebenone in Leber's hereditary optic neuropathy. Brain. 2011 Sep;134(Pt 9):2677–86. DOI: 10.1093/brain/awr170

44. Klopstock T, Metz G, Yu-Wai-Man P, Büchner B, Gallenmüller C, Bailie M, et al. Persistence of the treatment effect of idebenone in Leber's hereditary optic neuropathy. Brain. 2013 Feb;136(Pt 2):e230. DOI: 10.1093/brain/aws279

45. Carelli V, La Morgia C, Valentino ML, Rizzo G, Carbonelli M, De Negri AM, et al. Idebenone treatment in Leber's hereditary optic neuropathy. Brain. 2011 Sep;134(Pt 9):e188. DOI: 10.1093/brain/awr180

46. Mashima Y, Hiida Y, & Oguchi Y. Remission of Leber's hereditary optic neuropathy with idebenone. Vol. 340, The Lancet. 1992. p. 368–9. DOI: 10.1016/0140-6736(92)91442-B

47. Cwerman-Thibault H, Augustin S, Ellouze S, Sahel J-A, & Corral-Debrinski M. Gene therapy for mitochondrial diseases : Leber Hereditary Optic Neuropathy as the first candidate for a clinical trial. C R Biol. 2014;337:193–206. DOI: 10.1016/j.crvi.2013.11.011

48. Ratican SE, Osborne A, & Martin KR. Progress in Gene Therapy to Prevent Retinal Ganglion Cell Loss in Glaucoma and Leber's Hereditary Optic Neuropathy. Neural Plast. 2018;2018. DOI: 10.1155/2018/7108948

49. Guan MX. Mitochondrial 12S rRNA mutations associated with aminoglycoside ototoxicity. Mitochondrion. 2011;11(2):237–45. DOI: 10.1016/j.mito.2010.10.006

50. Ding Y, Leng J, Fan F, Xia B, & Xu P. The role of mitochondrial DNA mutations in hearing loss. Biochem Genet. 2013;51(7–8):588–602. DOI: 10.1007/s10528-013-9589-6

51. Jacobs HT, Hutchin TP, Käppi T, Gillies G, Minkkinen K, Walker J, et al. Mitochondrial DNA mutations in patients with postlingual, nonsyndromic hearing impairment. Eur J Hum Genet. 2005;13(1):26–33. DOI: 10.1038/sj.ejhg.5201250

52. Böttger EC, & Schacht J. The mitochondrion: A perpetrator of acquired hearing loss. Hear Res. 2013;303:12–9. DOI: 10.1016/j.heares.2013.01.006.

53. Zhao H, Young WY, Yan Q, Li R, Cao J, Wang Q, et al. Functional characterization of the mitochondrial 12S rRNA C1494T mutation associated with aminoglycoside-induced and non-syndromic hearing loss. Nucleic Acids Res. 2005;33(3):1132–9. DOI: 10.1093/nar/gki262

54. Shen SS, Liu C, Xu ZY, Hu YH, Gao GF, & Wang SY. Heteroplasmy levels of mtDNA1555A>G mutation is positively associated with diverse phenotypes and mutation transmission in a Chinese family. Biochem Biophys Res Commun. 2012;420(4):907–12. DOI: 10.1016/j.bbrc.2012.03.100

55. Gao Z, Chen Y, & Guan M-X. Mitochondrial DNA mutations associated with aminoglycoside induced ototoxicity. J Otol. 2017;12(1):1–8. DOI: 10.1016/j.joto.2017.02.001

56. Guthrie OW. Aminoglycoside induced ototoxicity. Toxicology. 2008;249(2–3):91–6. DOI: 10.1016/j.tox.2008.04.015

57. Ballana E, Morales E, Rabionet R, Montserrat B, Ventayol M, Bravo O, et al. Mitochondrial 12S rRNA gene mutations affect RNA secondary structure and lead to variable penetrance in hearing impairment. Biochem Biophys Res Commun. 2006;341(4):950–7. DOI: 10.1016/j.bbrc.2006.01.049

58. Lu J, Qian Y, Li Z, Yang A, Zhu Y, Li R, et al. Mitochondrial haplotypes may modulate the phenotypic manifestation of the deafness-associated 12S rRNA 1555A>G mutation. Mitochondrion. 2010;10(1):69–81. DOI: 10.1016/j.mito.2009.09.007

59. Konings A, Van Camp G, Goethals A, Van Eyken E, Vandevelde A, Ben Azza J, et al. Mutation analysis of mitochondrial DNA 12SrRNA and tRNASer(UCN) genes in non-syndromic hearing loss patients. Mitochondrion. 2008;8(5–6):377–82. DOI: 10.1016/j.mito.2008.08.001

60. Hobbie SN, Akshay S, Kalapala SK, Bruell CM, Shcherbakov D, & Bottger EC. Genetic analysis of interactions with eukaryotic rRNA identify the mitoribosome as target in aminoglycoside ototoxicity. Proc Natl Acad Sci. 2008;105(52):20888–93. DOI: 10.1073/pnas.0811258106

61. Drew RH. Aminoglycosides [Internet]. © 2019 UpToDate, Inc. 2018.

62. Raimundo N, Song L, Shutt TE, McKay SE, Cotney J, Guan MX, et al. Mitochondrial stress engages E2F1 apoptotic signaling to cause deafness. Cell. 2012;148(4):716–26. DOI: 10.1016/j.cell.2011.12.027

63. Foster II J, & Tekin M. Aminoglycoside induced ototoxicity associated with mitochondrial DNA mutations. Egypt J Med Hum Genet. 2016;17(3):287–93. DOI: 10.1016/j.ejmhg.2016.06.001

64. Ding Y, Xia B-H, Teng Y-S, Zhuo G-C, & Leng J-H. The Mitochondrial COI/tRNASER(UCN) G7444A Mutation may be Associated with Hearing Impairment in a Han Chinese Family. Balkan J Med Genet. 2017;20(2):43–50. DOI: 10.1515/bjmg-2017-0025

65. McKay SE, Yan W, Nouws J, Thormann MJ, Raimundo N, Khan A, et al. Auditory pathology in a transgenic mtTFB1 mouse model of mitochondrial deafness. Am J Pathol. 2015;185(12):3132–40. DOI: 10.1016/j.ajpath.2015.08.014

66. Chen T, Liu Q, Jiang L, Liu C, & Ou Q. Mitochondrial COX2 G7598A Mutation May Have a Modifying Role in the Phenotypic Manifestation of Aminoglycoside Antibiotic-Induced Deafness Associated with 12S rRNA A1555G Mutation in a Han Chinese Pedigree. Genet Test Mol Biomarkers. 2013;17(2):122–30. DOI: 10.1089/gtmb.2012.0251

67. Chen J, Yang L, Yang A, Zhu Y, Zhao J, Sun D, et al. Maternally inherited aminoglycoside-induced and nonsyndromic hearing loss is associated with the 12S rRNA C1494T mutation in three Han Chinese pedigrees. Gene. 2007;401(1–

2):4–11. DOI: 10.1016/j.gene.2007.06.009

68. Xing J, Liu X, Tian Y, Tan J, & Zhao H. Genetic and clinical analysis of nonsyndromic hearing impairment in pediatric and adult cases. Balk J Med Genet. 2016;19(1):35–42. DOI: 10.1515/bjmg-2016-0005

69. Pirvola U, Xing-Qun L, Virkkala J, Saarma M, Murakata C, Camoratto AM, et al. Rescue of hearing, auditory hair cells, and neurons by CEP-1347/KT7515, an inhibitor of c-Jun N-terminal kinase activation. J Neurosci. 2000 Jan 1;20(1):43–50. DOI: 10.1523/JNEUROSCI.20-01-00043.2000

70. Saunders Comprehensive Veterinary Dictionary. Real-Time PCR. In: Saunders Comprehensive Veterinary Dictionary. 3ed ed. Elsevier, Inc; 2007.

71. Higuchi R, Fockler C, Dollinger G, & Watson R. Kinetic PCR analysis: real-time monitoring of DNA amplification reactions. Biotechnology (N Y). 1993 Sep;11(9):1026–30.

72. Navarro E, Serrano-Heras G, Castaño MJ, & Solera J. Real-time PCR detection chemistry. Clin Chim Acta. 2015;439:231–50. DOI: 10.1016/j.cca.2014.10.017

73. Stephenson FH. Real-Time PCR. In: Leonard J, editor. Calculations for Molecular Biology and Biotechnology. 3rd ed. Academic Press; 2016. p. 215–320. DOI: 10.1016/B978-0-12-802211-5.00009-6

74. Farrar JS, & Wittwer CT. High-Resolution Melting Curve Analysis for Molecular Diagnostics [Internet]. Molecular Diagnostics: Third Edition. Elsevier Ltd; 2016. 79–102 p. DOI: 10.1016/B978-0-12-802971-8.00006-7

75. Matsuda K. PCR-Based Detection Methods for Single-Nucleotide Polymorphism or Mutation: Real-Time PCR and Its Substantial Contribution Toward Technological Refinement. In: Makowski G, editor. Advances in Clinical Chemistry. 1st ed. Elsevier Inc.; 2017. p. 45–72. DOI: 10.1016/bs.acc.2016.11.002

76. Wittwer CT, Herrmann MG, Moss AA, & Rasmussen RP. Continuous Fluorescence Monitoring of Rapid Cycle DNA Amplification. Biotechniques. 1997 Jan;22(1):130–8. DOI: 10.2144/97221bi01

77. Ririe KM, Rasmussen RP, & Wittwer CT. Product differentiation by analysis of DNA melting curves during the polymerase chain reaction. Anal Biochem. 1997 Feb 15;245(2):154–60. DOI: 10.1006/abio.1996.9916

78. Gundry CN, Vandersteen JG, Reed GH, Pryor RJ, Chen J, & Wittwer CT. Amplicon melting analysis with labeled primers: a closed-tube method for differentiating homozygotes and heterozygotes. Clin Chem. 2003 Mar;49(3):396–406.

79. Wittwer CT, Reed GH, Gundry CN, Vandersteen JG, & Pryor RJ. High-resolution genotyping by amplicon melting analysis using LCGreen. Clin Chem. 2003 Jun 1;49(6):853–60. DOI: 10.1373/49.6.853

80. Chambliss AB, Resnick M, Petrides AK, Clarke WA, & Marzinke MA. Rapid screening for targeted genetic variants via high-resolution melting curve analysis. Clin Chem Lab Med. 2017;55(4):507–16. DOI: 10.1515/cclm-2016-0603

81. Newton CR, Graham A, Heptinstall LE, Powell SJ, Summers C, Kalsheker N, et al. Analysis of any point mutation in DNA. The amplification refractory mutation system (ARMS). Nucleic Acids Res. 1989 Apr 11;17(7):2503–16. DOI: 10.1093/nar/17.7.2503

82. Bi R, Zhang AM, Yu D, Chen D, & Yao YG. Screening the three LHON primary mutations in the general Chinese population by using an optimized multiplex allele-specific PCR. Clin Chim Acta. 2010;411(21–22):1671–4. DOI: 10.1016/j.cca.2010.06.026

83. Abu-Amero KK. Leber's Hereditary Optic Neuropathy: The Mitochondrial Connection Revisited. Middle East Afr J Ophthalmol. 2011;18(1):17–23. DOI: 10.4103/0974-9233.75880

84. Ausubel FM, Brent R, Kingston RE, Moore DD, Seidman J, Smith JA, et al. Preparation and Analysis of DNA. In: Current Protocols in Molecular Biology. John Wiley & Sons; 1997. p. 2:0:1-2:14:8.

85. Ryan SE, Ryan F, Dwyer VO, & Neylan D. A real-time ARMS PCR / high-resolution melt curve assay for the detection of the three primary mitochondrial mutations in Leber ' s hereditary optic neuropathy. Mol Vis. 2016;22:1169–75.

86. Martins FTA, do Amor Divino Miranda PM, Amaral Fernandes MS, Maciel-Guerra AT, & Sartorato EL. Optimization of a genotyping screening based on hydrolysis probes to detect the main mutations related to leber hereditary optic neuropathy (LHON). Mol Vis. 2017;23(March):495–503.

87. Overbergh L, Giulietti A, Valckx D, & Mathieu C. Real-Time Polymerase Chain Reaction. In: Patrinos GP, Ansorge W, editors. Molecular Diagnostics. 2nd edition. San Diego, CA, USA: Elsevier Academic Press; 2010. p. 87–106.

88. Clay Montier LL, Deng JJ, & Bai Y. Number matters: control of mammalian mitochondrial DNA copy number. J Genet Genomics. 2009 Mar;36(3):125–31. DOI: 10.1016/S1673-8527(08)60099-5

89. Xia CY, Liu Y, Yang HR, Yang HY, Liu JX, Ma YN, et al. Reference intervals of mitochondrial DNA copy number in peripheral blood for Chinese minors and adults. Chin Med J (Engl). 2017 Oct 20;130(20):2435–40. DOI: 10.4103/0366-6999.216395

90. Pejznochova M, Tesarova M, Hansikova H, Magner M, Honzik T, Vinsova K, et al. Mitochondrial DNA content and expression of genes involved in mtDNA transcription, regulation and maintenance during human fetal development. Mitochondrion. 2010 Jun;10(4):321–9. DOI: 10.1016/j.mito.2010.01.006

91. Ding Y, Xia BH, Liu Q, Li MY, Huang SX, & Zhuo GC. Allele-specific PCR for detecting the deafness-associated mitochondrial 12S rRNA mutations. Gene. 2016;592(1):148–52. DOI: 10.1016/j.gene.2016.07.013

92. Han B, Zong L, Li Q, Zhang Z, Wang D, Lan L, et al. Newborn genetic screening for high risk deafness-associated mutations with a new Tetra-primer ARMS PCR kit. Int J Pediatr Otorhinolaryngol. 2013;77(9):1440–5. DOI: 10.1016/j.ijporl.2013.05.040

93. Wang C, Wang S, Chen H, & Lu D. Establishment of a Gene Detection System

for Hotspot Mutations of Hearing Loss. Biomed Res Int. 2018;2018(Article ID 6828306):1–8. DOI: 10.1155/2018/6828306

94. Zhang F, Xiao Y, Xu L, Zhang X, Zhang G, Li J, et al. Mutation analysis of the common deafness genes in patients with nonsyndromic hearing loss in linyi by SNPscan assay. Biomed Res Int. 2016;2016. DOI: 10.1155/2016/1302914

95. Du W, Cheng J, Ding H, Jiang Z, Guo Y, & Yuan H. A rapid method for simultaneous multi-gene mutation screening in children with nonsyndromic hearing loss. Genomics. 2014;104(4):264–70. DOI: 10.1016/j.ygeno.2014.07.009

96. Kato T, Nishigaki Y, Noguchi Y, Ueno H, Hosoya H, Ito T, et al. Extensive and rapid screening for major mitochondrial DNA point mutations in patients with hereditary hearing loss. J Hum Genet. 2010;55(3):147–54. DOI: 10.1038/jhg.2009.143

97. Wang X, Hong Y, Cai P, Tang N, Chen Y, Yan T, et al. Rapid and reliable detection of nonsyndromic hearing loss mutations by multicolor melting curve analysis. Sci Rep. 2017;7(February):1–8. DOI: 10.1038/srep42894

98. Eustace Ryan S, Ryan F, Barton D, O'Dwyer V, & Neylan D. Development and validation of a novel PCR-RFLP based method for the detection of 3 primary mitochondrial mutations in Leber's hereditary optic neuropathy patients. Eye Vis. 2015;2(1):18. DOI: 10.1186/s40662-015-0028-0

99. Krause KM, Serio AW, Kane TR, & Connolly LE. Aminoglycosides : An Overview. Cold Spring Harb Perspect Med. 2016;6(:a027029):1–18. DOI: 10.1101/cshperspect.a027029

Appendixes

Appendix 1. Supplementary Figure 1 Amplification Plot of the optimization step with 55ºC.

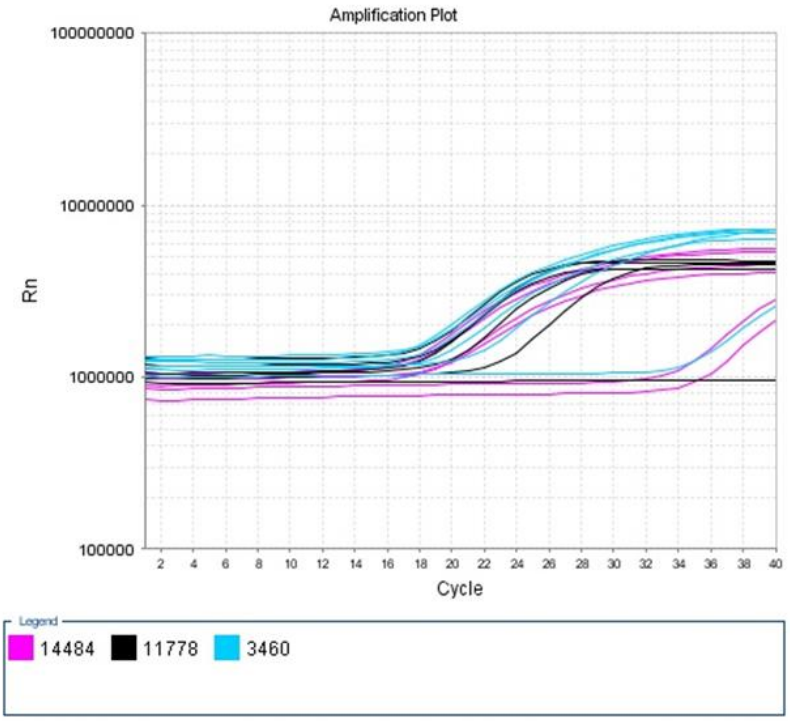

Appendix 2. Supplementary Figure 2 Melt curves for the optimization results at 55ºC. (2A) Normalized reporter melt curve results. (2B) derivative plot for all three targets.

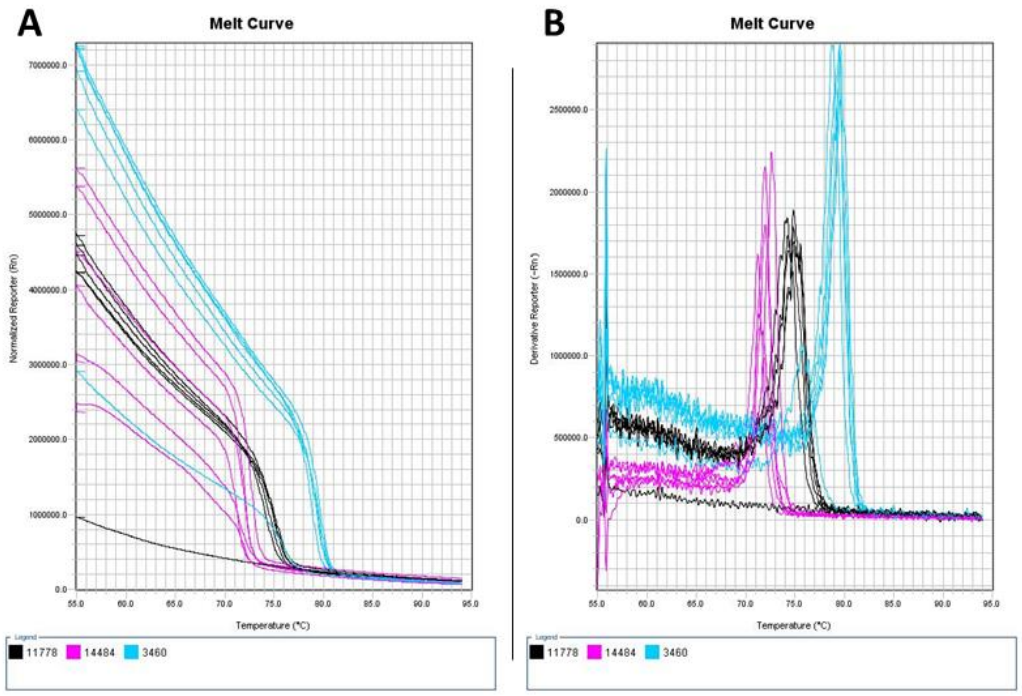

Appendix 3. Supplementary Figure 3 Aligned melt curves of HRM analysis of optimization step at 55ºC. The aligned melt curves are, top to bottom, for the m.3460G>A (A), m.11778G>A (B) and m.14484T>C (C) targets. The line of different color is the pathogenic sequence variant, from the positive sample.

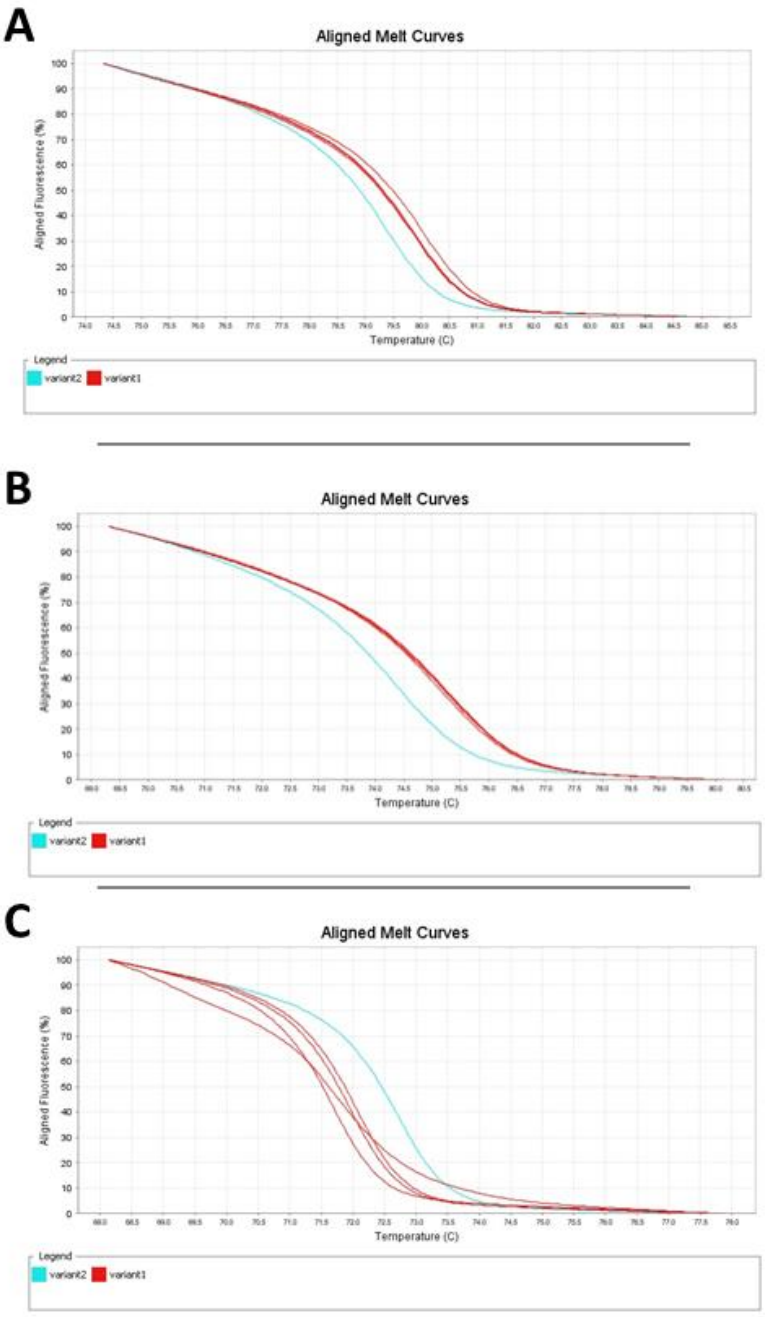

Appendix 4. Methodology Implementation

1.1. Primer Design

The design of primers was conducted using bioinformatic tools, namely *Primer3Plus* (http://www.bioinformatics.nl/primer3plus), *WASP* (http://bioinfo.biotec.or.th/WASP), *PrimerBLAST* (https://www.ncbi.nlm.nih.gov/tools/primer-blast/) and *Primer1* (http://primer1.soton.ac.uk/primer1.html).

Each obtained primer pair was processed by a series of bioinformatic tools, in order, *USCS In-Silico* (https://genome.ucsc.edu/cgi-bin/hgPcr), *USCS BLAT* (https://genome.ucsc.edu/cgi-bin/hgBlat), and *EndMemo - DNA Melting Temperature (Tm) Calculator* (http://endmemo.com/bio/tm.php). Firstly, the specificity of primers pairs was checked with *USCS In-Silico* by assessing the products to be amplified. Afterwards, the amplicon produced was checked for similarity within the human genome, namely looking for pseudogenes, with *USCS BLAT*. Values nearing 90% were considered acceptable. Finally, the amplified sequence was inserted in *EndMemo*, which predicts the amplicons' T_m. The prediction of HRM results was obtained, showing if the desired and undesired/nuclear amplicons were different enough from one another to allow discrimination. Thus, the sequences pertaining to i) wild-type (WT) amplicon, ii) mutant amplicon, and iii) any undesired pseudogenes were processed in *EndMemo*, and their T_m values should show a difference of >0.3ºC between each other.

For LHON, one primer pair (for m.3460G>A screening) produced by *Primer3Plus* had excellent specificity and was accepted. This primer pair had 100% specificity and the amplicon presented no similarities in the human genome. The two other primer pairs (for m.11778G>A and m.14484T>C screening) were obtained with *WASP*. These two pair were also specific, but their amplicons showed higher similarities with nuclear pseudogenes, with 92.5% and 93.4%, respectively, for m.11778G>A and m.14484T>C analysis. These values were the lowest found and considered low enough to accept the primers. This is related in Table 2.

Design of primers and amplicons, with high specificity and sensitivity attributes, was complex, due to the combination of the pseudogenes' presence and the required small size of the Real-Time PCR amplicon. The balance struck provided very good results.

1.2. Optimization of LHON protocol

For LHON screening, the MeltDoctor™ HRM Master Mix (with SYTO®9) was chosen and reaction mix and run set-up were performed following the dye manufacturer's instructions, with different annealing temperatures. Temperatures of 60ºC, 55ºC and 50ºC were tested, ultimately adopting the 55ºC temperature as optimal. Above this temperature amplification ceased and below it was found too unspecific. The optimization was processed with four samples (a positive control for each pathogenic sequence variant in analysis, and an overall negative control sample) along with a non-template control (NTC).

With those conditions, PCR amplification was good for all samples, without unspecific products found in amplification or melting curves, and the PCR data was correctly

processed, analyzed and identified by the HRM software (higher specificity and sensitivity).

1.3. Implementation of LHON protocol

The results were run in triplicate and submitted to confirmation runs randomly.

The analysis started with the 7500 Software, to confirm that amplification and melt curves were appropriate for HRM analysis, or if they had any issue that could detour the HRM analysis. Wells that showed uncomplete amplification, by failing to reach or having a low plateau, were excluded from analysis, at the beginning this was mainly due to the novelty of dealing with a new technique. Due to the use of triplicates any omission detected was possible without compromising analysis. The melt curves (both normative and derivative) were analyzed, to check for any unspecific products.

The HRM software analysis followed. Control assignment eased analysis, but mostly it was not necessary; manually matching variants from the controls with those of the samples was straightforward. However, in cases in which the software seemed to over distinguish variants (grouping was done in smaller intervals and more variants were adopted by the software for identification; it was possible to see that confidence values were low and a difference of <0.3ºC was often found between two variants) this tool was of some interest, helping the software to correctly group T_ms and, thus, assign variants correctly.

In cases in which triplicates presented more than one variant: i) if confidence values were similar, consider the 2/3 variant presented as correct; ii) the confidence value would be higher in one of the variants, and it would be considered that as correct, usually matched the 2/3 rule. These differences correlated with issues in amplification, namely one sample had less, or more, fluorescence than the other/s. Thus, checking the information simultaneously in the 7500 Software would be helpful.

To further assure results quality, and that the attribution of T_m and subsequent variant calling were not random, the controls' T_ms from all runs were compared. The values shifted between plates, but these variations were <0.3ºC. Moreover, they did so in a proportional manner, that is, if a positive control would shift, the negative controls' values would shift in the same proportion. This comes from a normal variation, from run to run, that might occur in these instruments; as it affected all wells in the plate equally, it has no effect in variant call.